

PERFORMANCE EVALUATION OF ARIZONA ASPHALT RUBBER MIXTURES USING ADVANCED DYNAMIC MATERIAL CHARACTERIZATION TESTS

Final Report

Prepared by

Kamil E. Kaloush, P.E., Assistant Professor, ASU
Matthew W. Witczak, Professor, ASU
George B. Way, P.E., ADOT

and

Aleksander Zborowski
Mohammad Abojaradeh
Andres Sotil

Graduate Research Assistants, ASU

Submitted to

FNF Construction, Inc.
Asphalt-Rubber Division
115 S. 48th Street
Tempe, AZ 85281



Arizona Department of Transportation
Materials Group
1221 North 21st Avenue
Phoenix, AZ 85009



July 2002



College of Engineering and Applied Sciences
Department of Civil and Environmental Engineering
Tempe, AZ 85287-5306

EXECUTIVE SUMMARY

The Arizona Department of Transportation (ADOT) has used Asphalt Rubber (AR) as a modified binder since the early 1970's. The primary purpose for using AR is to reduce reflective cracking in hot mix asphalt (HMA) rehabilitation overlays. In addition to this AR has been used to reduce maintenance, provide a smooth riding surface, with good skid resistance. The AR mix has also performed well in snow and ice conditions providing a tough surface that stands up well to snow plows.

The AR as tested in this study and used in Arizona is a mixture of approximately 20 percent ground tire rubber (crumb rubber) made from the recycling of used or defective tires. The ground tire rubber is added to hot paving grade asphalt at a high temperature and mixed with a high shear mixer. The mixing time and subsequent time of material interaction is generally 45 to 60 minutes. After the interaction, the hot AR product has acquired unique elastomeric properties. The hot AR is then pumped into a conventional hot plant and mixed with aggregate and placed like a conventional HMA, except for a few significant differences.

These significant differences relate to the gradation of the mineral aggregate and the percent binder. The AR hot mix is generally either a gap graded or open graded mix. The gap graded mix contains about 7.5 percent AR binder and is placed generally as the final structural course 1.5 to 2 inches in thickness. The open graded contains generally 9 percent binder and is placed as the final wearing course from 0.5 to 1.0 inch thick. The

mix designs for these two mixes are typically of a volumetric type and little has been published or researched about the binder or mix engineering properties in terms of the inputs needed for the new AASHTO 2002 Pavement Design Guide.

In the spring of 2001, ADOT in cooperation with FNF Construction Inc. entered into a research and testing plan with Arizona State University (ASU). The plan involves characterizing AR mixes and binders in order to determine their properties for future use in the AASHTO 2002 Pavement Design Guide. An additional part of the long-term plan is to begin building a database to support the new 2002 Pavement Design Guide. This research report represents the findings from this first project. The plan is to characterize AR mixes from several projects in order to represent different grades of AR binder, different aggregates and different climates representative of Arizona.

This first project, named Buffalo Range TI-Canyon Diablo (IM-040-D(1)P, Tracs # H4883) is located on Interstate 40 at Mile Posts 224.7 to 229.9, close to Winslow Arizona. The project elevation is approximately 5,000 feet and the region is considered a dry freeze zone according to SHRP. Air temperatures of over 100°F occur in the summer and temperatures below -20 degrees F occur in the winter. The Interstate truck traffic is quite heavy and averages 2.2 million ESAL's per year. The pavement was overlaid in 1988 with 4.5 inches of conventional HMA. By 2001 the pavement had 3 percent cracking and a 0.20 inches of rutting. However, these values are somewhat misleading since extensive patching maintenance averaging \$4,000 per mile were applied in 1998. This maintenance

activity masked the high degree of fatigue cracking and rutting. The AR overlay project was constructed by FNF Construction Inc. The project consisted of removing by milling off 2.5 inches of the old cracked pavement full width and replacing it with 2 inches of the AR gap graded mix followed by 0.5 inch of AR open graded mix. This is a relatively routine type of rehabilitation of older cracked pavements in Arizona. The construction took place in June of 2000. Materials for the ARAC – Gap Graded mixture and AR-ACFC – Open Graded mixture were collected during construction.

The focus of the laboratory experimental program was on conducting tests that were recommended by the NCHRP 9-19 Project. These tests dealt with recommending Simple Performance Tests (SPT) for the evaluation of asphalt mixtures. The goal was to also compare the performance of these AR mixtures to other conventional asphalt mixtures that are also being tested at ASU.

Conventional asphalt binder tests were conducted to develop information that will complement other mixture material properties such as fatigue cracking and permanent deformation. The conventional consistency tests (penetration, softening point and viscosity) were conducted on the Crumb Rubber Modified (CRM) binder to determine whether there were any unique characteristics or difficulties in handling the material. Consistency tests across a wide range of temperatures were conducted according to the accepted American Society for Testing and Materials (ASTM) practices. Based on the test results and analysis conducted in this study, the conventional asphalt cement tests were

shown to be adequate in describing the viscosity-temperature susceptibility of crumb rubber modified asphalt cement. This favorable viscosity-temperature susceptibility relationship also appeared to relate to the observed field performance behavior. Such behavior is characterized as less low temperature cracking and good resistance to permanent deformation at high temperatures.

Triaxial Shear Strength tests were conducted at unconfined and confined conditions (three different levels) at 100°F. These tests provided the standard cohesion and the angle of internal friction parameters of the mixtures. The Mohr-Coulomb failure envelope was developed for each tested mixture. In addition results from previously tested standard ADOT Salt River Base (SRB) mixture with binder PG64-22 were included in the analysis in order to compare its properties to those obtained for the AR. The results of the cohesion parameter showed that the asphalt rubber open graded mix (AR-ACFC) had much lower resistance to shearing stresses than the other two mixes. This observation must be supported by information that the AR-ACFC is utilized as a mixture for non-structural layer. For this Buffalo Range project, the AR-ACFC mix was placed as 0.5 in lift, and for that type of application, the shearing stress is not so critical. At the same time, the AR-ACFC mix had the highest value of angle of internal friction, which indicates that this material has the largest capacity to develop strength from the applied loads, and hence having smaller potential for permanent deformation. Similar results were observed for the ARAC mixtures as it had smaller cohesion than the SRB PG64-22, but also had larger angle of internal friction, and smaller potential for permanent deformation.

Repeated Load and Static Creep Permanent Deformation tests were conducted at two temperatures using unconfined and confined SPT protocols. Many test parameters were evaluated including tertiary flow (flow time and flow number of repetitions) as one of the SPT candidates. The test results obtained were compared to results available at ASU for conventional ADOT dense graded mixtures. For both tests, the ARAC mixture indicated superior performance, much higher resistance to permanent deformation compared to the standard ADOT SRB PG64-22 mixture. The AR-ACFC mix generally showed lower resistance to permanent deformation compared to the other tested mixtures. The poor performance was attributed to the lack of adequate laboratory confinement level applied, which does not represent the level of confinement that the material experiences in the field. In addition, few test specimens for the ARAC gap graded mix were prepared at lower air void content (7%) than that reported in the field (11%). The air voids variation test results showed that the ARAC mix compacted to 7% air voids would have much better performance and less potential for permanent deformation than the same mixture compacted to 11% air voids. Therefore, field compaction considerations should be carefully evaluated for this mixture. Overall, the permanent deformation test results were promising, in that utilizing the SPT candidate tests were able to verify the known field performance of the asphalt rubber mixtures.

Dynamic Complex Modulus (E^*) tests were also conducted at unconfined and confined conditions (three different levels), and the E^* master curves were developed for each mixture. The E^* test results for the AR mixes were compared with conventional dense

graded mixtures test results available from previous studies at Arizona State University. A modular (E^*) ratio was calculated for all mixtures using a conventional PG 64-22 mixture as a reference. A comparison of the modular ratios was done at 14°F and 100°F, for a selected test frequency of 10 Hz. For the unconfined tests, at 14°F, the AR exhibited the lowest modular ratio (lowest stiffness), and therefore the best desirable performance against cracking. At 100°F, the AR mixtures had comparatively the lowest stiffness values. However, when the comparison of the ratios was made using the confined test results, the AR mixtures showed higher ratios (modulus values), and therefore, the best performance against permanent deformation. Since the performance of the AR mixtures have been remarkable in the field, these results showed the importance of using confined laboratory tests when comparing the performance of open graded to dense graded mixtures.

The AR mixes were also subjected to fatigue and indirect tensile cracking tests. The results were compared to data and test results available at ASU for ADOT conventional dense graded mixtures. The goal was to start developing a database of typical ADOT AR mixture cracking (fatigue and thermal) properties and parameters for their use in the implementation of the new AASHTO 2002 Design Guide.

Constant Strain Fatigue tests were conducted at different test temperatures using the beam fatigue apparatus proposed by the Strategic Highway Research Program (SHRP). The fatigue models developed for the AR mixtures in this study had excellent measures of

accuracy and were rational in that lower fatigue life was obtained as the test temperature decreased. Furthermore, a comparison was made of the fatigue life obtained for the AR mixes with an ADOT PG 76-16 conventional dense graded mix. The fatigue life was found to be higher for asphalt rubber mixes compared to the conventional PG 76-16. The comparison was done at 70°F and at 50% reduction of initial stiffness for all mixtures. The ARAC mix resulted in approximately 3 times greater fatigue life than the conventional mix. On the other hand, the AR-ACFC mix resulted in 15 times greater fatigue life than the conventional mix. These order of magnitudes of fatigue life for the three mixtures were rational considering that the PG 76-16 mix had 4.20% binder content whereas the ARAC and AR-ACFC mixtures had 6.8% and 8.8%, respectively.

Both indirect tensile cracking tests (Strength and Creep) were carried out according to the procedure described in the draft indirect tensile tests protocol for the AASHTO 2002 Design Guide. The tests were carried out at three temperatures: 32, 14 and 5°F. The results of strain at failure showed that the AR-ACFC and ARAC mixes had higher values than the SRB PG64-22 mix. Mixtures with higher strain at failure have higher resistance to thermal cracking. The results of energy until failure and fracture energy from the indirect tensile strength test, as well as the results of the creep compliance from the indirect tensile creep test indicated that AR mixtures, and especially the AR-ACFC mix, are not sensitive to decrease in temperature compared to the SRB PG64-22 mixture. Both AR mixtures had higher energy values, which were indicative of more resistant to thermal cracking.

ACKNOWLEDGEMENT

The authors would like to acknowledge the following personnel for their assistance in this research study: Mr. Doug Forstie and Dr. Julie Nodes of the Arizona Department of Transportation, Mr. Mark Belshe of FNF Construction, Inc., Mr. Larry Ilg and Ms. Audra Merrick of ADOT Flagstaff District Office, Ms. Donna Carlson of the Rubber Pavement Association, Mr. Javed Bari and Mr. Kenny Witczak of Arizona State University. This work was sponsored by the Arizona Department of Transportation and FNF Construction Inc.

TABLE OF CONTENTS

	<u>Page</u>
EXECUTIVE SUMMARY	i
ACKNOWLEDGEMENT.....	viii
LIST OF TABLES	xii
LIST OF FIGURES	xiii
1. INTRODUCTION	17
1.1. Background	17
1.2. ASU Research Program	21
1.3. Study Objective.....	21
1.4. Scope of the Work.....	22
1.5. Specimens Preparation.....	23
1.6. Number of Tests.....	23
1.6.1. Test Program for ARAC – Asphalt Rubber GAP Graded Mix	23
1.6.2. Test Program for AR-ACFC – Asphalt Rubber OPEN Graded Mix.....	24
1.7. Report Organization.....	25
2. MIXTURE CHARACTERISTICS	26
2.1. Asphalt	26
2.2. Mixture Properties.....	26
2.3. Air Voids Measurement Using the CoreLok Device	28
3. BINDER CHARACTERIZATION	31
3.1. Introduction.....	31
3.2. Binder Consistency Tests – Viscosity Temperature Relationship	32
3.3. Testing Program.....	33
3.4. Results and Analysis	34
3.5. Asphalt Rubber Binder Handling Experience.....	43
3.6. Summary for the Binder Characterization.....	43
4. TRIAXIAL SHEAR STRENGTH TEST	45
4.1. Background for the Triaxial Shear Strength Test	45
4.2. Test Conditions for the Triaxial Shear Strength Test	47
4.3. Test Results and Analysis for the Triaxial Shear Strength	48
4.4. Summary for the Triaxial Shear Strength Test	49
5. PERMANENT DEFORMATION TESTS	51
5.1. Background for the Static Creep /Flow Time Tests.....	51
5.1.1. Modulus/Compliance Components	51
5.1.2. Mathematical Compliance Model.....	53
5.1.3. Evaluation of Flow Time	55

5.2. Background for the Repeated Load Permanent Deformation Test.....	57
5.3. Test Conditions for the Static Creep and Repeated Load Tests.....	64
5.4. Tests Results and Analysis.....	68
5.4.1. Static Creep/ Flow Time Test	68
5.4.2. Repeated Load/ Flow Number Test.....	73
5.5. Summary for the Permanent Deformation Tests	80
6. DYNAMIC MODULUS TEST.....	83
6.1. Background for the Dynamic (Complex) Modulus Test	83
6.2. General Test Description	85
6.3. Test Results and Analysis	88
6.3.1. ARAC Gap Graded Mixture	88
6.3.2. AR-ACFC OPEN Graded Mixture	95
6.3.3. Crumb Rubber Specimen.....	100
6.4. Comparison of Asphalt Rubber and Conventional Mixtures.....	102
6.5. Modular Ratio (R)	105
6.6. Witczak E* Predictive Equation Analysis	111
6.6.1. Assessing the applicability of the current version of the Predictive Equation on the Asphalt Rubber mixtures	113
6.6.1.1. Unconfined Test Results	113
6.6.1.2. Confined Test Results	116
6.6.2. Witczak et al. Dynamic Modulus Predictive Equation only for AR Mixtures	117
6.7. Summary of the Dynamic Modulus Tests	118
7. CRACKING TESTS	123
7.1. FATIGUE CRACKING TESTING.....	123
7.1.1. Background for the Flexural Beam Fatigue Test.....	123
7.1.2. Testing Equipment	125
7.1.3. Test Procedure and Calculations	127
7.1.4. Material And Specimen Preparation.....	130
7.1.4.1. Materials.....	130
7.1.4.2. Mold Assembly	130
7.1.4.3. Specimen Preparation	132
7.1.5. Testing Factorial	134
7.1.6. Test Conditions	134
7.1.7. Test Results and Analysis for the Flexural Beam Fatigue Test	135
7.1.8. Summary for the Flexural Beam Fatigue Test.....	140
7.2. THERMAL CRACKING	141
7.2.1. Indirect Tensile Tests.....	141
7.2.2. Background for the Indirect Tensile Strength Test.....	143
7.2.3. Background for the Indirect Tensile Creep Tests	146
7.2.3.1. Strain-Time Response Curve	147
7.2.3.2. Modulus/Compliance Components.....	148
7.2.4. Test Conditions for the Indirect Tensile Strength and Creep Tests	150

7.2.5. Tests Results and Analysis	151
7.2.5.1. Indirect Tensile Strength Test.....	151
7.2.5.2. Indirect Tensile Creep Test.....	159
7.2.6. Summary for the Indirect Tensile Tests.....	165
8. SUMMARY, CONCLUSIONS AND RECOMMENDATIONS.....	168
8.1. Summary	168
8.2. Conclusions and Recommendations	170
8.2.1. Binder Characterization.....	170
8.2.2. Triaxial Shear Strength Test.....	171
8.2.3. Permanent Deformation Tests	172
8.2.4. Dynamic (Complex) Modulus Test.....	173
8.2.5. Fatigue Cracking Testing.....	175
8.2.6. Thermal Cracking Tests.....	176
9. REFERENCES	178
APPENDIX A - BINDER TEST RESULTSERROR! BOOKMARK NOT DEFINED.	
APPENDIX B - TRIAXIAL SHEAR STRENGTH TEST RESULTSERROR! BOOKMARK NOT DEFINED.	
APPENDIX C - STATIC CREEP TEST RESULTSERROR! BOOKMARK NOT DEFINED.	
APPENDIX D - REPEATED LOAD TEST RESULTSERROR! BOOKMARK NOT DEFINED.	
APPENDIX E - DYNAMIC (COMPLEX) MODULUS TEST RESULTSERROR! BOOKMARK NOT DEFINED.	
APPENDIX F - FLEXURAL BEAM FATIGUE TEST RESULTSERROR! BOOKMARK NOT DEFINED.	
APPENDIX G - INDIRECT TENSILE STRENGTH TEST RESULTSERROR! BOOKMARK NOT DEFINED.	
APPENDIX H - INDIRECT TENSILE CREEP TEST RESULTSERROR! BOOKMARK NOT DEFINED.	

LIST OF TABLES

	<u>Page</u>
Table 1. Results of In-situ Air Voids Contents from Field Cores	26
Table 2. Average Mixture Properties	27
Table 3. Average Aggregate Gradations (w/o admixture)	27
Table 4. Summary of Consistency Tests: Asphalt Rubber (AR) and Virgin Asphalt Cements	35
Table 5. Summary of Viscosity-Temperature Regression Relationships	36
Table 6. Stress Level/ Temperature Combination Used for the Static Creep and Repeated Load Tests	67
Table 7. Master Summary of Static Creep Test Results.	68
Table 8. Master Summary of Repeated Load Test Results.....	73
Table 9. Summary of ϵ_p/ϵ_r Ratio for Repeated Load Test	74
Table 10. Dynamic Modulus Test Results for the AR-ACFC Mix Replicates - 70°F.....	87
Table 11. Tabular Summary of the Modular Ratio at 14°F and 10 Hz.....	106
Table 12. Tabular Summary of the Modular Ratio at 100°F and 10 Hz.....	107
Table 13. Tabular Summary of the Modular Ratio at 14°F and 10 Hz for 20-psi Confined Test Results	109
Table 14. Tabular Summary of the Modular Ratio at 100°F and 10 Hz for 20-psi Confined Test Results	110
Table 15. Input Parameters of ARAC and ACFC Mixtures for the Witczak Dynamic Modulus Predictive Equation.....	114
Table 16. Summary of Regression Coefficients for the Fatigue Relationships	136
Table 17 Summary of the Regression Coefficients for Generalized fatigue Equation.....	139
Table 18. Master Summary of the Indirect Tensile Strength Tests.	151
Table 19. Master Summary of Indirect Tensile Creep Test.	159

LIST OF FIGURES

	<u>Page</u>
Figure 1. Localization of the Buffalo Range TI-Canyon Diablo Project.....	19
Figure 2. Typical Section for the Buffalo Range TI-Canyon Diablo Project (6)	20
Figure 3. A View of the CoreLok Device (9)	28
Figure 4. Comparison of Air Voids by SSD and CoreLok Approach	30
Figure 5. Viscosity-Temperature Relationship for the PG 58-22 Binder, with and without Rubber Modification.....	37
Figure 6. Viscosity-Temperature Relationship of the AR PG 58-22 Binder at Different Aging Conditions	38
Figure 7. Viscosity-Temperature Relationship of the AR PG58-22 and PG76-16 Original Binders	40
Figure 8. Viscosity-Temperature Relationship of the AR PG58-22 and PG76-16 Binders After RTFO	41
Figure 9. Viscosity-Temperature Relationship of the AR PG58-28 and PG76-16 Binders After PAV100	42
Figure 10. Comparison of results for the Triaxial Shear Strength Test	48
Figure 11. Typical Test Results Between the Calculated Total Compliance and Time.	55
Figure 12. Total Axial Strain Vs. Time From an Actual Static Creep / Flow Time Test. ...	56
Figure 13. Typical Plot of the Rate of Change in Compliance Vs. Loading Time on a Log- Log Scale, Static Creep / Flow Time Test.	57
Figure 14. Typical Relationship Between Total Cumulative Plastic Strain and Number of Load Cycles.....	59
Figure 15. Regression Constants “a” and “b” When Plotted on a Log-Log Scale.	61
Figure 16. Permanent Deformation Parameters α and μ and the Flow Number.	61
Figure 17. Cumulative Permanent Strain Vs. Loading Cycles From a Repeated Load Test.	62
Figure 18. Regression Constants “a” and “b” from Log Permanent Strain – Log Number	63

Figure 19. Typical Plot of the Rate of Change in Permanent Strain Vs. Loading Cycles, Repeated Load Test.....	63
Figure 20. Vertical and Radial LVDTs' Set-Up for an Unconfined Test.....	65
Figure 21. Confined Test Set-Up	66
Figure 22. Test Set-Up Within Triaxial Cell with Mounted Radial LVDTs.	66
Figure 23. Static Creep Unconfined and Confined Test - Flow Time Results.	70
Figure 24. Static Creep Unconfined and Confined Test – Axial Strain at Flow Results....	72
Figure 25. Repeated Load Unconfined and Confined Test – Flow Number Results	75
Figure 26. Repeated Load Unconfined and Confined Test – Axial Strain Results	76
Figure 27. Comparison of ϵ_p/ϵ_r ratio for Repeated Load Test	77
Figure 28. (a) Typical Test Instrumentation – ARAC Test Specimen (b) Typical Confined	89
Figure 29. ARAC Gap Graded Mixture – Unconfined Test Results	90
Figure 30. ARAC Gap Graded Mixture – Confined Test Results – 10 psi	91
Figure 31. ARAC Gap Graded Mixture – Confined Test Results – 20 psi	92
Figure 32. ARAC Gap Graded Mixture – Confined Test Results – 30 psi	93
Figure 33. E* Master Curves for the ARAC Gap Graded Mixture	94
Figure 34. AR-ACFC Open Graded Mixture - Unconfined Test Results.....	96
Figure 35. AR-ACFC Open Graded Mixture – Confined Test Results - 10 psi.....	97
Figure 36. AR-ACFC Open Graded Mixture – Confined Test Results – 20 psi	98
Figure 37. AR-ACFC Open Graded Mixture - Confined Test Results – 30 psi	99
Figure 38. E* Master Curves for the AR-ACFC Open Graded Mixture	100
Figure 39. Crumb Rubber Sample: Effect of Loading Time and Temperature on the Measured Dynamic Modulus (Unconfined Test)	101
Figure 40. Unconfined Dynamic Modulus Master Curves for ARAC, AR-ACFC and Conventional PG 76-16 ADOT Mixture.....	102
Figure 41. Comparison of Measured Dynamic Modulus E* values at 10 Hz for the Asphalt Rubber and the PG 76-16 Mixtures at Selected Temperatures	103
Figure 42. Unconfined Dynamic Modulus Master Curves for ARAC, AR-ACFC and Conventional PG 64-22 ADOT Mixture.....	104

Figure 43. Comparison of Predicted and Measured Dynamic Modulus Values for the Asphalt Rubber Mixtures Using Current Version (1999) of the Witczak Predictive Equation – Arithmetic Space	115
Figure 44. Comparison of Predicted and Measured Dynamic Modulus Values for the Asphalt Rubber Mixture Using Current Version (199) of the Witczak Predictive Equation – Logarithmic Space	115
Figure 45. Predicted vs. Measured Dynamic Modulus Values for the AR Mixtures with New Equation Coefficients – Arithmetic Space	119
Figure 46. Predicted vs. Measured Dynamic Modulus Values for the AR Mixtures with New Equation Coefficients. – Logarithmic Space.....	119
Figure 47. Flexural Fatigue Apparatus	126
Figure 48. Loading Characteristics of the Flexural Fatigue Apparatus	127
Figure 49. Manufactured Mold for Beam Compaction	131
Figure 50. Top Loading Platen	132
Figure 51. Specimen sawing	133
Figure 52. Asphalt rubber GAP graded mix specimen	134
Figure 53. Controlled Strain Fatigue Relationships for the ARAC Mixture	136
Figure 54. Controlled Strain Fatigue Relationships for the AR-ACFC Mixture	137
Figure 55. Controlled Strain Fatigue Relationships for SRB, ARAC, and AR-ACFC mixes	139
Figure 56. Schematic Diagram of the Indirect Tensile Test	142
Figure 57. Illustration Showing the Determination of the Indirect Tensile Strength	145
Figure 58. Determination of Total Fracture Energy	145
Figure 59. Determination of Energy to Peak Load	146
Figure 60. Typical Strain-Time Response for HMA Mixtures for a Static Creep Test	148
Figure 61. Illustration of Creep Compliance versus Time from a Static Creep Test.....	149
Figure 62. Indirect Tensile Tests Set-Up.	150
Figure 63. Indirect Tensile Strength Test – Tensile Strength Results	152
Figure 64. Indirect Tensile Strength Test – Strain at Failure.....	153
Figure 65. Indirect Tensile Strength Test – Fracture Energy.....	154

Figure 66. Indirect Tensile Strength Test – Energy Until Failure	155
Figure 67. Indirect Tensile Strength Test – Summarized Results	156
Figure 68. Indirect Tensile Creep Test – Strain at $t = 1000s$	160
Figure 69. Indirect Tensile Creep Test – Creep Compliance at $t = 1000s$	161
Figure 70. Indirect Tensile Creep Test – Slope of the Compliance Curve	162
Figure 71. Indirect Tensile Creep Test – Intercept of the Compliance Curve	163
Figure 72. Indirect Tensile Creep Test – Summary of the Results	164

1. INTRODUCTION

1.1. Background

The Arizona Department of Transportation (ADOT) has used Asphalt Rubber (AR) as a modified binder since the early 1970's (1). The primary purpose for using AR is to reduce reflective cracking in hot mix asphalt (HMA) rehabilitation overlays (2,3). In addition to this AR has been used to reduce maintenance, provide a smooth riding surface, with good skid resistance. The AR mix has also performed well in snow and ice conditions providing a tough surface that stands up well to snow plows. Recently AR mixes have been recognized as a means of reducing the tire/ pavement interface noise (4).

The AR as tested in this study and used in Arizona is a mixture of approximately 20 percent ground tire rubber (crumb rubber) made from the recycling of used or defective tires. The ground tire rubber is added to hot paving grade asphalt at a high temperature and mixed with a high shear mixer. The mixing time and subsequent time of material interaction is generally 45 to 60 minutes (1). After the interaction the hot AR product has acquired unique elastomeric properties. The hot AR is then pumped into a conventional hot plant and mixed with aggregate and placed like a conventional HMA, except for a few significant differences.

These significant differences relate to the gradation of the mineral aggregate and the percent binder. The AR hot mix is generally either a gap graded or open graded mix. The gap graded mix contains about 7.5 percent AR binder and is placed generally as the final structural course 1.5 to 2 inches in thickness. The open graded contains generally 9

percent binder and is placed as the final wearing course from 0.5 to 1.0 inch thick. The mix designs for these two mixes are typically of a volumetric type and little has been published or researched about the binder or mix engineering properties in terms of the inputs needed for the new AASHTO 2002 Pavement Design Guide.

In the spring of 2001, ADOT in cooperation with FNF Construction Inc. entered into a research and testing plan with Arizona State University (ASU). The plan involves characterizing AR mixes in order to determine their properties for future use in the AASHTO 2002 Pavement Design Guide. An additional part of the long-term plan is to begin building a database to support the new 2002 Pavement Design Guide. This research report represents the findings from this first project. The plan is to characterize AR mixes from several projects in order to represent different grades of AR binder, different aggregates and different climates representative of Arizona.

This first project, named Buffalo Range TI-Canyon Diablo (IM-040-D(1)P, Tracs # H4883) is located on Interstate 40 at Mile Posts 224.7 to 229.9, close to Winslow Arizona as shown in Figure 1 (6). The project elevation is approximately 5,000 feet and the region is considered a dry freeze zone according to SHRP (7). Air temperatures of over 100°F occur in the summer and temperatures below -20 degrees F occur in the winter. The Interstate truck traffic is quite heavy and averages 2.2 million ESAL's per year. The pavement was overlaid in 1988 with 4.5 inches of conventional HMA. By 2001 the pavement had 3 percent cracking and a 0.20 inches of rutting (6). However, these values are somewhat misleading since extensive patching maintenance averaging \$4,000 per mile

were applied in 1998. This maintenance activity masked the high degree of fatigue cracking and rutting. The AR overlay project was constructed by FNF Construction Inc. The project consisted of removing by milling off 2.5 inches of the old cracked pavement full width and replacing it with 2 inches of the AR gap graded mix followed by 0.5 inch of AR open graded mix. A typical section for this project is shown in Figure 2. This is a relatively routine type of rehabilitation of older cracked pavements in Arizona. The construction took place in June of 2000. A change order was entered into between ADOT and FNF wherein FNF would sub-contract with ASU to provide special testing of the two AR mixes.

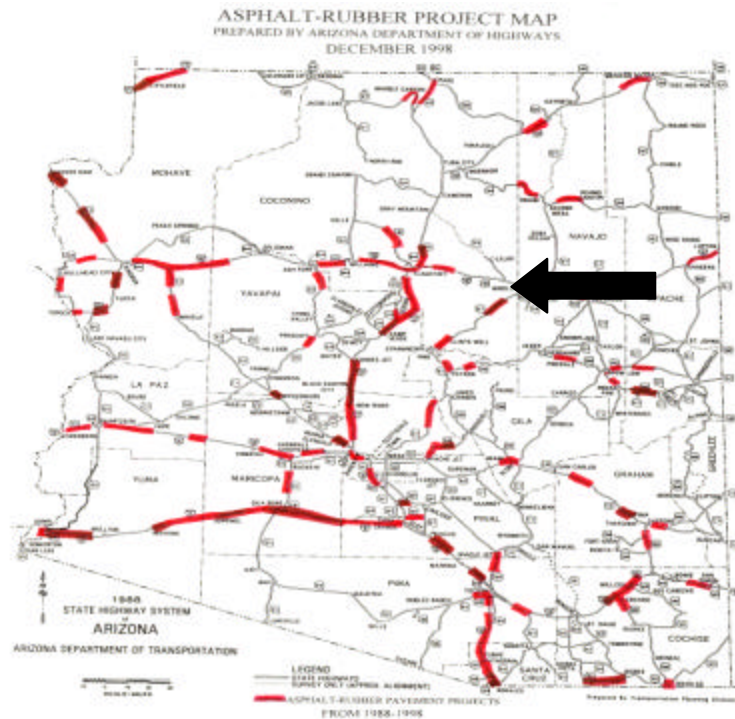
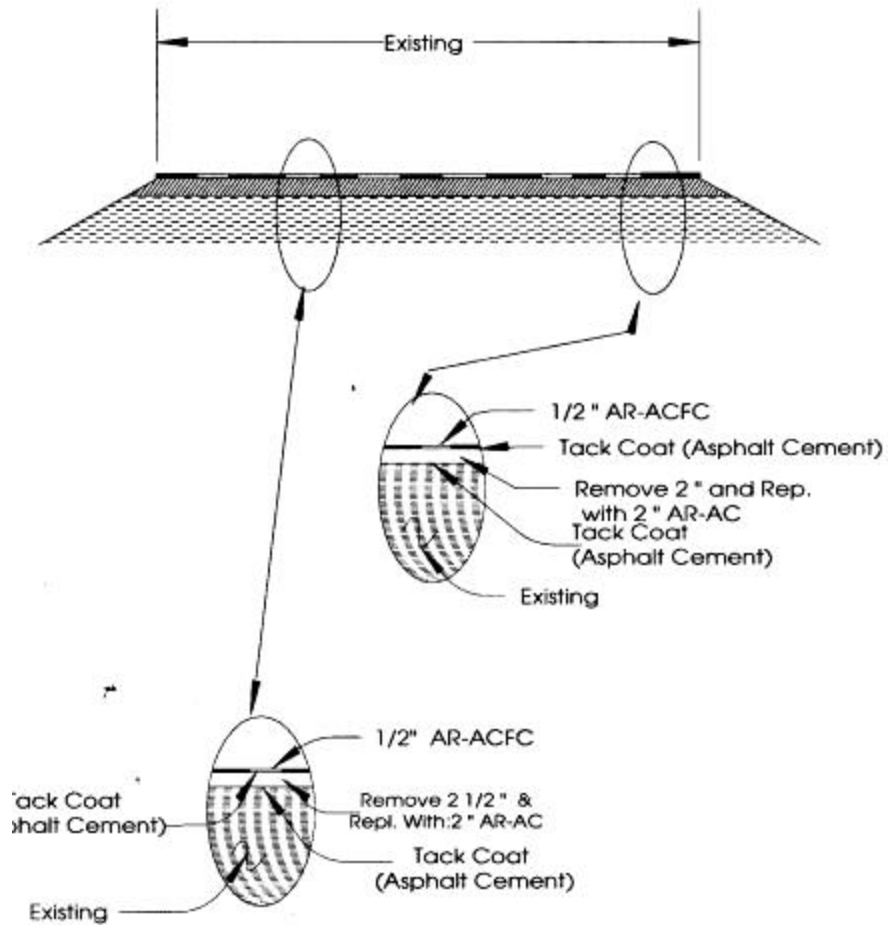


Figure 1. Localization of the Buffalo Range TI-Canyon Diablo Project

**TYPICAL SECTION
BUFFALO RANGE TI - CANYON DIABLO
040 CN 224 H488301C (IM 040-D-(1)P**



I 40 EB & WB MP 224.7 - 229.9

Figure 2. Typical Section for the Buffalo Range TI-Canyon Diablo Project (6)

1.2. ASU Research Program

In the last few years, the Department of Civil and Environmental Engineering at Arizona State University has been involved with several major asphalt mixtures characterization studies. These studies include the nationally recognized National Cooperative Highway Research Program (NCHRP) 9-19 project, under the leadership of Professor Matthew Witczak. The project deals with the development of Simple Performance Tests (SPT) for permanent deformation and cracking potential evaluation of asphalt mixtures. Furthermore, in July 1999, a long-range asphalt pavement research program was started with ADOT. The research program has the ultimate goal in implementing a methodology for Performance Related Specifications for asphalt pavements, and developing typical design input parameters for local conditions. Both of the above studies incorporated several mixture types; however, none of them included AR mixes, which are becoming widely used in the State of Arizona.

1.3. Study Objective

The objectives of this AR study are to conduct a laboratory experimental program to obtain typical engineering material properties for asphalt rubber mixtures used in Arizona; and to compare the performance of these AR mixtures to other conventional asphalt mixtures that are being tested at ASU. The testing of the AR open graded is the first of its kind to date and created many testing challenges.

1.4. Scope of the Work

Approximately 1000 pounds of samples from each of the two mixes were taken in five gallon buckets from eastbound direction during construction by FNF Construction, Inc. In addition to these, cores of the two AR compacted mixes were taken to determine the in-place air voids. The air voids from the cores are shown in Table 1. The reference air voids for the AR gap graded mix was selected to be 11% and for the AR open graded mix 18%. Plugs and beams were compacted to these air void values as close as practical.

Data obtained from tests of these mixtures were summarized in spreadsheets. The spreadsheet contained information such as binder information, aggregates, volumetric mix properties, and the results of the advanced dynamic material characterization tests. These tests include:

- Triaxial shear strength of the mixtures.
- Static creep and repeated load for permanent deformation evaluation.
- Dynamic (complex) modulus for stiffness evaluation.
- Flexural beam test for fatigue cracking evaluation.
- Indirect tensile tests for thermal cracking evaluation.

The test results were used, when possible, to establish a relative ranking of the mixtures, among others being tested at ASU, according to their expected rutting or cracking potential. The binder tests were conducted to develop information that will complement other mix material properties such as fatigue cracking and permanent deformation.

1.5. Specimens Preparation

The AR mix was transported to ASU laboratories, where it was re-heated and compacted with a “Servopac Gyratory Compactor” into a 6-in diameter gyratory mold. One 4-inch diameter sample was cored from each gyratory plug. The sample ends were sawed to arrive at typical test specimens of 4-inch in diameter and 6-inch in height. The plugs were prepared to be tested to obtain Simple Performance Test (SPT) permanent deformation (rutting) values consistent with the procedures developed as part of NCHRP 9-19. The beams were prepared by the method developed in SHRP and tested according to the test protocol AASHTO TP8-94 (23), and SHRP M-009 (24). The beams were prepared to determine the expected fatigue life of the two AR mixes. The disc specimens were prepared according to the “Test Method for Indirect Tensile Creep Testing of Asphalt Mixtures for Thermal Cracking” reported in NCHRP Report 465 (13).

Air voids, thickness and bulk specific gravities were measured for each test specimen and the samples were stored in plastic bags in preparation for the testing program.

1.6. Number of Tests

1.6.1. Test Program for ARAC – Asphalt Rubber GAP Graded Mix

Triaxial Shear Strength

3 Confinement Levels x 1 Temperature x 2 Replicates = 6 Tests

Static Creep / Flow Time

2 Confinement Levels x 1 Temperature (100°F) x 3 Replicates = 6 Tests

2 Confinement Levels x 1 Temperature (130°F) x 2 Replicates = 4 Tests

Unconfined Test of Mixture with 7% air voids @ Temperature 100°F = 2 Tests

Repeated Load / Flow Number

2 Confinement Levels x 1 Temperature (100°F) x 3 Replicates = 6 Tests

2 Confinement Levels x 1 Temperature (130°F) x 2 Replicates = 4 Tests

Unconfined Test of Mixture with 7% air voids @ Temperature 100°F = 3 Tests

Dynamic Complex Modulus

2 Confinement Levels x 5 Temperature x 6 Frequencies x 3 Replicates = 180 Tests

Indirect Tensile Creep

3 Temperature x 3 Replicates = 9 Tests

Indirect Tensile Strength

3 Temperature x 3 Replicates = 9 Tests

Beam Fatigue Test

3 Temperature x 6 Replicates = 18 Tests

1.6.2. Test Program for AR-ACFC – Asphalt Rubber OPEN Graded Mix

Triaxial Shear Strength

3 Confinement Levels x 1 Temperature x 2 Replicates = 6 Tests

Static Creep / Flow Time

2 Confinement Levels x 2 Temperature x 3 Replicates = 12 Tests

Repeated Load / Flow Number

2 Confinement Levels x 2 Temperature x 3 Replicates = 12 Tests

Dynamic Complex Modulus

4 Confinement Levels x 5 Temperature x 6 Frequencies x 3 Replicates = 360 Tests

Indirect Tensile Creep

3 Temperature x 3 Replicates = 9 Tests

Indirect Tensile Strength

3 Temperature x 3 Replicates = 9 Tests

Beam Fatigue Test

1 Temperature x 6 Replicates = 6 Tests

1.7. Report Organization

This report has been divided into eight chapters. Chapter 1 includes the introduction objectives, and scope of work. Chapter 2 presents data on the mixture characteristics. Chapters 3 summarize the binder characterization tests. Chapter 4 contains the test results for the triaxial shear strength test. Chapter 5 presents the test results for the permanent deformation tests; whereas Chapter 6 includes the stiffness test results. Fatigue and thermal cracking tests are included in Chapter 7. Chapter 8 presents the conclusions and recommendations of the study. All supporting test data and additional graphical plots are included in the appendices.

2. MIXTURE CHARACTERISTICS

2.1. Asphalt

The asphalt binder type CRA-2 manufactured by FNF Construction was used to produce AR-ACFC and ARAC mixtures. This binder type is a homogenous asphalt-rubber system created by blending the asphalt cement and the crumb rubber and then reacted at elevated temperatures for a minimum of 45 minutes. The asphalt cement PG58-22 manufactured by Copperstate and the crumb rubber produced by Recovery Technologies were used. The binder characterization is presented in Chapter 3.

2.2. Mixture Properties

The hot mix asphalt mixtures were obtained as loose mix samples taken behind the asphalt paver during construction. Therefore, the air void levels and binder contents in the laboratory-testing program simulated the properties of the field mixes as best as possible. The in-situ air voids contents were obtained from cores taken from each pavement section and are reported in Table 1. The original mix designs were done using the Marshall mix design method. Table 2 shows the target binder contents, air voids contents, and other volumetric properties of the mixtures. Table 3 shows the target aggregate gradations for the each mixture.

Table 1. Results of In-situ Air Voids Contents from Field Cores

Mix Type	SSD Air Voids (%)	CoreLok Air Voids (%)
ARAC	11.5	-
AR-ACFC	-	21.39

Table 2. Average Mixture Properties

Mixture	Asphalt Cement	Rubber %	AC %	Va %	G _{mm}		
					ADOT Rice Test	ASU Rice Test	ASU CoreLok
ARAC	PG 58-22	22.7	6.8	11.0	2.601	2.593	-
AR-ACFC	PG 58-22	22.7	8.8	18.0	2.549	2.528	2.556

Table 3. Average Aggregate Gradations (w/o admixture)

Sieve Size	ARAC	AR-ACFC
1 ½	100	100
1	100	100
¾	100	100
½	82	100
3/8	67	100
¼	48	63
#4	38	37
#8	22	8
#10	18	7
#16	12	6
#30	8	4
#40	6	4
#50	5	3
#100	2	1
#200	1.8	1.4

2.3. Air Voids Measurement Using the CoreLok Device

Because of the high air void content of the two mixes, and especially the open graded mixture, it was necessary to use the CoreLok device to accurately determine the in-place air voids of the mixes as well as the air voids for laboratory specimens.

The CoreLok Air Voids determination procedure involves placing a dry specimen into a plastic, puncture resistant bag. The sample is then placed into the CoreLok chamber as shown in Figure 3. Closing the chamber door automatically starts the vacuum process. In approximately 2 minutes, the sample is vacuumed to 29.7 in Hg. The specimen is now sealed within the bag in an evacuated state. The sample is then completely immersed in water and weighted. Knowing the weight in air of the bag, the sample, and the combined weight of the bag and sample under water allows for calculation of the air voids content. The entire process takes less than five minutes with very high degree of repeatability.



Figure 3. A View of the CoreLok Device (9)

Comparison analysis of air voids determined by the Saturated Surface Dry (SSD) and CoreLok methods were conducted during this research project. As shown in Figure 4, the results of air voids obtained from the CoreLok method were higher than these from the SSD for both mixtures. The general trend is that the higher air voids the bigger the difference between both test methods. The reason for this difference is that when using the SSD method there is unavoidable leak of water from the specimen within the time between weighting the sample under water and in air at saturated surface dry condition. This leak is larger when higher air voids are present in the sample.

It is also noted that the variability of air voids measured between these two methods for gap graded mixture was 0.24%. For the open graded mixture the difference was higher, 3.46%. In both cases, the tested specimens were laboratory, gyratory compacted specimens, cored to 100mm in diameter and 150mm in height.

The results also indicated that texture of sample affected the difference between methods. Bigger difference 4.35% for open graded mix was observed for uncured plugs, which texture was rougher and contained more voids in the surface.

Comparison Of Air Voids By SSD and CoreLok

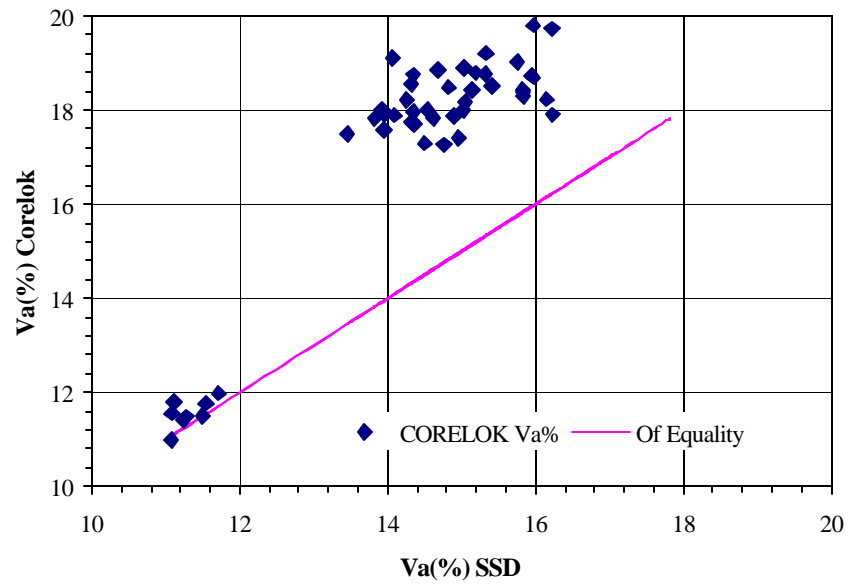


Figure 4. Comparison of Air Voids by SSD and CoreLok Approach

3. BINDER CHARACTERIZATION

3.1. Introduction

The characterization of the AR binder properties will be used as direct input to estimate the overall Complex Modulus-Reduced Time Master Curve of the specific asphalt mixture used in the pavement design process. One of the key elements for the successful implementation of the new AASHTO 2002 Pavement Design Guide is to have a database of material characterization and properties of all typical materials used within the agency. In addition, the research team suspected that the results of the rubber modified asphalt binder characterization using conventional tests might reveal some of this material's unique temperature susceptibility properties.

Conventional asphalt binder tests (penetration and viscosity) were conducted to develop information that will complement other mixture material properties such as fatigue cracking and permanent deformation. It was anticipated that since Asphalt Rubber (AR) is a mixture of approximately 20% ground tire rubber and 80% virgin asphalt binder, it might not be a good candidate for such testing. Nevertheless, conventional consistency tests were conducted on the AR asphalt binder to determine whether there were any unique characteristics or difficulties in handling the material.

Consistency tests across a wide range of temperatures were conducted according to the accepted American Association of State Highway and Transportation Officials (AASHTO), and/or American Society for Testing and Materials (ASTM) practices. The remainder of this section will go into greater detail with regard to the test methods,

challenges and the surprising good degree of correlations found from the measurements.

3.2. Binder Consistency Tests – Viscosity Temperature Relationship

Witczak et al experience with applying conventional / standard binder consistency tests to modified asphalt cements had shown that they can be rational and can be used as a general guide (10). Notwithstanding the concerns of the asphalt cement modifier manufacturers recommendation that these test not be used for mixing and compaction temperatures. In this study, the consistency tests are being used for descriptive comparative purposes and not for specification control.

Most refined asphalt cements, with the exception of heavily air blown or high wax content crudes, exhibit a linear relationship when plotted on a log-log viscosity (centipoises) versus log temperature (in degree Rankine: $R = F + 459.7^{\circ} F$) scale (ASTM D 2493). In this study, centipoises was selected for this type of plots because the test results are reported in these units. The approach uses only viscosity units (centipoise) to define the viscosity-temperature relationship. In order to make use of all consistency tests variables over a wide range of temperatures, it was necessary to convert all penetration (pen) and softening point (T_{RB}) measurements into viscosity units. Penetration data was converted to viscosity units by the following model developed at the University of Maryland as a part of a Strategic Highway Research Program (SHRP) study (11). It should be noted that the following equation is applicable over a very wide range of penetration from 3 to 300.

$$\log \eta = 10.5012 - 2.2601 \times \log(\text{pen}) + 0.00389 \times \log(\text{pen})^2 \quad (3.1)$$

Note that the viscosity obtained from the above equation is in poise. The second consistency variable point defined by the softening point (T_{RB}) is converted to viscosity units by the approach suggested by Shell Oil researchers. It states that all asphalts at their softening point (T_{RB}), will yield a penetration of approximately 800 and a viscosity of 13,000 poises. The third group of viscosity values at high temperature was obtained by use of the Brookfield Viscometer.

Using the above three methods, all penetration and softening point results can be shown or converted to viscosity units, which along with the Brookfield test results can then be used as direct viscosity measurements to obtain a viscosity (η) - temperature (T_R) relationship from the following regression equation (12):

$$\log \log \eta(\text{centipoise}) = A_i + VTS_i \times \log T_R \quad (3.2)$$

In Equation (3.2), A_i and VTS_i represents regression coefficients, which describe the unique consistency-temperature relationship of any blend. The VTS term in this equation represents the slope of the regression equation, which is also interpreted as the Viscosity Temperature Susceptibility parameter. For example, a larger (negative) slope value defines a higher temperature susceptibility of the binder.

3.3. Testing Program

The crumb rubber modified asphalt cement in this study used PG 58-22 base asphalt cement with approximately 20% crumb rubber. The samples obtained were from the

interacted final product that had been blended in the field at the hot mix plant site. The blend was achieved at 325°F for a minimum of 45 minutes.

In the laboratory, the research team used the standard asphalt cement consistency tests for each of the modified and virgin binders. The tests were run at Original conditions as well as Rolling Thin Film Oven (RTFO) and Pressure Aging Vessel (PAV) aged conditions. Additional tests were also available in the ASU database on a variety of virgin binders that are being used by the Arizona Department of Transportation.

3.4. Results and Analysis

Table 4 shows the average test results for all tests; Appendix A contains details of the tests conducted. In general, the crumb rubber modified asphalt exhibited lower penetration values than the virgin binder, especially at the higher temperature. This was also true for the RTFO and PAV aging conditions. For the Brookfield viscosity tests, the test temperature range varied as shown (200 to 350°F). The results show that, generally, the viscosity values of the crumb rubber modified asphalt cement were higher than that of the virgin binder for the test temperature range between 200 and 350°F. Higher viscosity values are desirable for better resistance to permanent deformation.

Table 4. Summary of Consistency Tests: Asphalt Rubber (AR) and Virgin Asphalt Cements

Test	Temp (°C)	Temp (°F)	Original			RTFO			PAV100		
			Virgin PG 58-22	AR PG 58-22	Virgin PG 76-16	Virgin PG 58-22	AR PG 58-22	Virgin PG 76-16	Virgin PG 58-22	AR PG 58-22	Virgin PG 76-16
Penetration (0.1 mm)	15	59	34.2	28.7	10.3	21.8	11.7	7.5	10.2	7.3	5.7
	25	77	112.2	46.7	24.7	66.2	30.3	18.2	30.0	14.3	13.7
Rotational Viscosity (cP)	60	140	82,000	-	1,048,000	175,750	-	-	-	-	-
	70	158	-	-	-	-	-	-	285,933	-	4,723,200
	80	176	9,413	-	69,000	17,142	-	15,800	79,000	-	986,368
	100	212	2,250	47,000	9,283	4,588	-	17,150	10,854	-	76,117
	121	250	588	10,500	2,193	1,013	44,250	3,400	2,098	235,000	7,868
	135	275	288	5,600	827	450	18,833	1,250	923	78,000	2,857
	150	302	-	-	-	-	-	-	-	29000	-
	177	350	63	1700	121	75	4333	150	103	6900	381
Softening Point (°C)	-	-	47	59.5	63.3	51.3	79.5	63.8	58	99.75	76

The softening point test results showed similar trends. The AR had higher softening point than either the PG 58-22 or PG 76-16 at RTFO and PAV aging conditions.

Regression analysis were conducted on the AR and virgin binders used in this study using the consistency data shown in Table 4. The results of A_i and $VT S_i$ are shown in Table 5. In addition, the test results for an ADOT PG 76-16 virgin asphalt cement are also shown in this table. Using these regression results, graphical plots were generated to evaluate the viscosity-temperature relationship for both binders. This type of analysis was considered as the most logical way to interpret the effect of rubber modification on the asphalt cement binder. Detailed analysis of the test results are also shown in Appendix A.

Table 5. Summary of Viscosity-Temperature Regression Relationships

Binder	Aging	Regression Coefficients		
		A	VT S	R ²
Virgin PG 58-22	Original	10.8750	-3.6588	0.9965
	RTFO	10.7630	-3.6076	0.9973
	PAV 100	10.7320	-3.5827	0.9971
AR PG 58-22	Original	7.6903	-2.4795	0.9890
	RTFO	7.3611	-2.3444	0.9963
	PAV 100	7.1468	-2.2534	0.9984
Virgin PG 76-16	Original	10.8690	-3.6295	0.9986
	RTFO	10.6420	-3.5420	0.9989
	PAV 100	10.0130	-3.3005	0.9950

Figure 5 shows a comparison of the viscosity-temperature relationship for the PG 58-22 binder with and without rubber modification. It can be clearly shown that the crumb rubber modified binder has much lower slope with increasing temperature, a behavior highly desirable for resistance to permanent deformation. In addition, it clearly appears that these conventional binder tests are adequate in describing the viscosity-temperature susceptibility of the crumb rubber modified binder, and as indicated by the high degree of the coefficient of determination $R^2 = 0.989$.

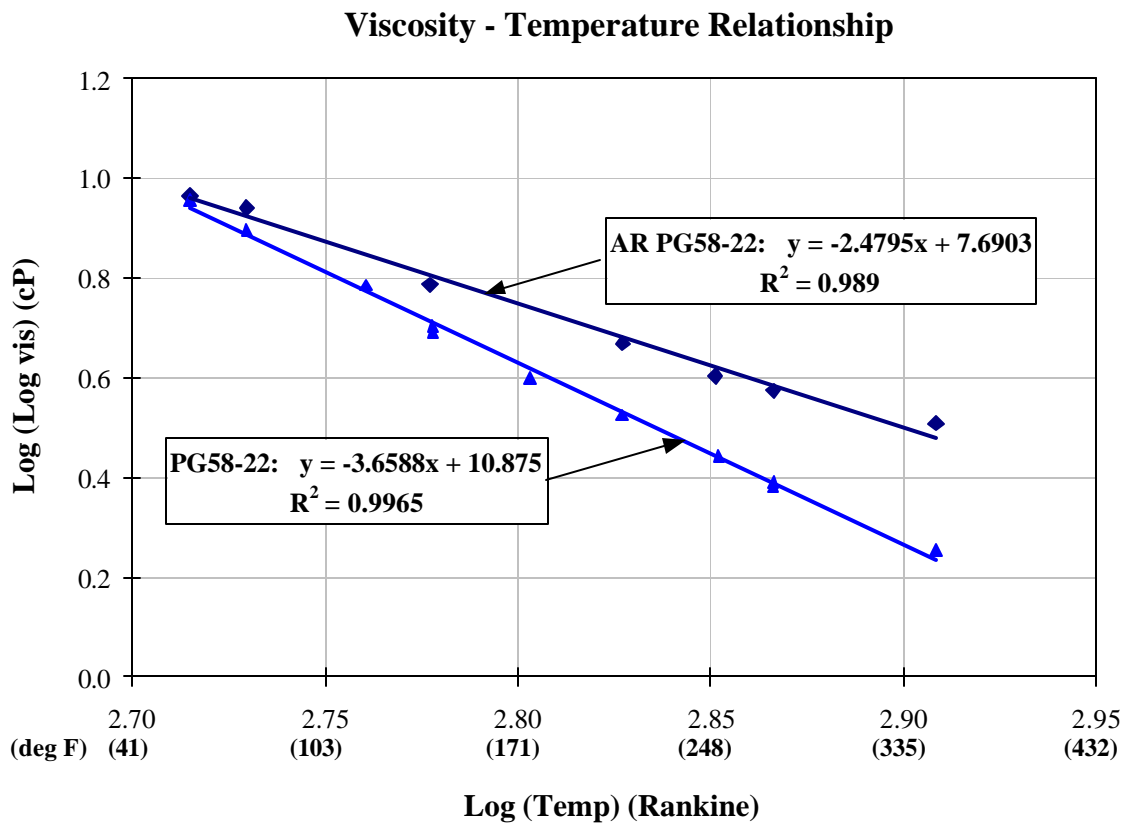


Figure 5. Viscosity-Temperature Relationship for the PG 58-22 Binder, with and without Rubber Modification

Figure 6 shows a comparison of the viscosity-temperature relationships for the AR PG 58-22 original binder and at the two aging conditions. In Figure 6 it can be clearly shown that despite the effect of different aging on the crumb rubber modified binder, the conventional binder tests are still adequate in describing the viscosity-temperature susceptibility of the crumb rubber modified binder. An aging index comparison between the virgin and crumb

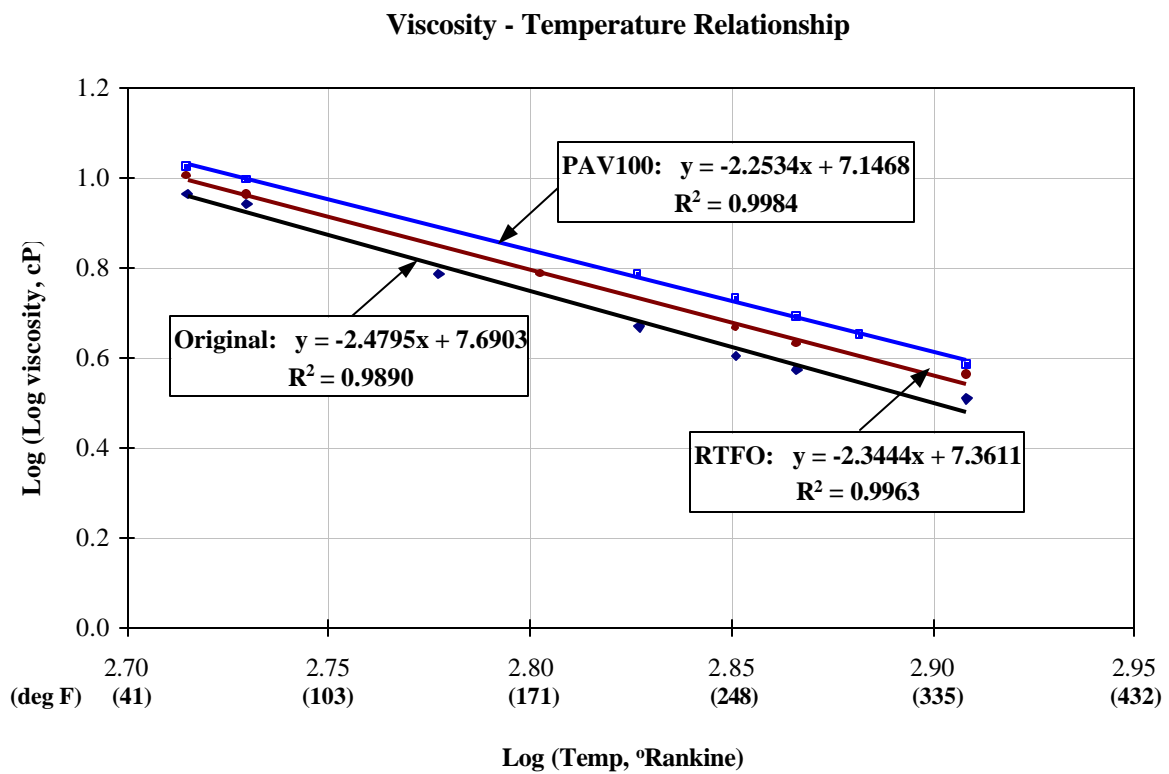


Figure 6. Viscosity-Temperature Relationship of the AR PG 58-22 Binder at Different Aging Conditions

rubber modified binder was not attempted simply because a direct comparison should not be made. The amount of material aged, which in one way correspond to a film thickness of an aggregate in the mix, were kept the same for all tests and at the different aging conditions. If a true comparison needs to be made, the amount of binder (e.g. in the PAV pan) should be increased to represent an increased film thickness on the aggregate in the mix. The AR mixtures have much higher binder content than conventional mixtures, and one would expect the film thickness of the binder on the aggregate to be much larger as well. Therefore, it is expected that if the amount of material / binder layer thickness in a PAV pan was increased, the aging characteristic measured would be different than those for standard tests.

Figure 7 through 9 compare the viscosity-temperature relationship for the crumb rubber modified binder (AR PG 58-22) and a conventional ADOT PG 76-16 binder at the different aging conditions. In all three plots, the relationship developed relate to the observed field performance behavior of the AR mixtures. The plots indicate that the AR mixes would provide good resistance to permanent deformation (rutting) at high temperatures. At the same time, the AR mixes would be less susceptible to low temperature cracking than the PG 76-16 mix. Note that the regression lines reverse in order at the lower temperature side of the plot. The above results confirm some of the unique temperature susceptibility properties of the crumb rubber modified binders/ mixes.

Viscosity - Temperature Relationship (Original Binder)

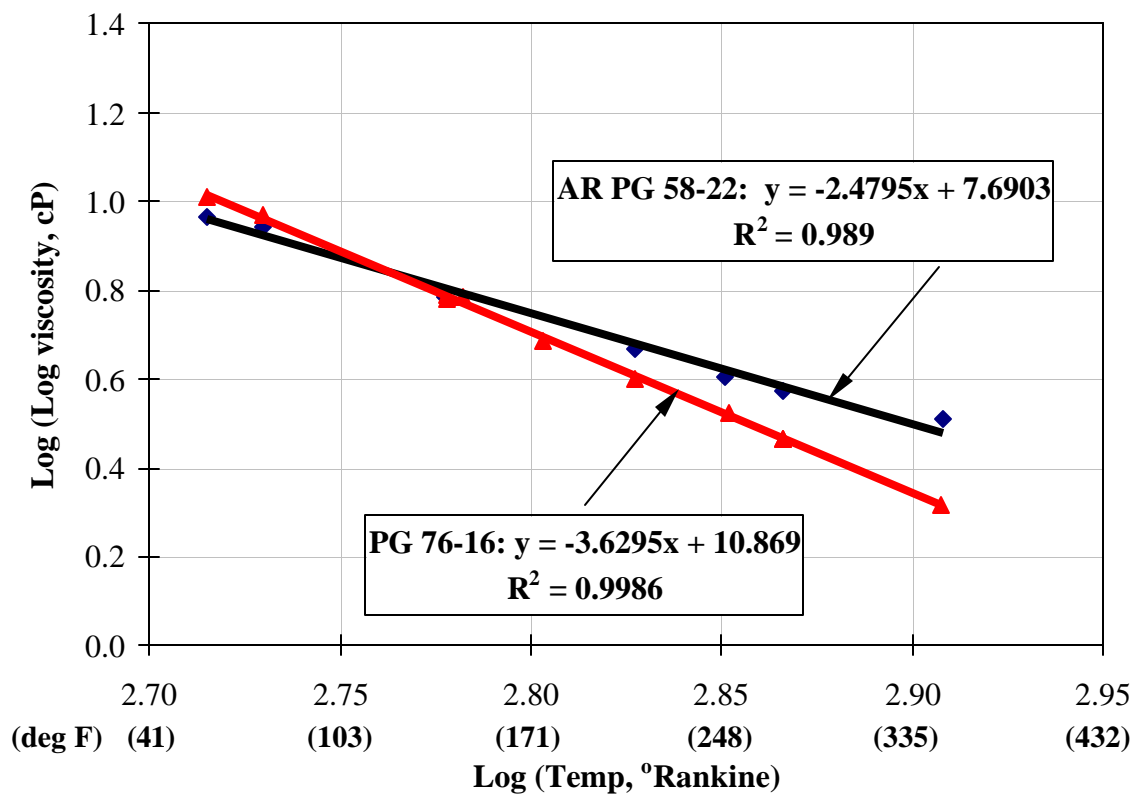


Figure 7. Viscosity-Temperature Relationship of the AR PG58-22 and PG76-16 Original Binders

Viscosity - Temperature Relationship (RTFO)

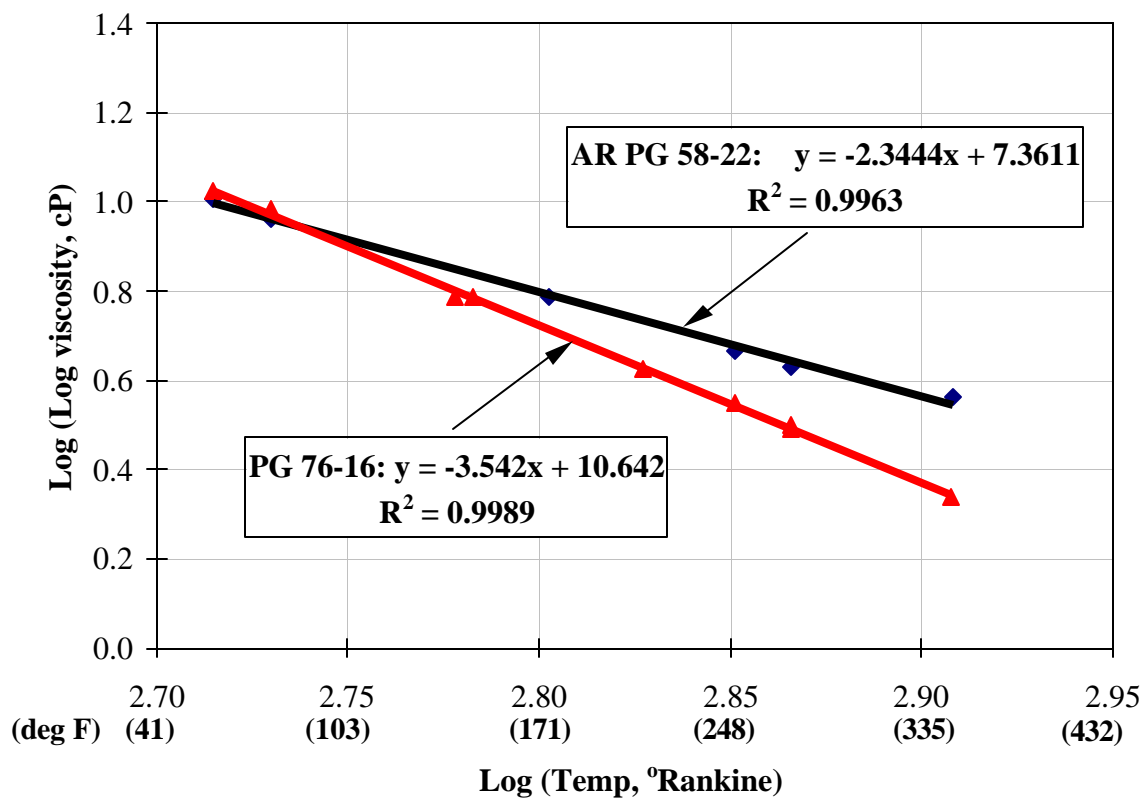


Figure 8. Viscosity-Temperature Relationship of the AR PG58-22 and PG76-16 Binders After RTFO

Viscosity - Temperature Relationship (PAV100)

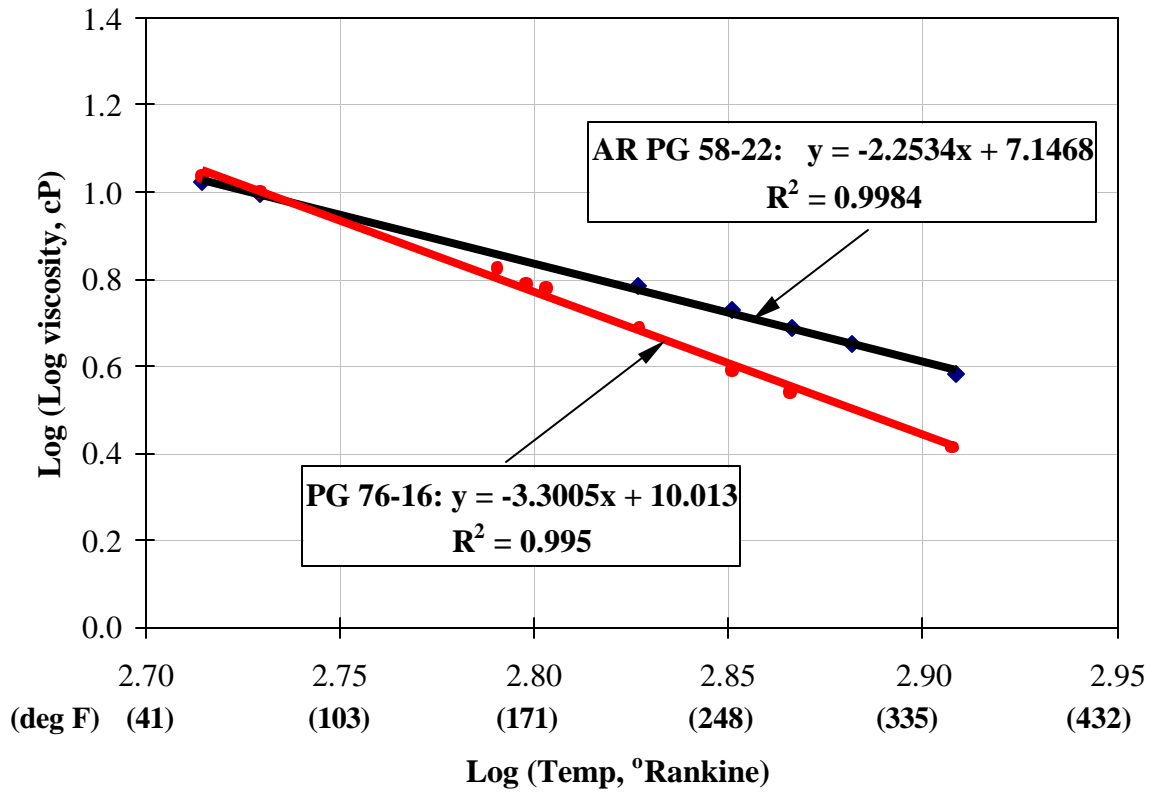


Figure 9. Viscosity-Temperature Relationship of the AR PG58-28 and PG76-16 Binders After PAV100

3.5. Asphalt Rubber Binder Handling Experience.

The following remarks were reported by the laboratory technician handling the asphalt rubber binder, and also conducting the tests.

- Extra-time to preheat the material was needed (20 to 30 minutes) to obtain a fluidity of the binder that will ease its handling, mixing and pouring.
- More AR binder material was needed for test preparation than for a conventional binder. This was necessary because the recovery of all binder from the different tins and pans was harder than for conventional binders.
- More AR binder materials also necessitated doing more runs of the RTFO and PAV aging conditioning. At least twice the amount of binder material was needed.
- In the RTFO conditioning, the standard amount of materials (35 grams per bottle) seemed to be excessive as the binder spilled out of the bottle. About 10 grams per bottle was typically lost in the process.

3.6. Summary for the Binder Characterization

The overall effort in this study was aimed at characterizing the properties of virgin and crumb rubber modified (CRM) asphalt cements for their use in the new AASHTO 2002 Pavement Design Guide. Conventional asphalt binder tests were conducted to develop information that was anticipated to complement mixture material properties such as fatigue cracking and permanent deformation. The conventional consistency tests were conducted on the CRM binder to determine whether there were any unique characteristics

or difficulties in handling the material.

Consistency tests across a wide range of temperatures were conducted according to the accepted American Society for Testing and Materials (ASTM) practices. Based on the test results and analysis conducted in this study, the following conclusion are made:

- The conventional asphalt cement tests were shown to be adequate in describing the viscosity-temperature susceptibility of crumb rubber modified asphalt cement.
- This favorable viscosity-temperature susceptibility relationship appears to relate to observed field performance behavior. Such behavior is characterized as less low temperature cracking and good resistance to permanent deformation at high temperatures.
- The A and VTS parameters developed for the crumb rubber modified binder provide the very necessary input to predict mixture stiffness (E^*) that is the building block used in the new 2002 Design Guide. Furthermore, This building block is used to derive virtually all other stress and strain calculations needed for new and existing pavement rehabilitation analysis.

4. TRIAXIAL SHEAR STRENGTH TEST

4.1. Background for the Triaxial Shear Strength Test

The Triaxial Shear Strength Test has been recognized as the standard test for determining the strength of materials for over 50 years. The results from these tests provide a fundamental basis, which can be employed in analyzing the stability of asphalt mixtures. This is because the stresses acting on the laboratory specimen during the test truly simulate the state of stresses existing in the pavement provided certain specimen boundary and geometry conditions are met. In general, there has been reluctance to adopt this test as a routine test procedure because of the degree of difficulty in performing the test. However, with the improvement in testing equipment and computerized data acquisition systems, an increased interest in the use of the triaxial strength test has been extended to more than just a research tool.

The shear strength of an asphalt mixture is developed mainly from two sources:

- 1) the cementing action of the binder, which is commonly referred to as “cohesion” from Mohr plots;
- 2) strength developed by the aggregate matrix interlock from the applied loads, commonly referred to as “ ϕ ” or the angle of internal friction.

The major role and interaction of both of these terms varies substantially with rate of loading, temperature, and the volumetric properties of the mixture.

Triaxial tests are run at different confining pressures to obtain the Mohr-Coulomb failure

envelope. The Mohr-Coulomb failure envelope is defined as:

$$\tau_{ff} = c + \sigma_{ff} \tan \phi \quad (4.1)$$

where,

τ_{ff} = shear stress at failure on failure plane

σ_{ff} = normal stress at failure on failure plane

c = intercept parameter, cohesion

$\tan \phi$ = slope of the failure envelope (ϕ is the angle of internal friction)

Typical “c” values for conventional AC mixtures are in the range of 5 and 35 psi; whereas typical “ ϕ ” values range between 35 and 48°.

Typical triaxial tests require testing specimens at three or more levels of lateral confinement to accurately develop the failure envelope. Although each test may be run on a single specimen, replicate specimens are desired if higher reliability is required.

Specimen size and preparation are also important factors needed to be considered in the testing protocols. Normally, a sample with a height to diameter ratio of 2 is used in order to eliminate the effects of friction against the loading platens and interference of shear cones within the specimen. According to the modified sample preparation protocols used in NCHRP Report 465 (13) (sawed specimen ends and the use of thin lubricated membranes), a sample size of 100mm (4 inches) in diameter and 150mm (6 inches) in height was recommended. This size was judged sufficient in providing representative (reproducible) material properties provided the ends are parallel and well lubricated. More details on this aspect can be found in reference (14).

4.2. Test Conditions for the Triaxial Shear Strength Test

Three triaxial strength tests, one unconfined and two confined were conducted for each of the AR mixtures. In addition results from previously tested standard ADOT Salt River Base (SRB) mixture with binder PG64-22 were reported in order to compare its properties to those obtained for the AR. These tests provided the standard cohesion “c” and the angle of internal friction “ ϕ ” parameters for each AR mixture. The test was carried out on cylindrical specimens, 100mm (4 inches) in diameter and 150mm (6 inches) in height, prepared as described previously. The tests were conducted at 100°F. In addition to the unconfined test, two additional confining pressures were used: 138, and 276 kPa (20 and 40 psi). The specimens were loaded axially to failure, at the selected constant confining pressure, and at a strain rate of 0.05 in/in/min (1.27mm/mm/min). An IPC Universal Testing Machine (UTM 100) electro- hydraulic system was used to load the specimens. The machine was equipped to apply up to 100 psi (690 kPa) confining pressure and 22,000 lbs (100 KN) maximum vertical load. The load was measured through the load cell, whereas, the deformations were measured through the actuator Linear Variable Differential Transducer (LVDT). Thin and fully lubricated membranes at the sample ends were used to reduce end friction. All tests were conducted within an environmentally controlled chamber throughout the testing sequence, controlled within $\pm 1^\circ\text{F}$ throughout the entire test.

4.3. Test Results and Analysis for the Triaxial Shear Strength

The results for the triaxial strength tests for all three mixtures are summarized and reported in Appendix B. The maximum deviator stress, normal stress and percent strain at failure were summarized for each test condition. Shear strength parameters, cohesion “c”, friction angle “ ϕ ”, and shear strength equations using Mohr-Coulomb failure envelopes were developed for each mixture and are included in Tables B-1, B-2, and B-3 of Appendix B.

Figure 10 shows plots of the Mohr-Coulomb failure envelope represented by the cohesion “c” and angle of internal friction “ ϕ ” for three tested mixtures.

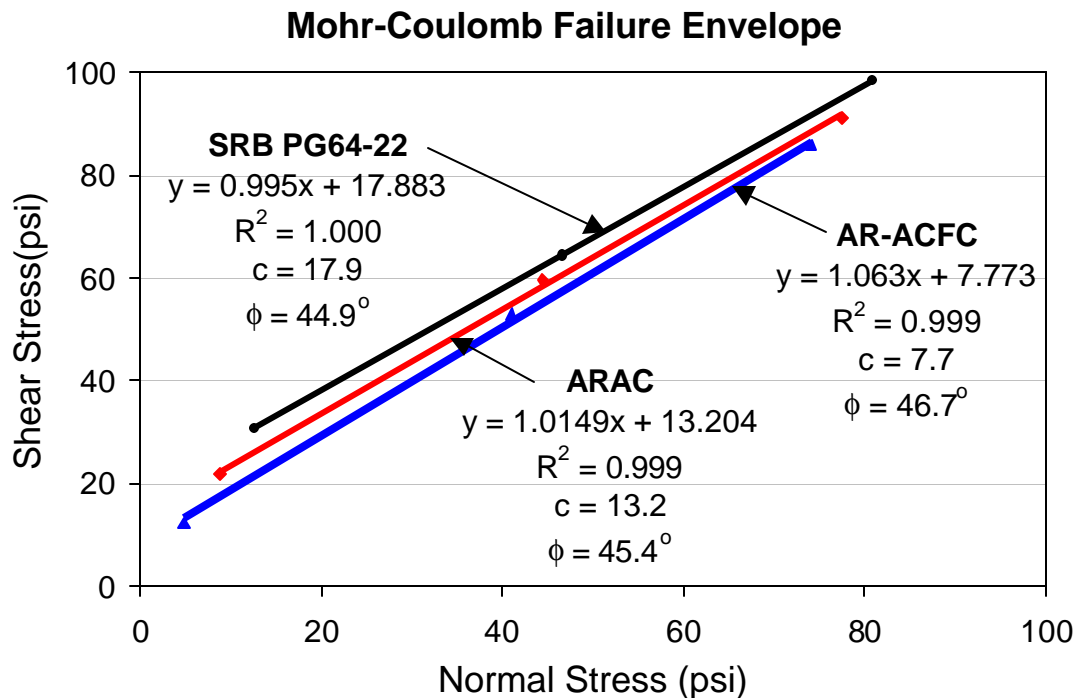


Figure 10. Comparison of results for the Triaxial Shear Strength Test

The parameters “ c ” and “ ϕ ” are the strength indicators of the mix. The larger the “ c ” value, the larger the mix resistance to shearing stresses. In addition, the larger the “ ϕ ” value, the larger the capacity of the asphalt mixture to develop strength from the applied loads, and hence the smaller the potential for permanent deformation.

When all three mixes were compared the highest difference was observed for the cohesion parameter. The SRB PG64-22 mix has 133% higher cohesion than AR-ACFC, and 35% higher cohesion than ARAC. In the same time both asphalt rubber mixes have higher angle of internal friction compared to the standard ADOT mixture, but the difference between AR-ACFC and SRB PG64-22 is only 1.8 degree which is about 4% and the difference between ARAC and SRB PG64-22 is 0.5 degree which is about 1%. In addition, it can be observed that the difference in shear strength between the mixtures decreases as the level of confinement increases. This is especially true for the AR-ACFC mixture.

4.4. Summary for the Triaxial Shear Strength Test

Based on the test results and analysis the following conclusions can be made:

- The results of the cohesion parameter showed that the asphalt rubber open graded mix (AR-ACFC) has much lower resistance to shearing stresses than the other two mixes. This observation must be supported by information that the AR-ACFC is utilized as a mixture for non-structural layer. For this Buffalo Range project it was placed in 0.5 in lift, and for that type of application, the

shearing stress is not so critical. At the same time, the AR-ACFC mix has the highest value of angle of internal friction, which indicates that this material has the largest capacity to develop strength from the applied loads, and hence the smallest the potential for permanent deformation.

- Comparing the results for the SRB PG64-22 and ARAC mixtures it can be observed that although the ARAC mix has smaller cohesion than the SRB PG64-22, it has also larger angle of internal friction, and smaller potential for permanent deformation.
- Analyzing the failure envelope trendlines shown in Figure 10, it can be noticed that at higher confinements level, there are smaller difference in shear stress between all three mixtures. Theoretically, a confinement level exists at which for the same normal stress, there is equal shear stress for all three mixtures.

5. PERMANENT DEFORMATION TESTS

5.1. Background for the Static Creep /Flow Time Tests

In a static creep / flow time test, a total strain – time relationship for a mixture is obtained experimentally in the lab (15). The static creep is a fundamental test because the rate of cumulative strain and the time at which tertiary deformation occurs for an asphalt mixture was found to be dependent on the temperature, deviator and confining stresses applied, and mix quality (16). While the creep test has been used in the pavement community for many decades; the starting point of tertiary deformation, or flow time, concept also obtained from a creep test, had been evaluated for asphalt mixtures by Witczak et al at the University of Maryland (UMd) and later on at Arizona State University (15,17).

The static creep test, using either one cycle load/unload or cyclic loading is capable of providing much information concerning the material response characteristics. The interpretation of the strain/time response of a material undergoing a static creep test provides significant parameters, which describe the instantaneous elastic/plastic and viscoelastic/plastic components of the material response.

5.1.1. Modulus/Compliance Components

In mechanics, the term "modulus" represents the ratio of stress to strain on a deformable body. In creep testing, several unique moduli can be defined dependent upon the particular strain value used. The "resilient" modulus is:

$$E_R = \frac{\sigma_d}{\epsilon_r} \quad (5.1)$$

The "pure" elastic (instantaneous) modulus is:

$$E_e = \frac{\sigma_d}{\epsilon_e} \quad (5.2)$$

The "creep" or time dependent modulus is:

$$E_c = \frac{\sigma_d}{\epsilon(t)} \quad (5.3)$$

Where $\epsilon_p, \epsilon_e, \epsilon(t)$ are the resilient, elastic and total strains as shown in Figure 15. The "modulus" of a material is a very important property that relates stress to strain. However, for viscoelastic materials, it is more advantageous to use the term "compliance" or $D(t)$. Compliance is the reciprocal of the modulus and is expressed by:

$$D(t) = E(t)^{-1} = \frac{\epsilon(t)}{\sigma_d} \quad (5.4)$$

The main advantage of its use in viscoelasticity/plasticity is that it allows for the separation of the various strain components (e.g., $\epsilon_e, \epsilon_p, \epsilon_{ve}$, and ϵ_{vp}) at a constant stress level. Thus, the time dependent strain $\epsilon(t)$ can be simply expressed by:

$$\begin{aligned} \epsilon(t) &= \sigma_d * D(t) \\ &= \sigma_d (D_e + D_p + D_{ve}(t) + D_{vp}(t)) \end{aligned} \quad (5.5)$$

The stress used to calculate compliance in the above equations is defined as the following:

$$\sigma_d = \sigma_1 - \sigma_3 \quad (5.6)$$

where:

σ_d = deviator stress (psi)

σ_1 = vertical stress (psi)

σ_3 = confining pressure (psi)

The creep test can be conducted at both unconfined and triaxial / confined conditions. For the unconfined condition, $\sigma_d = \sigma_1$ ($\sigma_3=0$) while for the triaxial / confined condition, $\sigma_d = \sigma_1 - \sigma_3$. The vertical stress (σ_1) is calculated by the following equation:

$$\sigma_1 = \frac{P}{A} \quad (5.7)$$

where:

σ_1 = vertical stress (psi)

P = vertical load applied (lb)

A = area of cross section of specimen (in²)

Therefore, compliance values calculated in the above equations are "true" compliance values as both stress and strain computed are in the same axis or direction.

5.1.2. Mathematical Compliance Model

In general, power models for compliance only model the secondary (linear) phase of the creep curve.

One type, often mentioned in literature, uses the following compliance model:

$$D' = D(t) - D_o = a_1 t^{m_1} \quad (5.8)$$

where:

D' = viscoelastic compliance component at any time

$D(t)$ = total compliance at any time

D_o = instantaneous compliance ($= D_e + D_p$)

t = loading time

a_1, m_1 = materials regression coefficients

In the above model, $D(t)$ and t are obtained from the static creep (load only) test. It is necessary to estimate the D_o value before the regression can be performed to obtain the materials coefficients, a_1 and m_1 . One approach used to estimate D_o is to estimate the time at which D_o is calculated. A time of 0.1 second is generally selected for all mixes and stress levels.

The regression coefficients "a" and "m" are generally referred to as the compliance parameters. These parameters are the general indicators of the permanent deformation behavior of the materials. In general, the larger the value of "a", the larger the $D(t)$ value, lower the $E_c(t)$ value and hence larger the potential permanent deformation of the material. In addition, for a constant "a" value, as the slope parameter "m" is increased, the larger the potential for permanent deformation will be.

5.1.3. Evaluation of Flow Time

Figure 11 shows typical test results between the calculated total compliance and time. It can be seen from this figure that the total compliance can be divided into three major zones. They are:

- (1) Primary zone,
- (2) Secondary zone,
- (3) Tertiary flow zone.

In the primary creep phase, the strain rate decreases; in the secondary creep phase the creep rate is constant; and in the tertiary creep phase the creep rate increases. At low stress levels, the material mainly exhibit primary creep, that is the creep rate slowly decreases to zero as the total strain reaches a certain value.

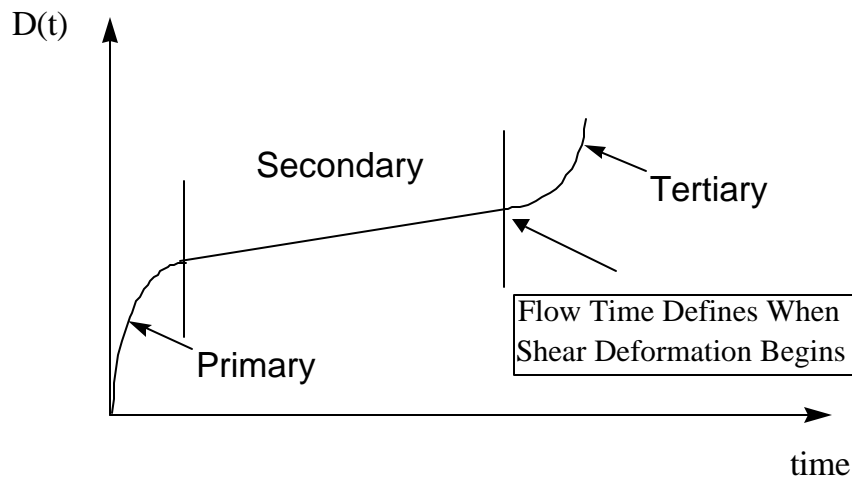


Figure 11. Typical Test Results Between the Calculated Total Compliance and Time.

This also suggests that at this very low stress level the creep rate in the secondary phase may approach zero. At high stress levels, the constant secondary creep rate phase depends on the stress level applied. Ideally, the large increase in compliance generally occurs at a constant volume within the tertiary zone. The flow time, F_T , is therefore defined as the time when shear deformation, under constant volume, starts. The flow time is also viewed as the minimum point in the relationship of rate of change of compliance versus loading time. Figure 12 and 13 show typical static creep test plots. The first shows the total compliance versus loading time on a log-log scale. The estimation of compliance parameters "a" and "m" are obtained from the regression analysis of the linear portion of the curve. The second plot shows a plot of the rate of change in compliance versus loading time in log-log scale along with the calculated value of the flow time.

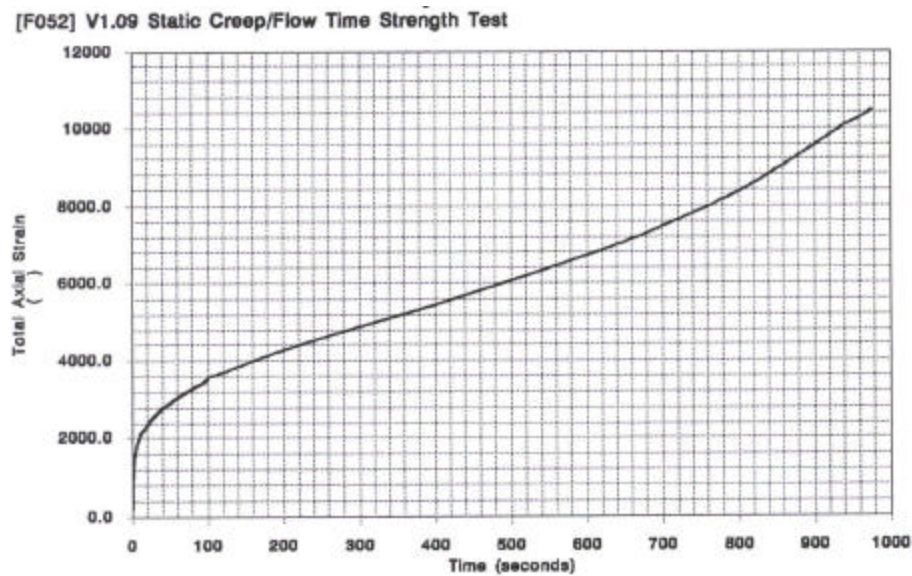


Figure 12. Total Axial Strain Vs. Time From an Actual Static Creep / Flow Time Test.

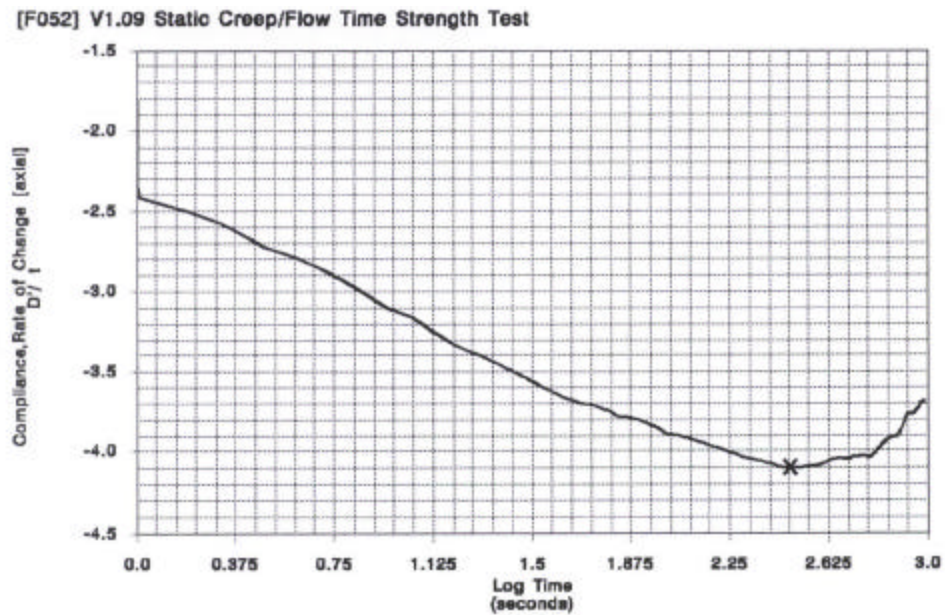


Figure 13. Typical Plot of the Rate of Change in Compliance Vs. Loading Time on a Log-Log Scale, Static Creep / Flow Time Test.

5.2. Background for the Repeated Load Permanent Deformation Test

Another approach to determine the permanent deformation characteristics of paving materials is to employ a repeated dynamic load test for several thousand repetitions and record the cumulative permanent deformation as a function of the number of cycles (repetitions) over the test period. This approach was employed by Monismith et al. in the mid 1970's using uniaxial compression tests (18). Several research studies conducted by Witczak et al, used a temperature of 100°F or 130 °F, and at 10, 20, or 30 psi unconfined deviator stress level (15). A haversine pulse load of 0.1 sec and 0.9 sec dwell (rest time) is applied for the test duration of approximately 3 hours. This approach results in approximately 10,000 cycles applied to the specimen. Brown and Cooper used a range of

various levels of confining pressure for the repeated load test (21). A stress level of 14.4 psi (100 kPa) was subsequently adopted as the standard for their tests. The test was conducted at 104°F (40°C).

A number of parameters describing the accumulated permanent deformation response can be obtained from the test. Figure 14 illustrates the typical relationship between the total cumulative plastic strain and number of load cycles. Like the creep test, the cumulative permanent strain curve is generally defined by three zones: primary, secondary, and tertiary. In the primary zone, permanent deformations accumulate rapidly. The incremental permanent deformations decrease reaching a constant value in the secondary zone. Finally, the incremental permanent deformations again increase and permanent deformations accumulate rapidly in the tertiary zone. The starting point, or cycle number, at which tertiary flow occurs was referred to as the “Flow Number” by Witczak.

Typical permanent deformation parameters, which are obtained and analyzed from the repeated load permanent deformation test, include the intercept (a , μ) and slope (b , α) parameters. The permanent deformation properties (α , μ) have been used as input for predictive design procedures (22). It is emphasized that all of the parameters derived from the linear (secondary) portion of the cumulative plastic strain – repetitions curve ignore the tertiary zone of material deformability. Thus, all four of the parameters noted (α , μ , b , a) are regression constants of a statistical model that is only based upon the “linear” secondary phase of the plastic strain – repetition curve.

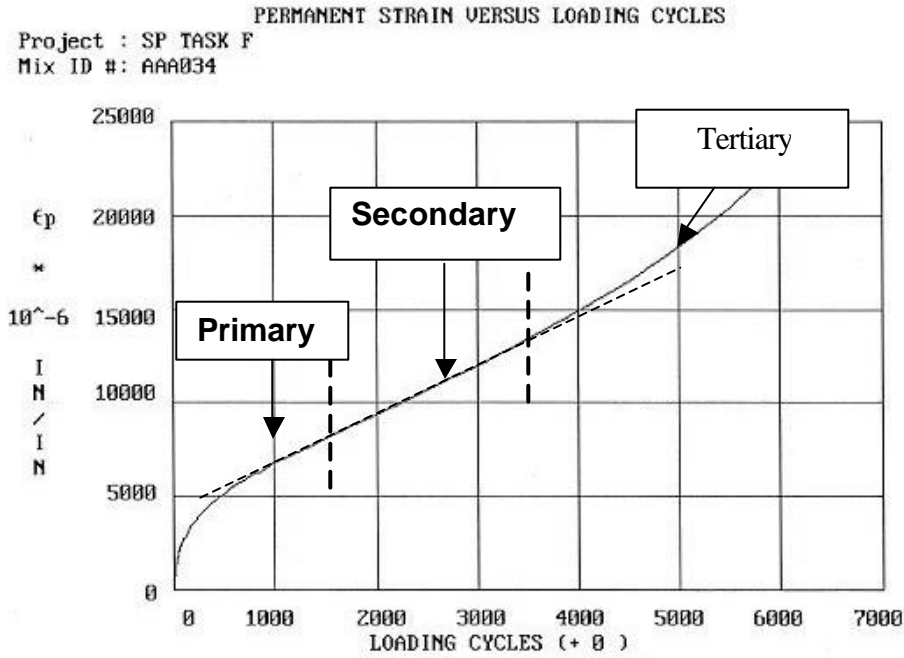


Figure 14. Typical Relationship Between Total Cumulative Plastic Strain and Number of Load Cycles.

The log-log relationship between the permanent strain and the number of load cycles can be expressed by the classical power model:

$$\epsilon_p = aN^b \quad (5.10)$$

Where "a" and "b" are regression constants depending upon the material-test combination conditions. Figure 15 illustrates the relationship when plotted on a log-log scale. The intercept "a" represents the permanent strain at $N=1$, whereas, the slope "b", represents the rate of change in permanent strain as a function of the change in loading cycles ($\log(N)$). An alternative form of the mathematical model used to characterize the plastic strain per

load repetition (ϵ_{pn}) relationship can be expressed by:

$$\frac{\partial \epsilon_p}{\partial N} = \epsilon_{pn} = \frac{\partial (aN^b)}{\partial N} \quad (5.11)$$

or

$$\epsilon_{pn} = abN^{(b-1)} \quad (5.12)$$

The resilient strain (ϵ_r) is generally assumed to be independent of the load repetition value (N). As a consequence, the ratio of plastic to resilient strain components of the material in question can be defined by:

$$\frac{\epsilon_{pn}}{\epsilon_r} = \left(\frac{ab}{\epsilon_r} \right) N^{b-1} \quad (5.13)$$

letting: $\mu = \frac{ab}{\epsilon_r}$ and $\alpha = 1-b$ one obtains:

$$\frac{\epsilon_{pn}}{\epsilon_r} = \mu N^{-\alpha} \quad (5.14)$$

In the above equation, ϵ_{pn} is the permanent or plastic strain due to a single load application; i.e., at the N^{th} application. μ (μ) is a permanent deformation parameter representing the constant of proportionality between permanent strain and elastic strain (i.e. plastic strain at $N=1$). α (α) is a permanent deformation parameter indicating the rate of decrease in incremental permanent deformation as the number of load applications increases.

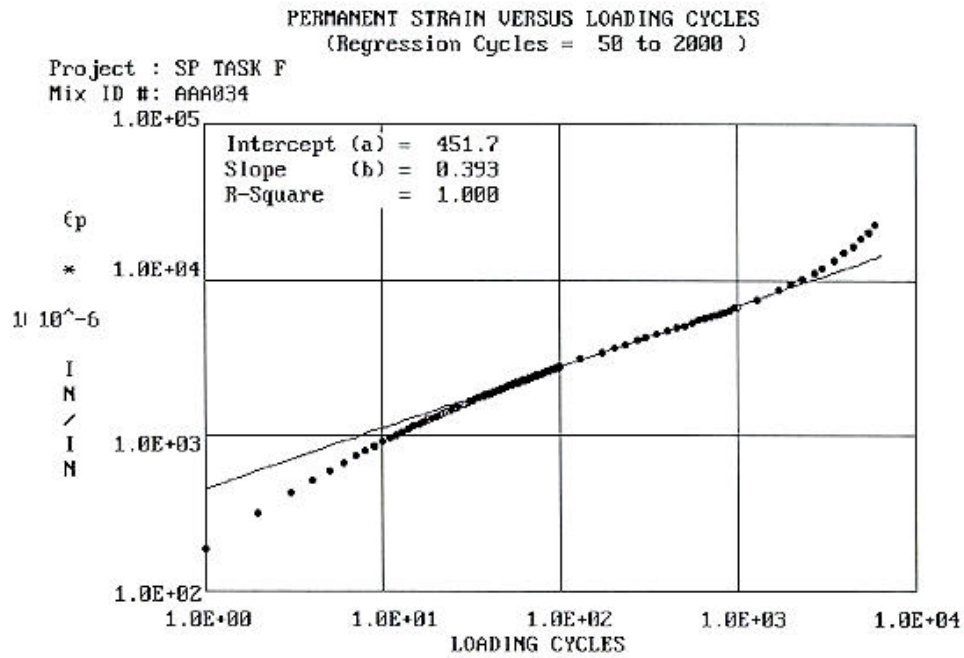


Figure 15. Regression Constants “a” and “b” When Plotted on a Log-Log Scale.

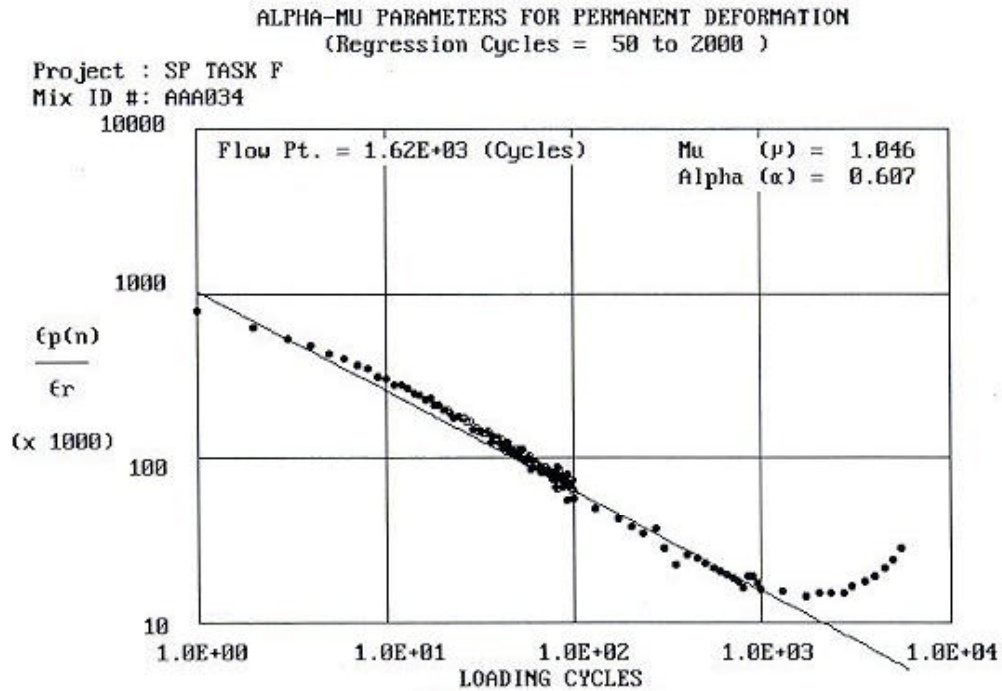


Figure 16. Permanent Deformation Parameters α and μ and the Flow Number.

Figure 16 illustrates the above relationship and the occurrence of the flow point when the rate of decrease in permanent strain is constant.

Figure 17 through 19 show typical plots for an actual repeated load test conducted. Figure 18 shows a typical plot of the total permanent strain versus loading cycles on a log-log scale. The estimation of parameters "a" and "b" are obtained from the regression analysis of the linear portion of the permanent strain – number of cycles data in Figure 18.

Figure 19 shows a plot of the rate of change in permanent strain versus loading cycles on a log-log scale. The flow number of cycles is recorded where the minimum slope is shown.

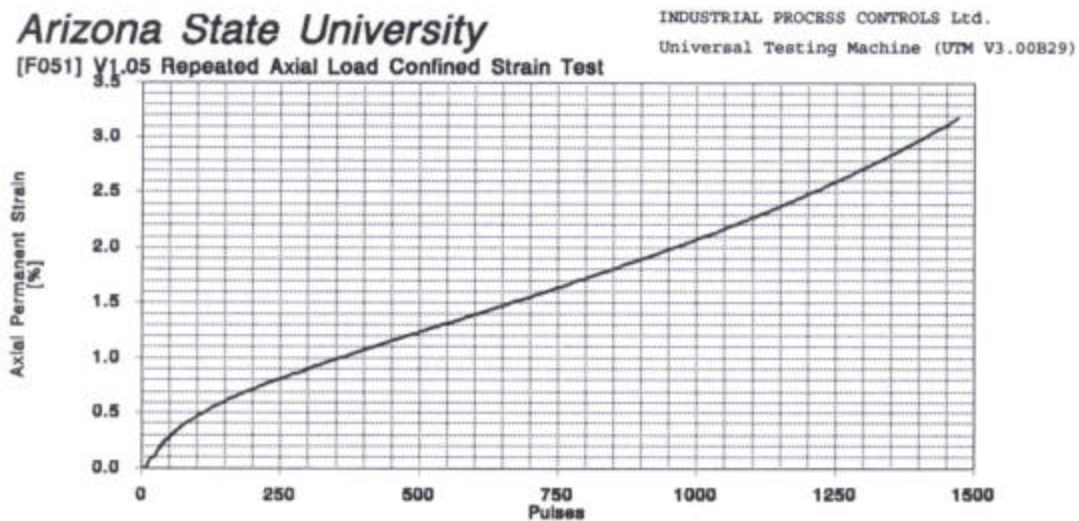


Figure 17. Cumulative Permanent Strain Vs. Loading Cycles From a Repeated Load Test

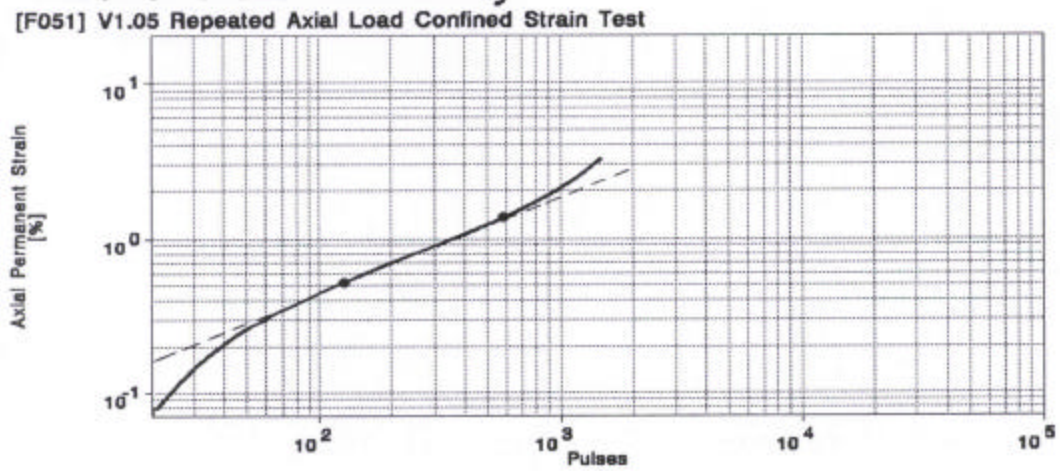


Figure 18. Regression Constants “a” and “b” from Log Permanent Strain – Log Number of Loading Cycles Plot, Repeated Load Test.

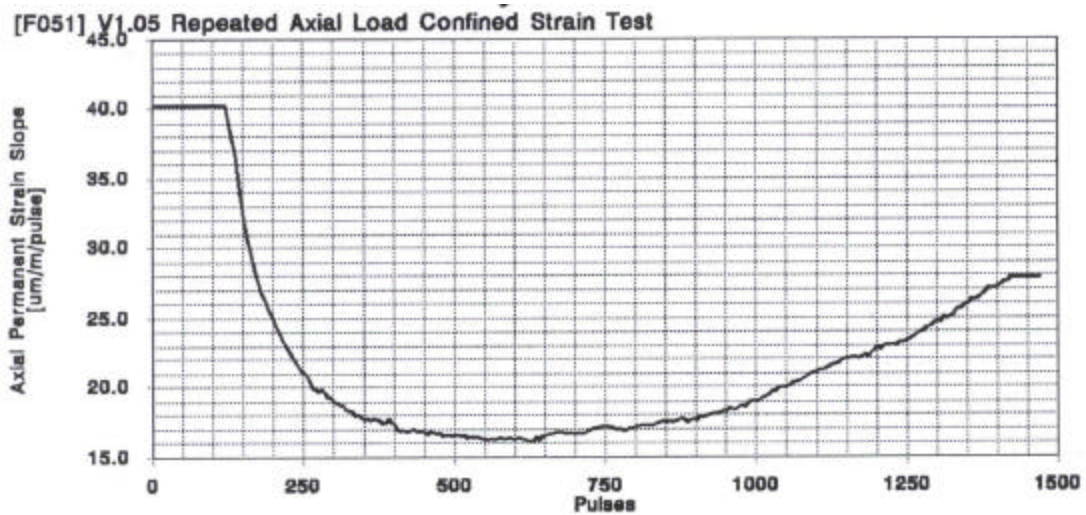


Figure 19. Typical Plot of the Rate of Change in Permanent Strain Vs. Loading Cycles, Repeated Load Test

5.3. Test Conditions for the Static Creep and Repeated Load Tests

Static creep and repeated load tests, confined and unconfined, were conducted using at least two replicate test specimens for each mixture. When material availability was not of concern, three replicates were used. When the equivalent test results for the standard ADOT mixture (SRB PG64-22) were available, they were compared to the results of the AR mixtures. All tests were carried out on cylindrical specimens, 100mm (4 inches) in diameter and 150mm (6 inches) in height.

For the static creep tests, a static constant load was applied until tertiary flow occurred. For the repeated load tests, a haversine pulse load of 0.1 sec and 0.9 sec dwell (rest time) was applied for a target of 300,000 cycles. This number was less if the test specimen failed under tertiary flow before reaching this target level.

An IPC Universal Testing Machine (UTM 25-14P) electro- pneumatic system was used to load the specimens. The machine is equipped to apply up to 90 psi (620 kPa) confining pressure and 5,500 lb (24.9 KN) maximum vertical load. The load was measured through the load cell, whereas, the deformations were measured through six spring-loaded LVDTs. Two axial LVDTs were mounted vertically on diametrically opposite specimen sides. Parallel studs, mounted on the test specimen, placed 100mm (4 inches) apart and located at the center of the specimen were used to secure the LVDTs in place. The studs were glued using a commercial 5-minute epoxy. An alignment rod with a frictionless bushing was used to keep the studs aligned at extreme failure conditions. Figure 20 shows a photograph of an actual specimen set-up for unconfined test. For radial deformations, four

externally mounted LVDTs aligned on diametrical and perpendicular lines were located at the center of the specimen and along opposite specimen sides. The radial LVDT's set-up is also shown in Figure 20. Thin and fully lubricated membranes at the test specimen ends were used to warrant frictionless surface conditions. All tests were conducted within an environmentally controlled chamber throughout the testing sequence (i.e., temperature was held constant within the chamber to $\pm 1^{\circ}\text{F}$ throughout the entire test). Figure 20 showed typical unconfined test set up for either a static creep and/or the repeated load test. Figure 21 and 22 show the same but for a confined test set-up.



Figure 20. Vertical and Radial LVDTs' Set-Up for an Unconfined Test



Figure 21. Confined Test Set-Up



Figure 22. Test Set-Up Within Triaxial Cell with Mounted Radial LVDTs.

A complete matrix of the stress level/ temperature combinations used for the Static Creep and Repeated Load tests is shown in Table 6. In addition to original testing program, five specimens of the ARAC mixture were compacted to 7% air voids in order to evaluate the mixture properties at this lower air voids level. These specimens were tested in unconfined conditions at temperature of 100°F.

It is emphasized that the stress levels combinations in the below table were primarily selected because of the need to compare the AR mixture's values to previously determined values from other studies (conventional ADOT mixture). The confining pressure in the conventional mixture study was selected on the low side to force the specimen to fail within a reasonable testing time period. Previous research studies conducted by the research team utilized a confinement level of 20 psi for dense graded mixture.

Table 6. Stress Level/ Temperature Combination Used for the Static Creep and Repeated Load Tests

Test Type	Stress Type *		Test Temperature			
			37.8°C (100°F)		54.4°C (130°F)	
			Unconfined	Confined	Unconfined	Confined
Static Creep/ Flow Time	σ_3	(kPa)	0	69	0	69
		(psi)	0	10	0	10
	σ_d	(kPa)	105	1145	69	825
		(psi)	15	166	10	120
Repeated Load/ Flow Number	σ_3	(kPa)	0	69	0	69
		(psi)	0	10	0	10
	σ_d	(kPa)	105	1145	69	1145
		(psi)	15	166	10	166

* σ_3 – confining stress

σ_d – deviator stress

5.4. Tests Results and Analysis

5.4.1. Static Creep/ Flow Time Test

The results for the static creep unconfined and confined tests for all three mixtures are summarized and reported in Appendix C. A master summary table for all mixtures, temperatures, and stress level combinations reported in Appendix C is shown in Table 7. The table contains final average values used in the comparison analysis of rubber asphalt mixtures and the standard ADOT mixture. These properties include the Flow Time, percent of axial strain at flow (flow time), Creep Modulus at flow, and the compliance parameters (a - intercept, m - slope, and D_0 - instantaneous compliance). It is noted that at 100°F, the results for the SRB PG 64-22 were not available.

Table 7. Master Summary of Static Creep Test Results.

Mix	Target AV%	Temp °F	S_3 (psi)	S_d (psi)	Axial Flow Time (sec)	Axial Strain @ failure (%)	Creep Modulus @ failure (psi)	Inst. Compl. $D_0 \times 10^{-3}$ (1/psi)	Intercept $a \times 10^{-3}$ (1/psi)	Slope m
AR-ACFC	18.0	100	0	15	987	3.15	470	0.056	0.113	0.559
	18.0	130	0	10	108	3.39	297	0.188	0.607	0.378
	18.0	100	10	166	3	4.85	3,253	0.038	0.136	0.709
	18.0	130	10	120	2	4.24	2,550	0.076	0.207	0.553
ARAC	11.0	100	0	15	4,299	4.29	355	0.053	0.293	0.281
	11.0	130	0	10	23,826	1.87	558	0.033	0.201	0.217
	7.0	100	0	15	175,140	2.45	631	0.013	0.015	0.489
	11.0	100	10	166	10	5.54	3,029	0.021	0.076	0.633
	11.0	130	10	120	3	6.15	1,570	0.080	0.270	0.824
SRB PG64-22	7.0	130	0	10	135	0.28	3,303	0.045	0.046	0.406
	7.0	130	10	120	8	0.66	21,780	0.008	0.014	0.594

Figure 23 shows a comparison of Flow Time at the different test conditions. For the unconfined tests at 100°F, the ARAC mixture at 11% Air Voids (AV) had much higher Flow Time (over 4 times higher for unconfined test and 3 times higher for confined test) compared to the AR-ACFC mixture. At 130°F the ARAC mixture shows superior flow time properties compared to the AR-ACFC and the standard ADOT dense graded mixtures. The ARAC mix flow time is 175 times higher than that of the SRB PG64-22 mix. It is also noted that the SRB PG64-22 had 25% higher Flow Time than the AR-ACFC mix.

The results for the confined tests conducted at both temperatures were concluded as not reliable, especially at 130°F. This was because the stress levels combinations selected resulted in rapid failure (flow time) of the test specimens (2 to 10 seconds). This was too short to develop proper compliance curves. Nevertheless, the results are shown in Figure 4 for completeness purposes.

Considering the sensitivity of the ARAC mixture to air voids variation it can be observed (from Figure 23) that mixtures compacted to 7% air voids had 40 times higher flow time to failure compared to the mixture compacted to 11% air voids. Therefore, field compaction considerations should be carefully evaluated for this mixture.

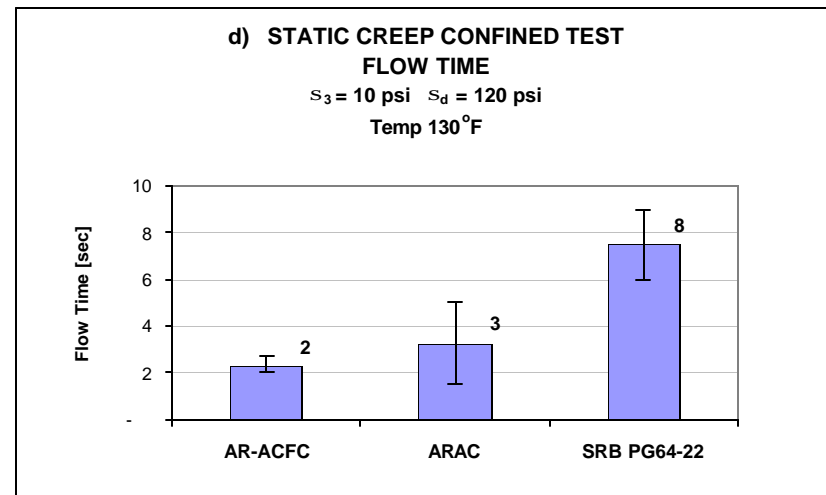
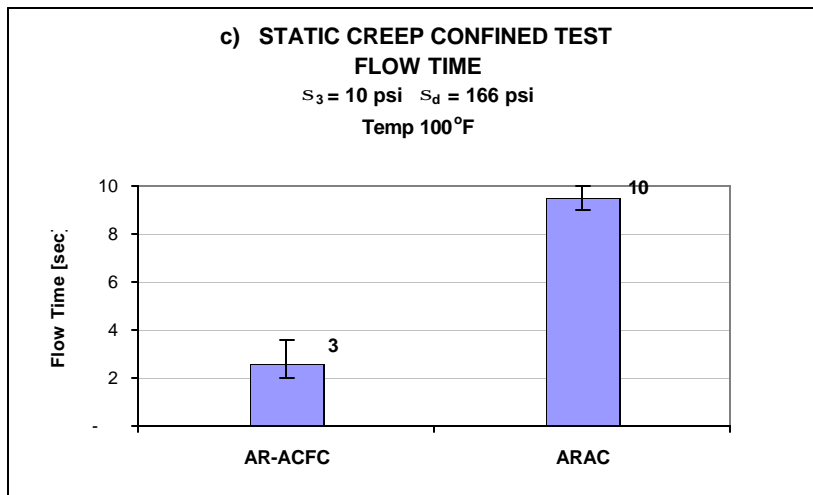
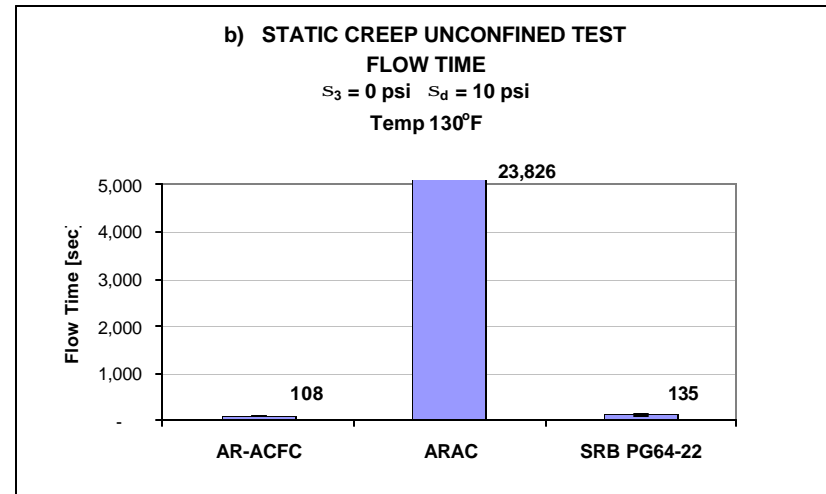
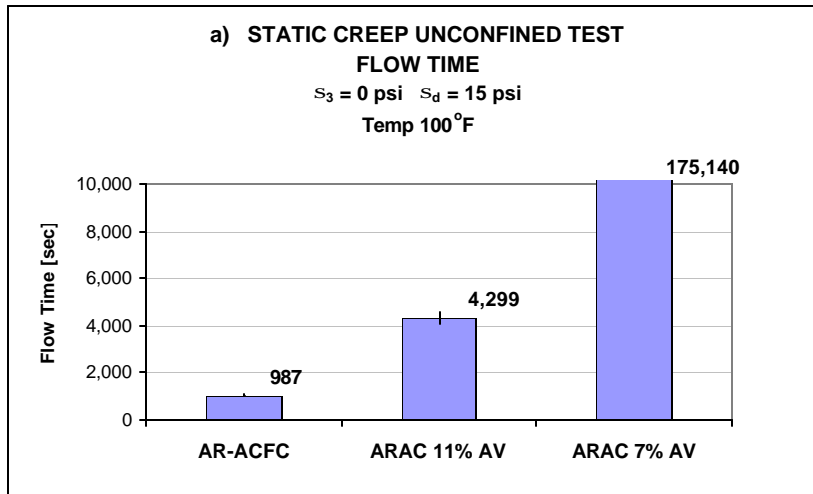


Figure 23. Static Creep Unconfined and Confined Test - Flow Time Results.

Figure 24 shows summary plots for the strain at failure. For the unconfined test results at 100oF, the ARAC 11%AV mix had 35% higher strain at failure than the AR-ACFC mix. This was 14% higher for the confined test. In addition, for the unconfined tests conducted at 130oF, the ARAC mix showed over 5 times higher strain at failure than the SRB PG64-22 mix. Higher strains at failure are indicative of good mixture stability to the applied loads.

The results of the slope parameter of the compliance curve for the unconfined tests at 100oF showed that the SRB PG64-22 mix had higher slope than the asphalt rubber mixtures. Higher slope values are indicative of susceptibility of the mixture to permanent deformation. Because of the lack of the confinement in the unconfined tests the AR-ACFC mix had twice as high slope as the ARAC 11%AV mixture. However, a comparison of the slope parameter for the confined tests at 130oF, the ARAC mix at 11%AV had the lowest slope followed by the AR-ACFC and the SRB PG 64-22 mixtures. The ARAC mix at 11%AV had the highest slope, probably due to the higher air voids present in this mix. Overall, the asphalt rubber mixtures showed good permanent deformation characteristics compared to the conventional SRB PG 64-22 dense graded mixture.

The results of the Creep Modulus at failure conducted in unconfined conditions and at 100°F show 32% higher value for the AR-ACFC mix comparing to the ARAC 11%AV, and 9 times higher value for the SRB PG64-22 mix compared to the ARAC 11%AV.

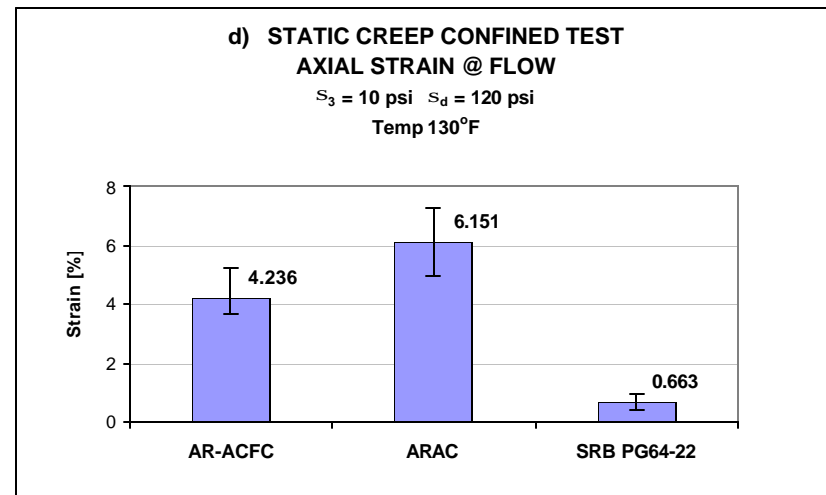
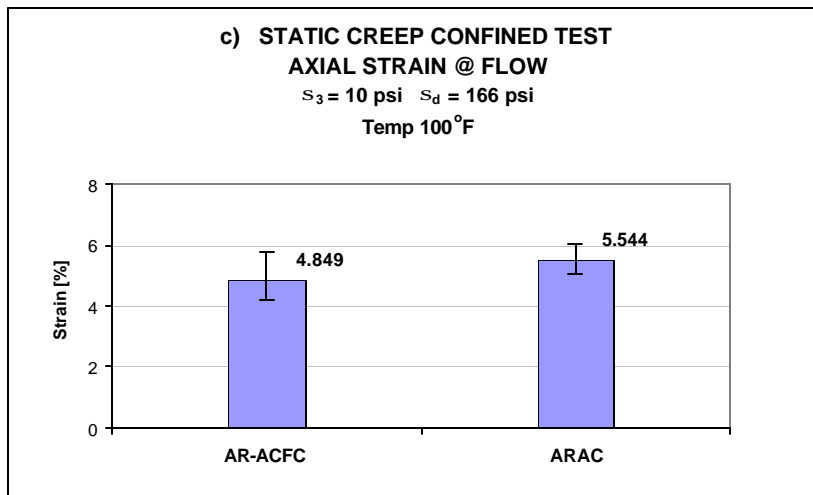
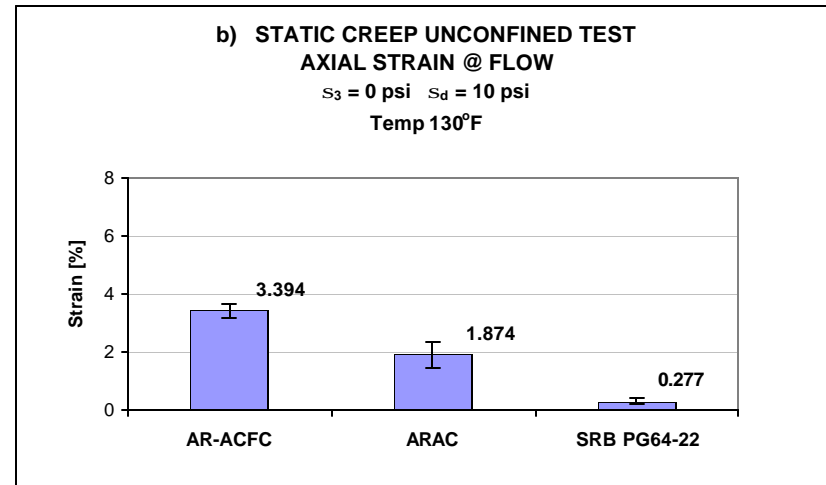
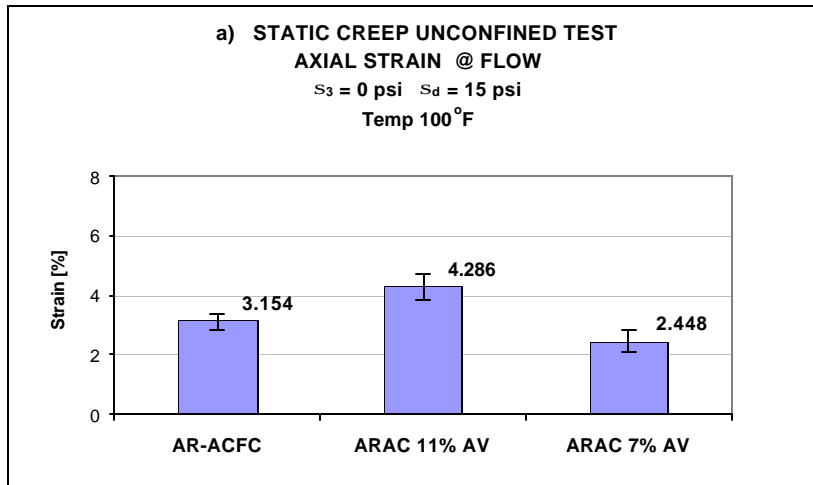


Figure 24. Static Creep Unconfined and Confined Test – Axial Strain at Flow Results

5.4.2. Repeated Load/ Flow Number Test

The results for the repeated load unconfined and confined tests for all three mixtures are summarized and reported in Appendix D. A master summary table for all mixtures, temperatures, and stress level combinations reported in Appendix D is shown in Table 8. The table contains final average values used for the analysis and comparison of the AR and standard ADOT mixtures. Table 8 includes the flow number, percent of axial strain at failure (flow), Resilient Modulus at failure, and the permanent deformation parameters (a – intercept and b - slope). At 100°F, the results for the SRB PG 64-22 mixture were not available.

Table 8. Master Summary of Repeated Load Test Results

Mix	Target VA %	Temp °F	S ₃ (psi)	S _d (psi)	Axial Flow Number	Axial Strain (%)	Resilient Modulus @ failure (psi)	Intercept a x10 ⁻³ (1/psi)	Slope b
AR-ACFC	18.0	100	0	15	6,985	3.510	64,558	0.388	0.482
	18.0	130	0	10	605	2.727	26,937	1.200	0.425
	18.0	100	10	166	124	8.796	168,426	3.529	0.623
	18.0	130	10	166	25	9.193	51,342	4.464	0.825
ARAC	11.0	100	0	15	8,445	4.190	120,087	0.607	0.427
	11.0	130	0	10	12,118	3.120	43,712	0.863	0.346
	7.0	100	0	15	248,585	1.405	146,063	1.110	0.188
	11.0	100	10	166	2,289	10.711	156,838	3.830	0.361
	11.0	130	10	166	91	8.634	120,935	2.658	0.656
SRB PG64-22	7.0	130	0	10	738	0.327	70,558	0.043	0.607
	7.0	130	10	166	172	4.987	109,741	0.993	0.687

Table 9 presents the results of the permanent to resilient strain ratio (ϵ_p/ϵ_r). This was an important property that the testing program needed to establish for asphalt rubber mixtures, for its future use in the AASHTO 2002 Pavement Design Guide. The design guide uses this ratio in the model that predicts permanent deformation in the asphalt layer.

A comparison of the results for all tested mixtures in unconfined and confined state at 100 and 130°F are shown in Figure 25 through 27.

Table 9. Summary of ϵ_p/ϵ_r Ratio for Repeated Load Test

Mix	Target VA%	Temp °F	S ₃ (psi)	S _d (psi)	Average Flow Number	e _p [%] at Failure	e _r [%] at Failure	e _p /e _r at Failure
AR-ACFC	18.00	100	0	15	6,985	3.468	0.024	145
	18.00	130	0	10	605	2.564	0.031	83
	18.0	100	10	166	124	8.950	0.416	16
	18.0	130	10	166	25	9.193	0.520	20
ARAC	11.00	100	0	15	8,445	4.182	0.013	340
	11.00	130	0	10	12,118	3.121	0.022	142
	7.00	100	0	15	248,585	1.405	0.010	134
	11.0	100	10	166	2,289	10.711	0.246	62
	11.0	130	10	166	91	8.546	0.142	61
SRB PG64-22	7.00	130	0	10	738	0.313	0.014	23
	7.0	130	10	166	169	4.987	0.159	33

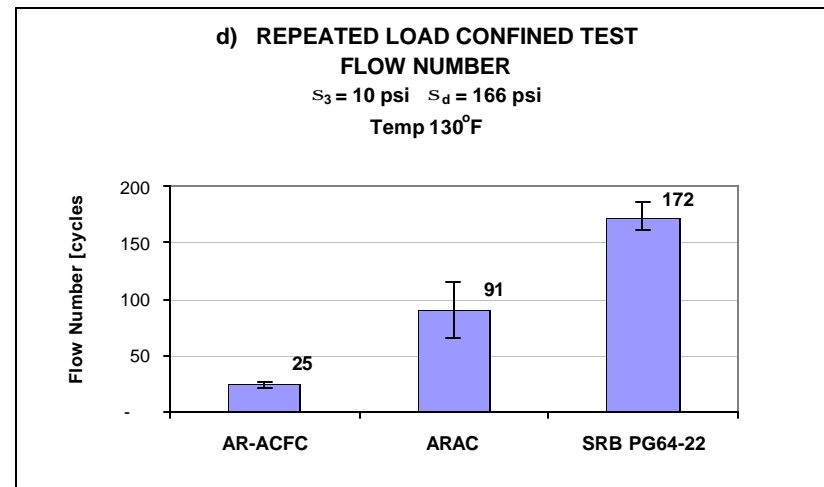
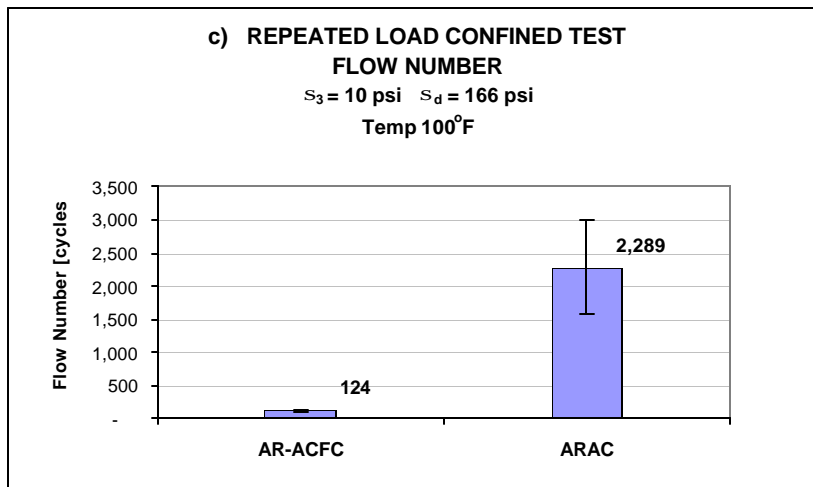
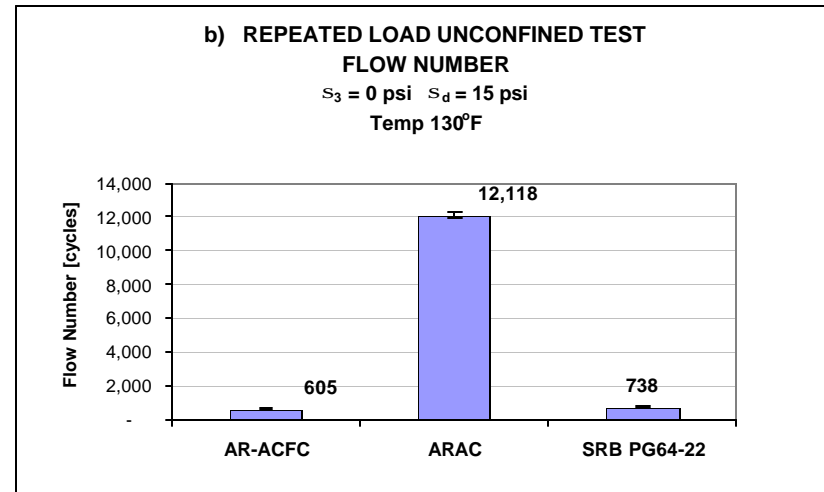
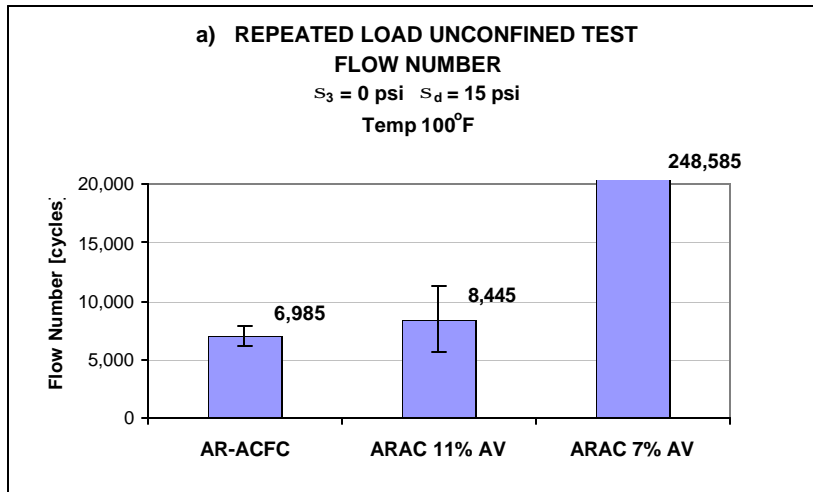


Figure 25. Repeated Load Unconfined and Confined Test – Flow Number Results

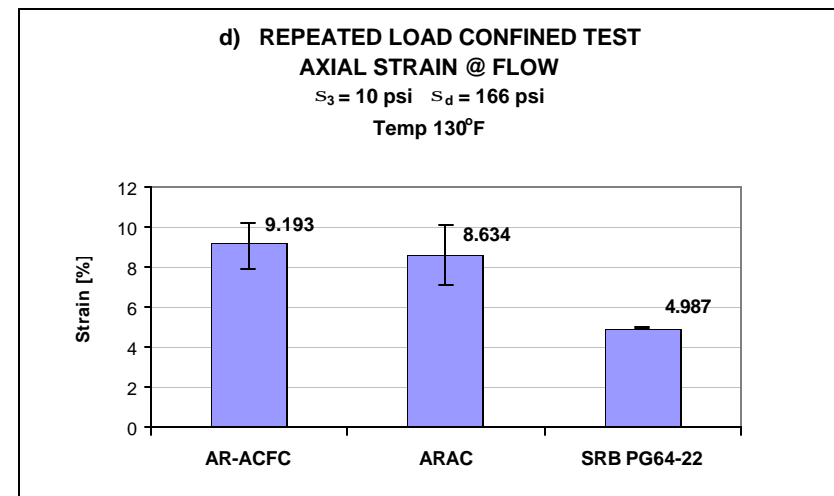
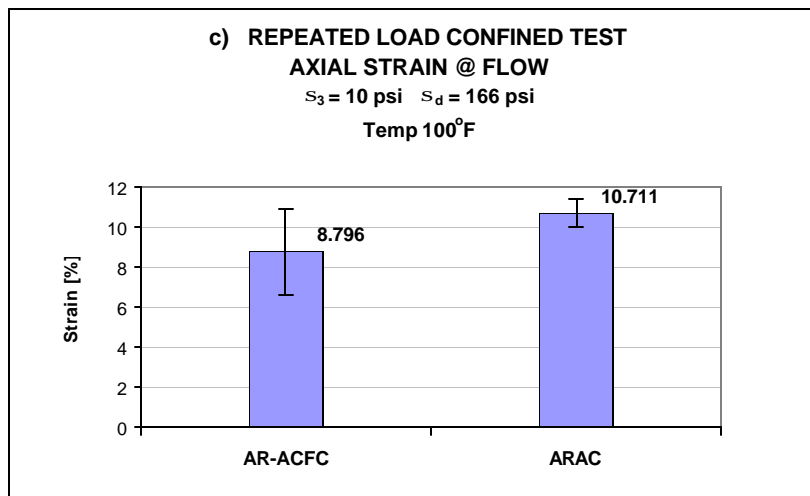
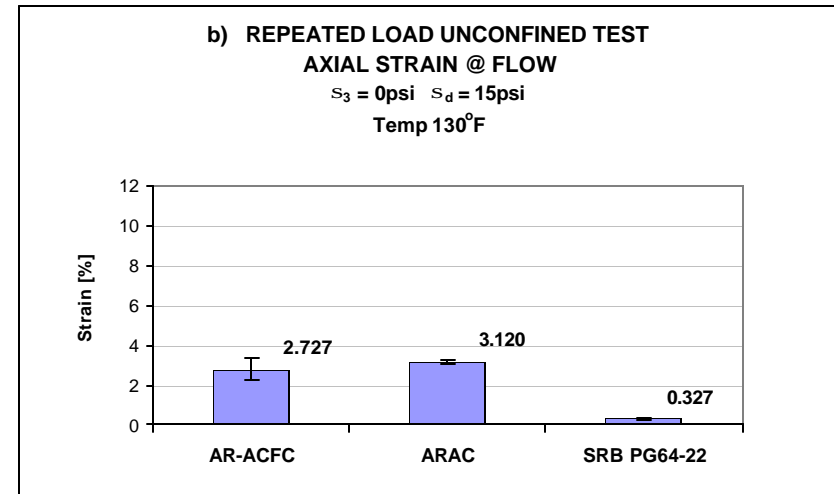
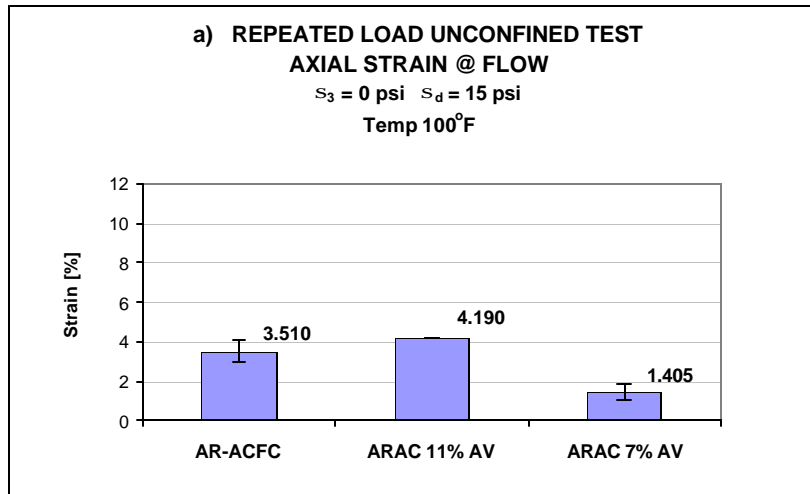


Figure 26. Repeated Load Unconfined and Confined Test – Axial Strain Results

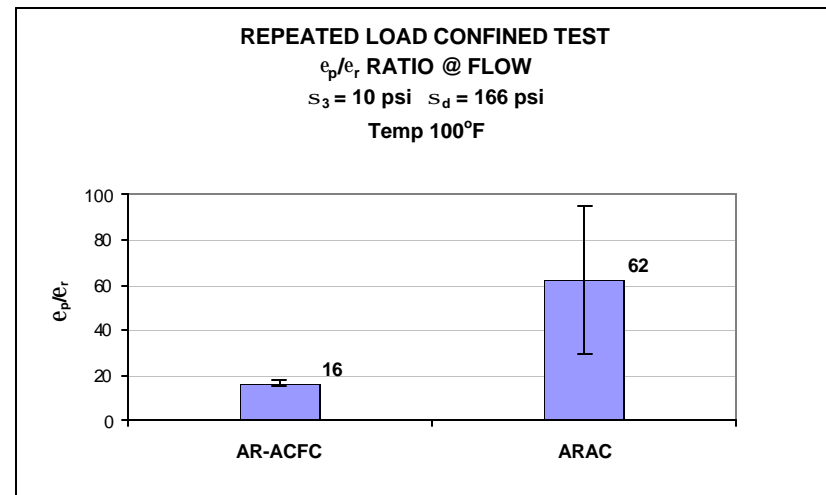
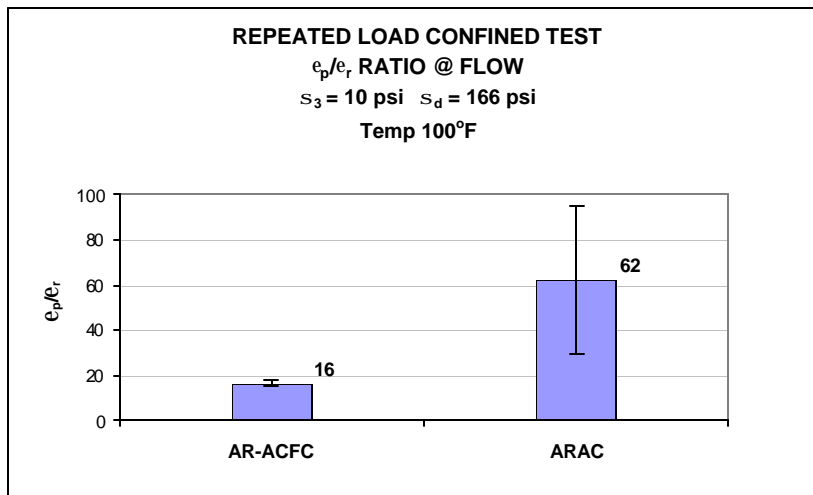
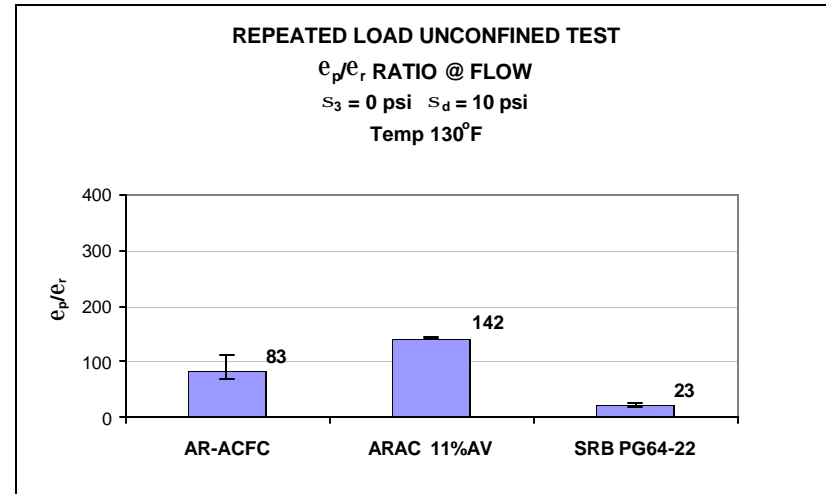
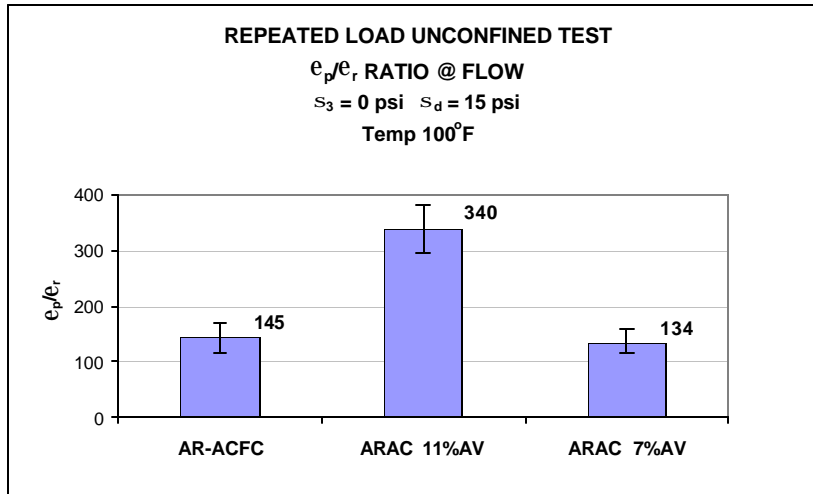


Figure 27. Comparison of ϵ_p/ϵ_r ratio for Repeated Load Test

The results of the flow number for the unconfined tests at 100°F (Figure 25) shows 20% higher flow number for the ARAC 11%AV mixture compared to the AR-ACFC mix, and over 18 times higher flow number for the confined test. For the unconfined tests conducted at 130°F, very similar trend to the Static Creep test was observed. The ARAC 11%AV mix showed over 16 times higher Flow Number than the SRB PG64-22 mix, and the difference between the AR-ACFC and SRB PG64-22 mixtures was relatively small (about 22%).

The results for the confined tests conducted at 130°F showed about 90% higher flow number for the SRB PG64-22 mix compared to the ARAC mix, and about 7 times higher flow number compared to the AR-ACFC mix. Similarly to the Static Creep test, the short time to failure (25 to 172 pulses) made the results unreliable.

Considering the mixture sensitivity to air voids changes, it was observed that the ARAC mix with 7% air voids had 30 times higher flow number compared to the ARAC mix with 11% air voids. This was similar to observation made with the static creep tests. Again, field compaction considerations should be further evaluated for this mixture.

The results of axial strain at failure (Figure 26) showed very similar trends to the static creep test. The ARAC 11%AV mix showed higher strains at failure than the AR-ACFC mix, but at the same time its failure (flow number) occurred later. It is also worth mentioning that in the repeated load test, the difference in the strain levels between both

AR mixtures were not as large as the static creep test, although still significantly higher than the SRB PG 64-22 mix. Larger strains at failure are indicative of good mixture stability to the applied loads.

The results of ϵ_p/ϵ_r ratio at failure (Figure 27) for the unconfined tests at 100°F, showed that the ARAC mix with 11% air voids had 2.5 times higher ratio than the AR-ACFC mix and the ARAC mix with 7% air voids. The difference between the AR-ACFC and ARAC 7%AV mixes is negligible. At 130°F, the ARAC 11%AV mix had 71% higher ratio than the AR-ACFC mix and 5 times higher ratio than the SRB PG64-22 mix.

For the confined tests at 100°F, the ARAC mix indicated 3.8 times higher ratio than the AR-ACFC mix. At 130°F, the ARAC mix has 3 times higher ratio than the AR-ACFC and 2 times higher ratio than the SRB PG64-22 mixture.

The above results indicated that the ϵ_p/ϵ_r ratio at failure is different for AR mixtures compared to conventional mixtures. It is also dependant on the test temperature, mix aggregate grading, confinement condition, and the mix air voids content. Higher ϵ_p/ϵ_r ratio at failure may be indicative of better mixture resistance to permanent deformation. Further testing and analysis in this area needs to be addressed for the AR mixtures.

Considering the slope of the compliance curve it was observed that for the unconfined test at 130°F the ARAC mix had 23% smaller slope than the AR-ACFC mix, and 75% smaller slope than the SRB 64-22 mix. At 100°F the ARAC 11%AV mix had more than 2 times

larger slope than the ARAC 7%AV mixture.

The results of the slope parameter of the permanent strain curve for the unconfined tests at 130°F showed that the SRB PG64-22 mix had much higher slope than the asphalt rubber mixtures. Higher slope values are indicative of greater susceptibility of the mixture to permanent deformation. A comparison of the slope parameter for the confined tests at 130°F showed that the ARAC mix at 11%AV had the lowest slope followed by the SRB PG 64-22 mix and then the AR-ACFC mix. Similar to the static creep test results, and considering the unconfined tests at 100oF, the ARAC 11%AV mix had more than 2 times larger slope than the ARAC 7%AV mixture. Overall, the asphalt rubber mixtures showed good permanent deformation characteristics compared to the conventional SRB PG 64-22 dense graded mixture.

5.5. Summary for the Permanent Deformation Tests

Repeated load and static creep permanent deformation tests were conducted at two temperatures using unconfined and confined SPT protocols. The test results obtained were compared to results available at ASU for conventional ADOT dense graded mixtures (SRB PG 64-22). Based on the test results and analysis, the following conclusions are made:

- In both unconfined tests (Static Creep and Repeated Load) conducted at 130oF, the ARAC mixture indicated superior performance, much higher resistance to permanent deformation compared to the standard ADOT SRB PG64-22 mixture.

- The ARAC mixture failure (flow) occurred after reaching 5 to 10 times larger strain than the SRB PG64-22 mix. Larger strain at failure are indicative of good mixture stability to the applied loads.
- The trends for the Static Creep and the Repeated Load tests were very similar, and the ARAC mix performed very well in both tests. However, better results were observed in the Static Creep test. Therefore, improved mixture stability under static load may also be expected from the ARAC mixture.
- The AR-ACFC mix generally showed lower resistance to permanent deformation (in both unconfined and confined tests) compared to the other tested mixtures.
 - For the unconfined tests, this was attributed to several factors: much higher air voids, lack of confinement that this material normally experience in the field, and higher binder content. Note that the AR-ACFC mix is a material designed for non-structural layers and its thickness usually does not exceed 1 inch.
 - For the confined tests, the laboratory poor performance was attributed to the lack of adequate confinement level applied, which does not represent the level of confinement that the material experiences in the field. Therefore, the open graded friction course (AR-ACFC mix) should not be compared in a routine testing mode (that was utilized in this study) to materials like the ARAC – Gap graded asphalt concrete or the Salt River Base dense graded mixtures, when resistance to permanent deformation is considered.

- Experience from the confined tests in this study showed that the selected stress level combinations in the laboratory were not effective and further work on selecting appropriate stress levels for these confined tests should be conducted.
- The air voids sensitivity study showed that the ARAC mix compacted to 7% air voids would have much better performance and less potential for permanent deformation than the same mixture compacted to 11% air voids. This finding is consistent with observations found for dense graded mixes. Therefore, it would be advisable to use a similar type of compaction quality control for the AR gap graded mixtures.
- This study showed promising results of utilizing the flow time / flow number of repetitions parameters to evaluate / verify the field performance of the asphalt rubber mixtures.

6. DYNAMIC MODULUS TEST

6.1. Background for the Dynamic (Complex) Modulus Test

For linear viscoelastic materials such as asphalt mixes, the stress to strain relationship under a continuous sinusoidal loading is defined by a complex number called the complex modulus E^* (ASTM D3497). The complex modulus has a real and imaginary part that defines the elastic and viscous behavior of the linear viscoelastic material. The absolute value of the complex modulus $|E^*|$, is defined as the dynamic modulus. Mathematically, the dynamic modulus is defined as the maximum (peak) dynamic stress (σ_o) divided by the recoverable axial strain (ϵ_o):

$$|E^*| = \sigma_o / \epsilon_o \quad (6.1)$$

By current practice, dynamic modulus testing of asphaltic materials is conducted on unconfined cylindrical specimens having a height to diameter ratio equal to 1.5 and uses a uniaxially applied sinusoidal (haversine) stress pattern (13). Under such conditions, the sinusoidal stress at any given time t , is given as:

$$\sigma_t = \sigma_o \sin(\omega t) \quad (6.2)$$

where:

σ_o = peak dynamic stress amplitude (psi).

ω = angular frequency in radian per second.

t = time (sec).

The subsequent dynamic strain at any given time is given by:

$$\epsilon_t = \epsilon_o \sin(\omega t - \phi) \quad (6.3)$$

where:

ϵ_o = peak recoverable strain (in/in).

ϕ = phase lag or angle (degrees).

The phase angle is simply the angle at which the ϵ_o lags σ_o , and is an indicator of the viscous (or elastic) properties of the material being evaluated. Mathematically this is expressed as:

$$\phi = (t_i / t_p) \times (360) \quad (6.4)$$

where:

t_i = time lag between a cycle of stress and strain (sec).

t_p = time for a stress cycle (sec).

The complex modulus E^* is comprised of both a real and imaginary portion. This can be written as:

$$E^* = E' + iE'' \quad (6.5)$$

with

$$E' = (\sigma_o / \epsilon_o) \times \cos \phi \quad (6.5a)$$

and

$$E'' = (\sigma_o / \epsilon_o) \times \sin \phi \quad (6.5b)$$

The E' value is generally referred to as the storage or elastic modulus component of the complex modulus, while E'' is referred to as the loss (viscous) modulus. The loss tangent ($\tan \phi$) is the ratio of the energy lost to the energy stored in a cyclic deformation and is equal to:

$$\tan \phi = E'' / E' \quad (6.5c)$$

For a pure elastic material, $\phi = 0$ and it is observed that the complex modulus E^* is equal to the absolute value, or dynamic modulus. For pure viscous materials, $\phi = 90^\circ$ (10).

6.2. General Test Description

Dynamic Modulus tests were conducted unconfined, as well as using three levels of confinements: 10, 20, and 30 psi. Test specimens used were cored from laboratory compacted Gyratory plugs approximately 6.0 inches in diameter and 6.0 inches high, to arrive at test specimens with a diameter of 4.0 inches and an approximate height of 6.0 inches. For each mixture, a full factorial of test frequencies (0.1, 0.5, 1, 5, 10, and 25 Hz) and temperatures (14, 40, 70, 100, and 130°F) were used. Each specimen was tested in an increasing order of temperature, i.e. 20, 40, 70, 100, and 130°F. For each temperature level, specimens were tested in a decreasing order of frequency (25, 10, 5, 1, 0.5, and 0.1 Hz). This temperature-frequency sequence was carried out to cause minimum damage to the specimen before the next sequential test. At cold temperatures and high frequency level, the material behaves stronger compared to warmer temperatures and at low frequency levels.

For the ARAC Gap Graded mixture, three replicate specimens were used for the unconfined test, and three additional replicate specimens (total of six specimens) were used for all the confined tests in an increasing order of confinement (10, 20, and 30 psi). This was mainly done because the amount of material available for the ARAC mixture was limited. For the AR-ACFC Open Graded mixture, material availability was not an

issue; therefore three replicate specimens were used for the unconfined tests and at each level of confinement (total of twelve specimens). However, a round of unconfined tests were performed at room temperature (70°F) on all twelve specimens to ensure that they are true replicates and provide comparable results. Table 10 shows a list of the replicates used and their respective test assignment (whether it is unconfined or confined test). Additional tests were performed on a formed (molded) crumb rubber specimen consisting of 80% crumb rubber and 20% urethane. This was done because the results of the ARAC and AR-ACFC mixtures showed a different behavior at higher temperatures. For that, the crumb rubber sample was prepared and tested unconfined at 70, 100, and 130°F using the same frequency levels. For this crumb rubber sample, a total of 18 dynamic modulus tests were performed.

A servo hydraulic testing machine was used to load the specimens. The load was varied with temperature to keep the specimen response within a linear range (initial microstrains about 20-25 micro-strains). A dynamic sinusoidal stress (continuous wave) was applied and measured through the machine load cell, whereas, the deformations were measured using spring-loaded LVDT's (Linear Variable Differential Transducers). The specimen instrumentation method used was the one developed by the ASU Research Team (36). The LVDT's were secured in place using brackets and studs glued on to the specimen; guiding rods were added to the instrumentation for alignment especially at high temperatures. A typical set-up of the test specimen instrumentation is shown in Figure 28.

Table 10. Dynamic Modulus Test Results for the AR-ACFC Mix Replicates - 70°F

Specimen ID	Dynamic Stress (kPa)	Dynamic Modulus @25 Hz (MPa)	Phase Angle @25 Hz (deg)	Axial Strain @25 Hz (mstr)	Axial Strain @0.1 Hz (mstr)	Air Void, Va (%)	Test Condition Assignment
AR-ACFC-04	50	2469	23.3	20.0	72.4	17.5	Unconfined
AR-ACFC-06	60	2849	24.0	20.7	83.9	17.7	Unconfined
AR-ACFC-07	60	3101	21.3	19.5	59.4	17.7	Unconfined
AR-ACFC-08	60	2835	26.1	20.8	74.6	18.5	Conf. 10psi
AR-ACFC-11	75	3357	21.7	22.1	90.5	18.5	Conf. 10psi
AR-ACFC-12	70	2894	29.0	24.1	94.0	18.5	Conf. 10psi
AR-ACFC-13	65	3098	24.1	20.9	70.3	18.4	Conf. 20psi
AR-ACFC-15	68	2825	25.6	23.8	87.8	18.1	Conf. 20psi
AR-ACFC-19	68	3028	25.8	22.2	82.6	18.1	Conf. 20psi
AR-ACFC-09	75	3615	30.8	20.3	77.5	17.9	Conf. 30 psi
AR-ACFC-14	75	3554	21.3	21.1	80.1	18.3	Conf. 30 psi
AR-ACFC-16	75	3874	22.2	19.5	73.7	18.4	Conf. 30 psi

6.3. Test Results and Analysis

Table E-1 through Table E-4 located in Appendix E show the test results of axial strain, dynamic modulus, and phase angle at 25 and 0.1 Hz for the ARAC Gap Graded mixture replicate specimens at each test temperature. Table E-5 through Table E-8 provide the same information for the AR-ACFC Open Graded mixture. Table E9 provides the results for the crumb rubber sample tested unconfined at 70, 100, and 130°F.

Table E-10 through Table E-18 summarize the measured dynamic modulus and phase angles obtained for each mixture and replicate specimen. These summary tables also contain the volumetric properties of each specimen/mixture (Gmm %, AC %, Va %, and aggregate type).

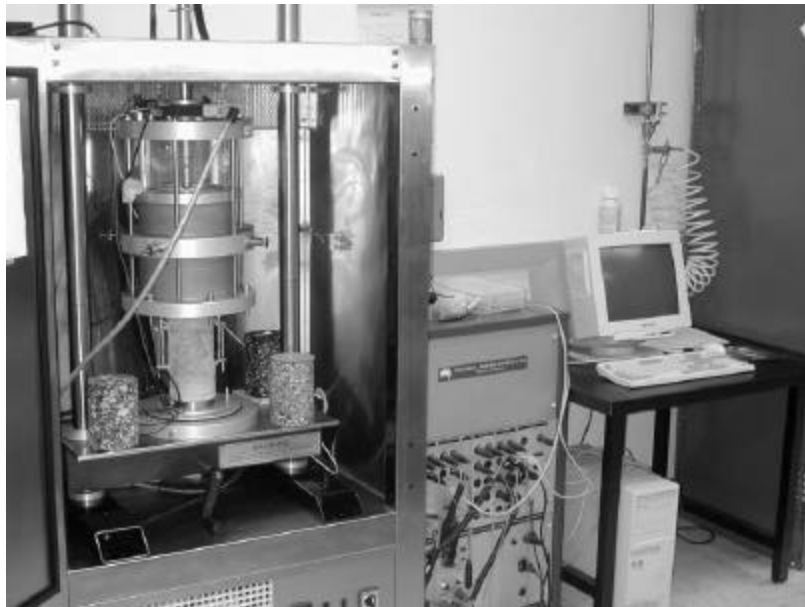
The following subsections include data analysis for the three different mixtures: ARAC-Gap Graded mixture, AR-ACFC-Open Graded mixture, and the crumb rubber specimen.

6.3.1. ARAC Gap Graded Mixture

Figure 29 through 32 are plots of (a) the effect of loading time on the measured dynamic modulus for a selected replicate test, (b) its corresponding shift factors plot, and (c) the master curve developed using the average of the three replicates. The plots show the results for the unconfined as well as the three levels of confinement (10, 20, 30 psi) tests.

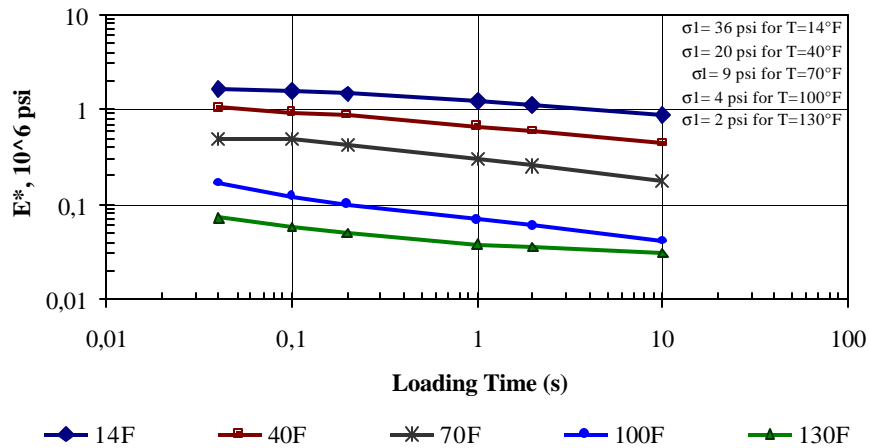


(a)

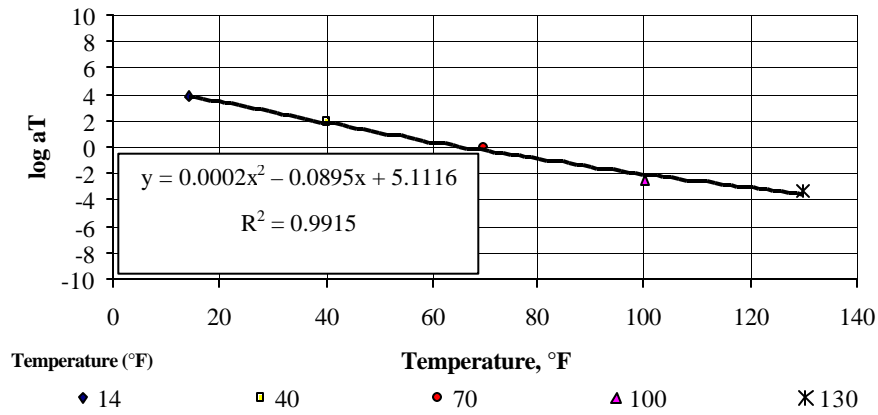


(b)

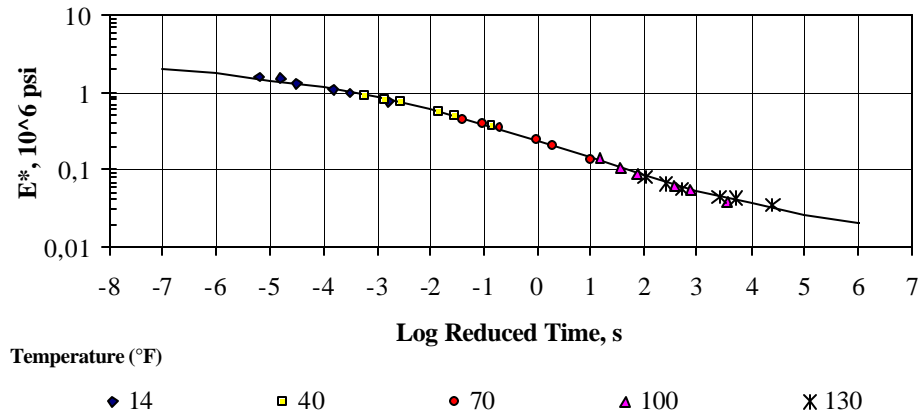
Figure 28. (a) Typical Test Instrumentation – ARAC Test Specimen (b) Typical Confined Test Set-Up



a) Effect of Loading Time and Temperature on Measured Dynamic Modulus E^* - Replicate #2

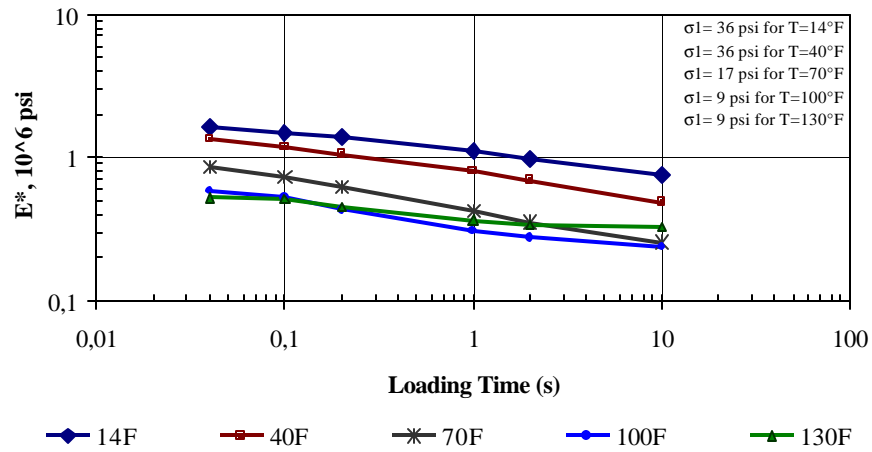


b) Shift Factors for ARAC Gap Graded Mixture (Average of three replicates)

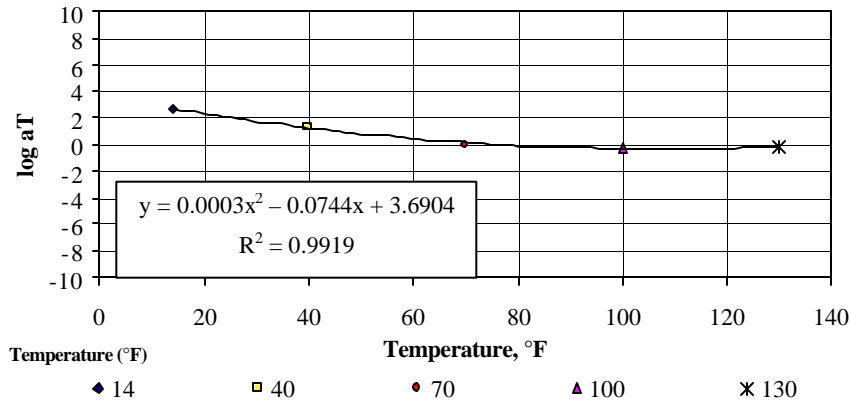


c) Master Curve for ARAC Gap Graded Mixture (Average of three replicates)

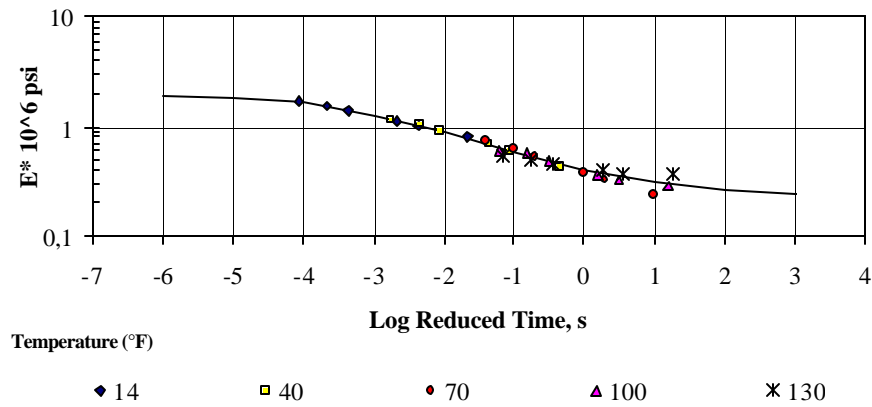
Figure 29. ARAC Gap Graded Mixture – Unconfined Test Results



a) Effect of Loading Time and Temperature on Measured Dynamic Modulus E^* - Replicate #2

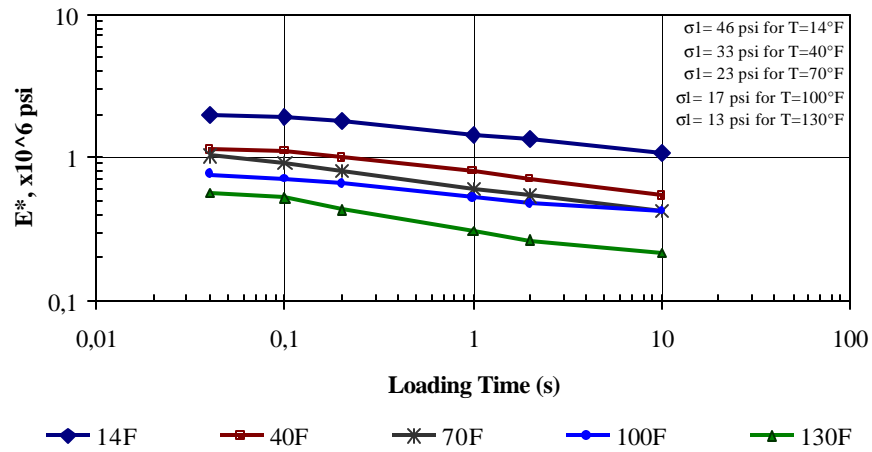


b) Shift Factors for ARAC GAP Graded Mixture (Average of three replicates)

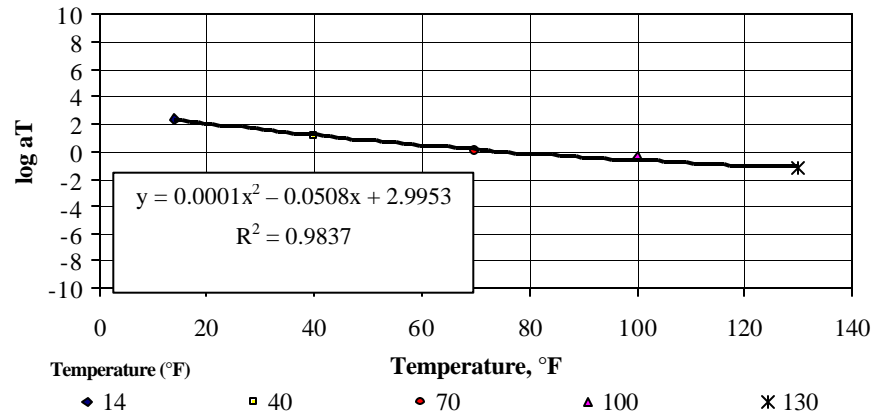


c) Master Curve for ARAC Gap Graded Mixture (Average of three replicates)

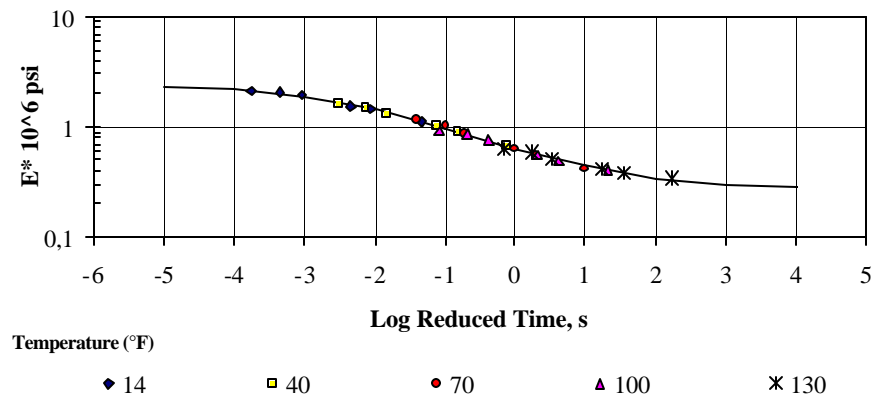
Figure 30. ARAC Gap Graded Mixture – Confined Test Results – 10 psi



a) Effect of Loading Time and Temperature on Measured Dynamic Modulus E^* - Replicate #2

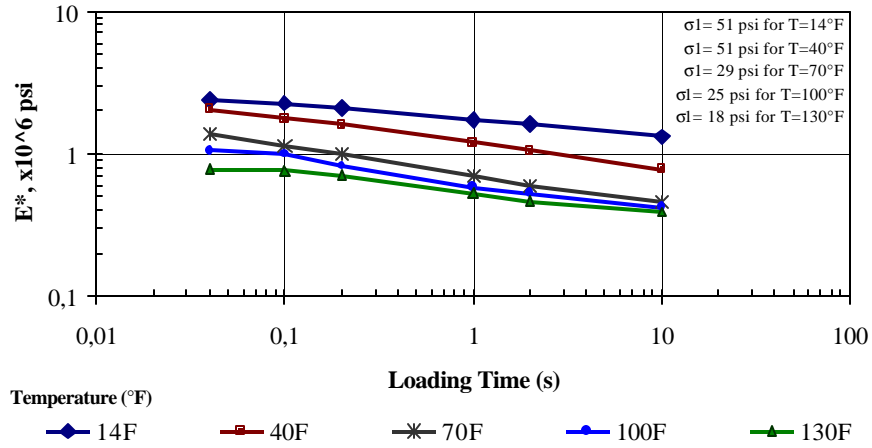


b) Shift Factors for ARAC GAP Graded Mixture (Average of three replicates)

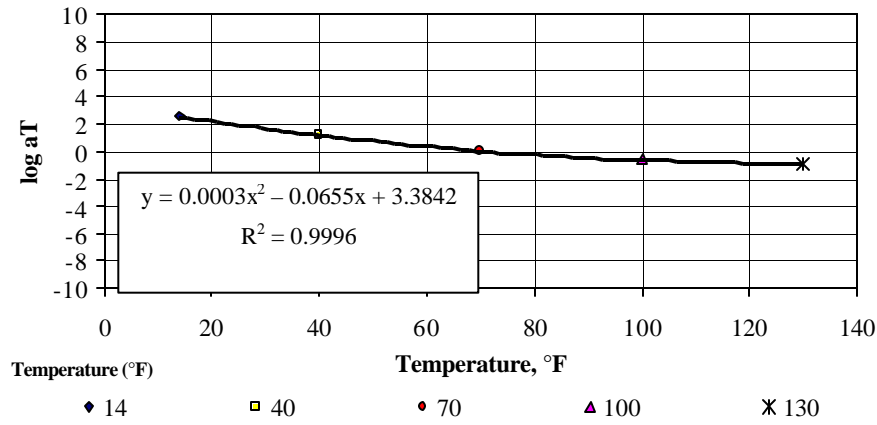


c) Master Curve for ARAC Gap Graded Mixture (Average of three replicates)

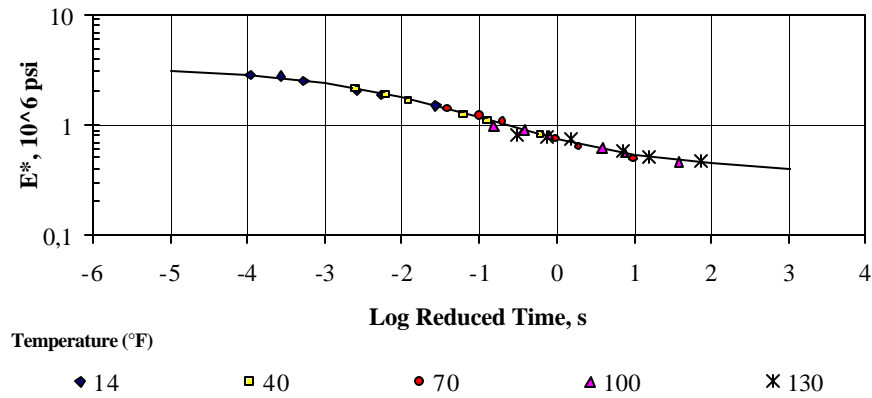
Figure 31. ARAC Gap Graded Mixture – Confined Test Results – 20 psi



a) Effect of Loading Time and Temperature on Measured Dynamic Modulus E^* - Replicate #3



b) Shift Factors for ARAC GAP Graded Mixture (Average of three replicates)



c) Master Curve for ARAC Gap Graded Mixture (Average of three replicates)

Figure 32. ARAC Gap Graded Mixture – Confined Test Results – 30 psi

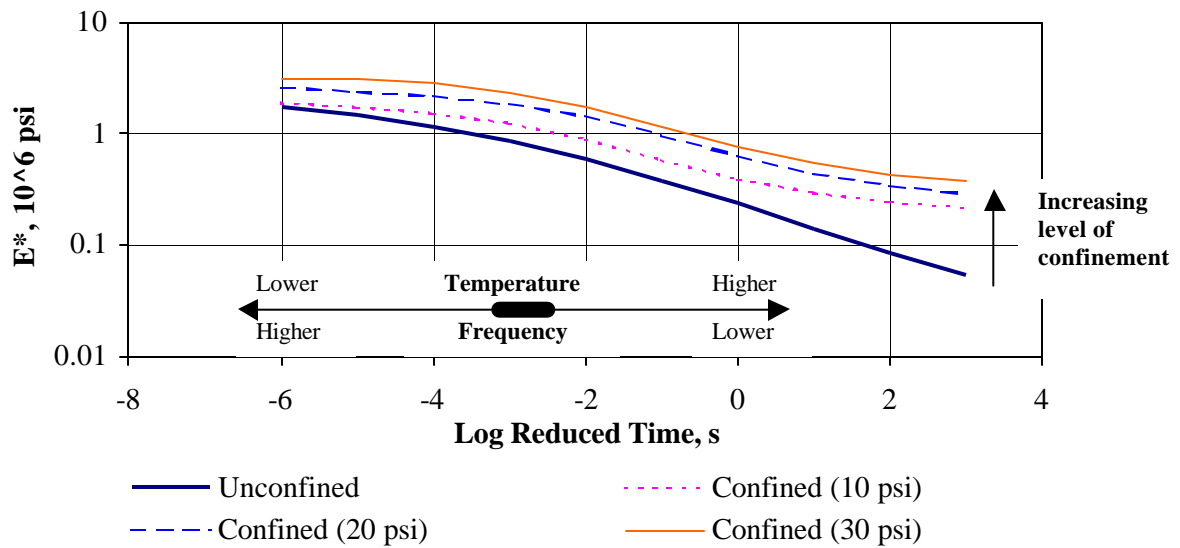


Figure 33. E* Master Curves for the ARAC Gap Graded Mixture

Figure 33 shows a comparison of the master curves results obtained for the unconfined and confined tests. Table E-19 through Table E-22 contain additional information on the regression coefficients for the master curves, and a table summarizing the data obtained for each test.

The comparison of the results for the unconfined and confined tests in Figure 33 shows that there is a significant increase in the E* values with confinement at higher temperatures and lower frequencies, compared to the low temperature part of the curve. The difference in E* results between the unconfined and confined tests at higher temperatures become less as the confinement is increased (400% increment from unconfined conditions to a 10-psi confinement, 25% from 10 to 20-psi confinement, and 11% increment from 20 to 30-psi confinement). This increment is reduced at lower

temperatures between the unconfined and confined tests, but remained significant between the different levels of confinement.

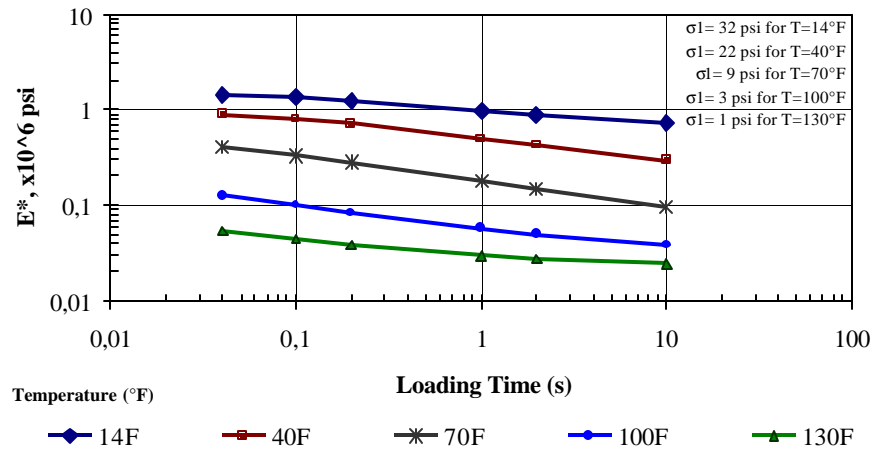
In addition, as shown in Figure 30 (a) and (b) there were cases where the E^* values of the specimens at 100 or 130 degrees were equivalent to those at 70 or 100 degrees respectively. It has been surmised that this is due in large measure to the decreased role of the asphalt cement in relationship to the increased role of the rubber particles, at higher temperatures. Further analysis on this observation is presented in Section 6.3.3.

6.3.2. AR-ACFC OPEN Graded Mixture

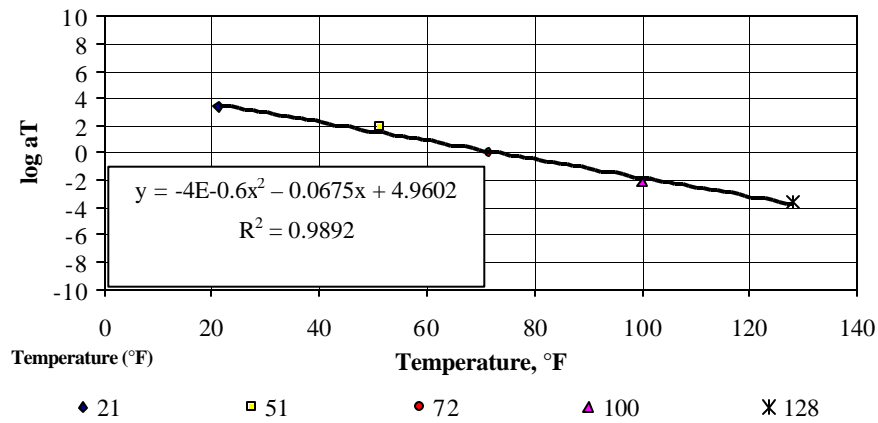
Figure 34 through 37 are plots of (a) the effect of loading time on the measured dynamic modulus for a selected replicate test, (b) its corresponding shift factors plot, and (c) the master curve developed using the average of the three replicates. The plots show the results for the unconfined as well as the three levels of confinement (10, 20, 30 psi) test. Figure 38 shows a comparison of the master curves obtained for the unconfined and confined tests. Table E-23 and Table E-26 contain additional information on the regression coefficients for the master curves, and a table summarizing the data obtained for each test.

Similar trends to the ARAC mixture were observed for the AR-ACFC mixture.

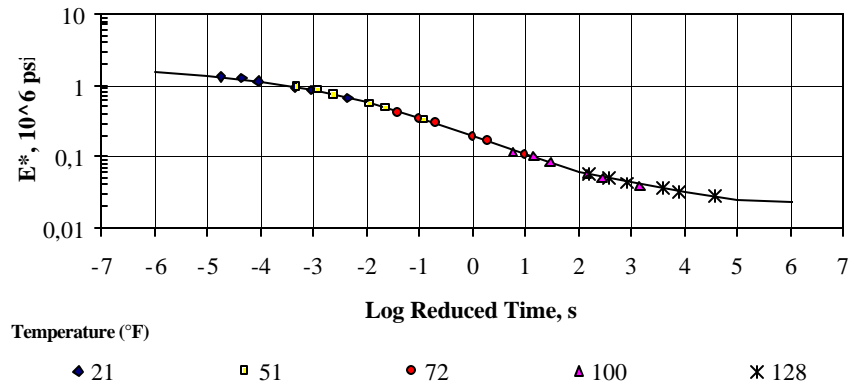
Figure 38 shows a significant increase in the E^* values with confinement at higher temperatures and lower frequencies, compared to the low temperature part of the curve.



a) Effect of Loading Time and Temperature on Measured Dynamic Modulus E^* - Replicate #2

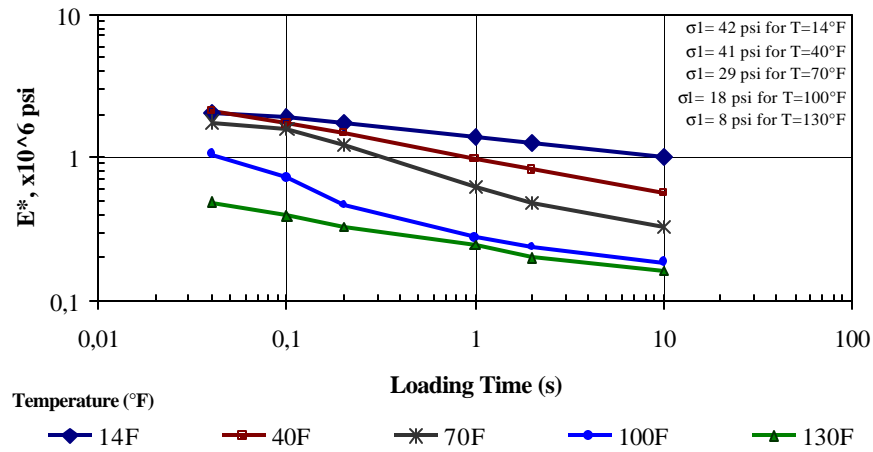


b) Shift Factors for AR-ACFC Open Graded Mixture (Average of three replicates)

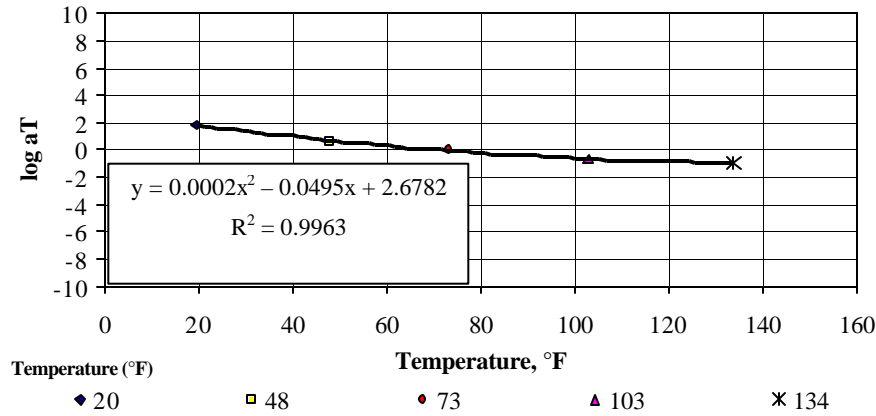


c) Master Curve for AR-ACFC Open Graded Mixture (Average of three replicates)

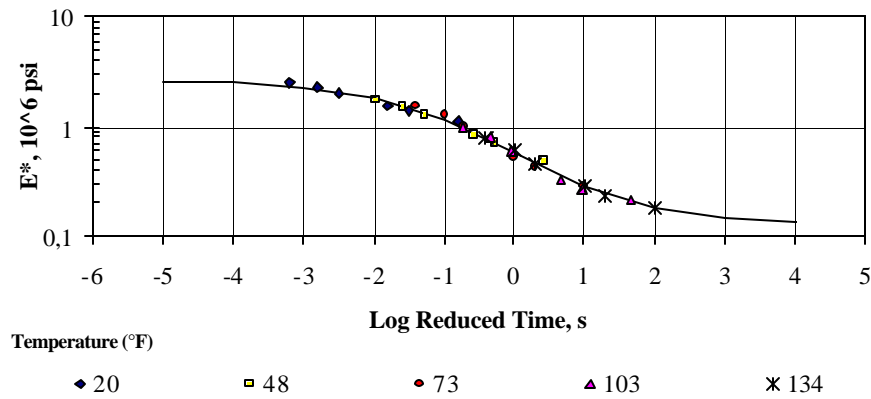
Figure 34. AR-ACFC Open Graded Mixture - Unconfined Test Results



a) Effect of Loading Time and Temperature on Measured Dynamic Modulus E^* - Replicate #1

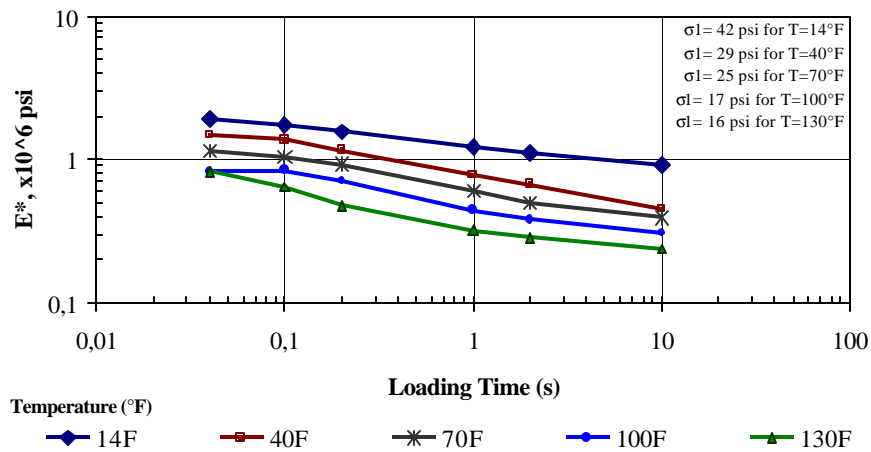


b) Shift Factors for AR-ACFC Open Graded Mixture (Average of three replicates)

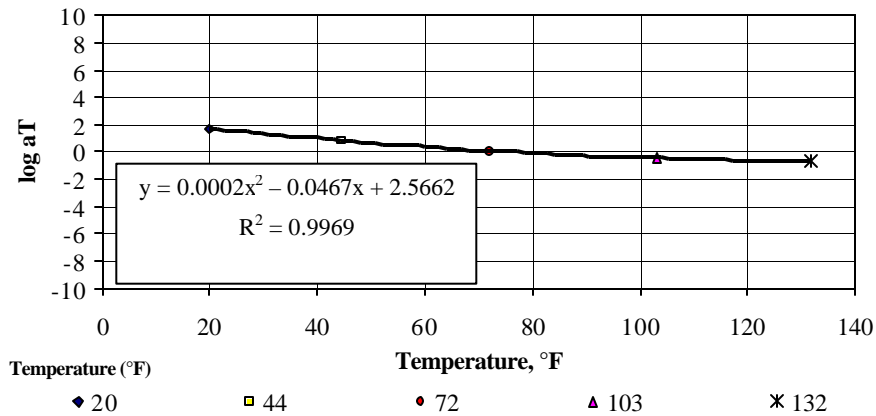


c) Master Curve for AR-ACFC Open Graded Mixture (Average of three replicates)

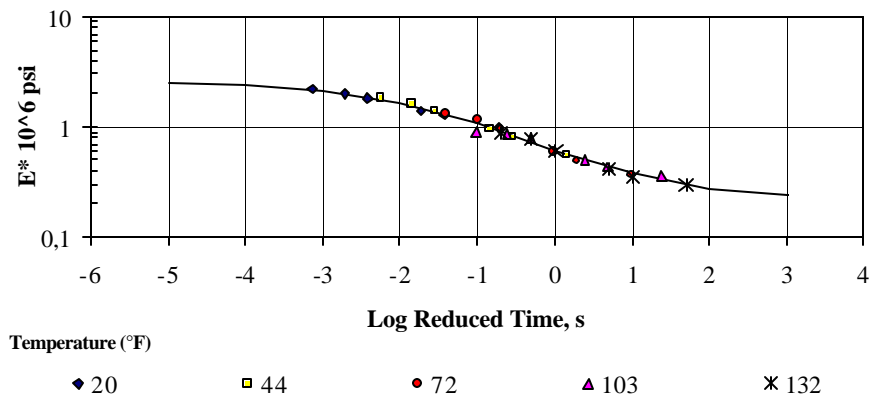
Figure 35. AR-ACFC Open Graded Mixture – Confined Test Results - 10 psi



a) Effect of Loading Time and Temperature on Measured Dynamic Modulus E^* - Replicate #3

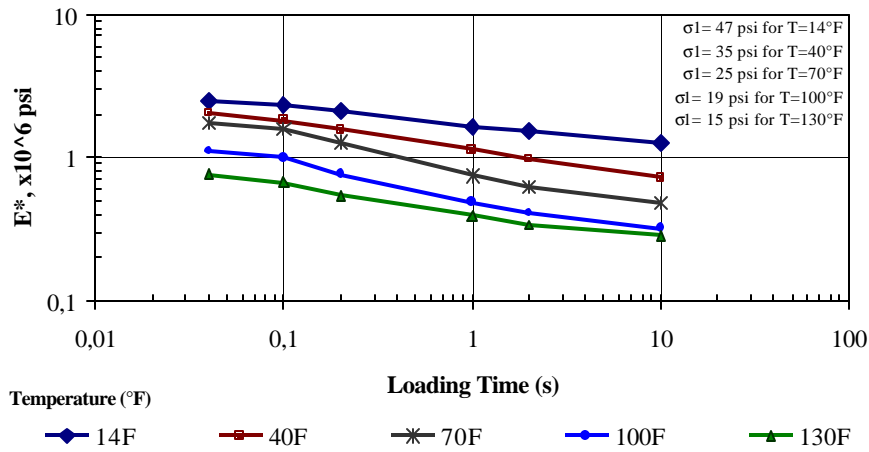


b) Shift Factors for AR-ACFC Open Graded Mixture (Average of three replicates)

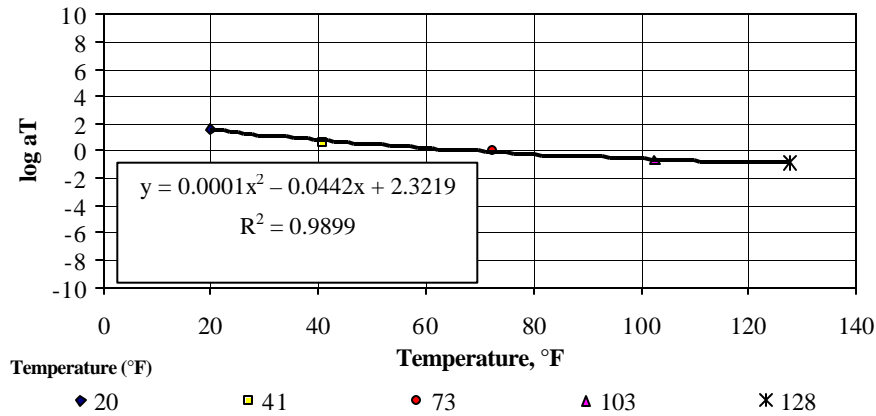


c) Master Curve for AR-ACFC Open Graded Mixture (Average of three replicates)

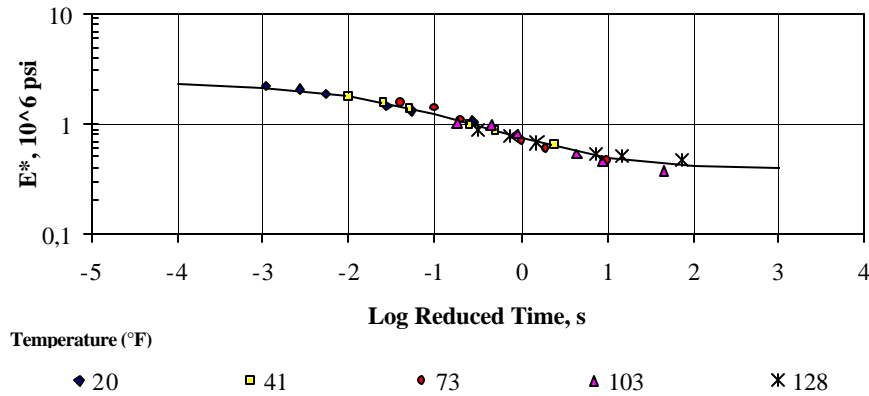
Figure 36. AR-ACFC Open Graded Mixture – Confined Test Results – 20 psi



a) Effect of Loading Time and Temperature on Measured Dynamic Modulus E^* - Replicate #1



b) Shift Factors for AR-ACFC Open Graded Mixture (Average of three replicates)



c) Master Curve for AR-ACFC Open Graded Mixture (Average of three replicates)

Figure 37. AR-ACFC Open Graded Mixture - Confined Test Results – 30 psi

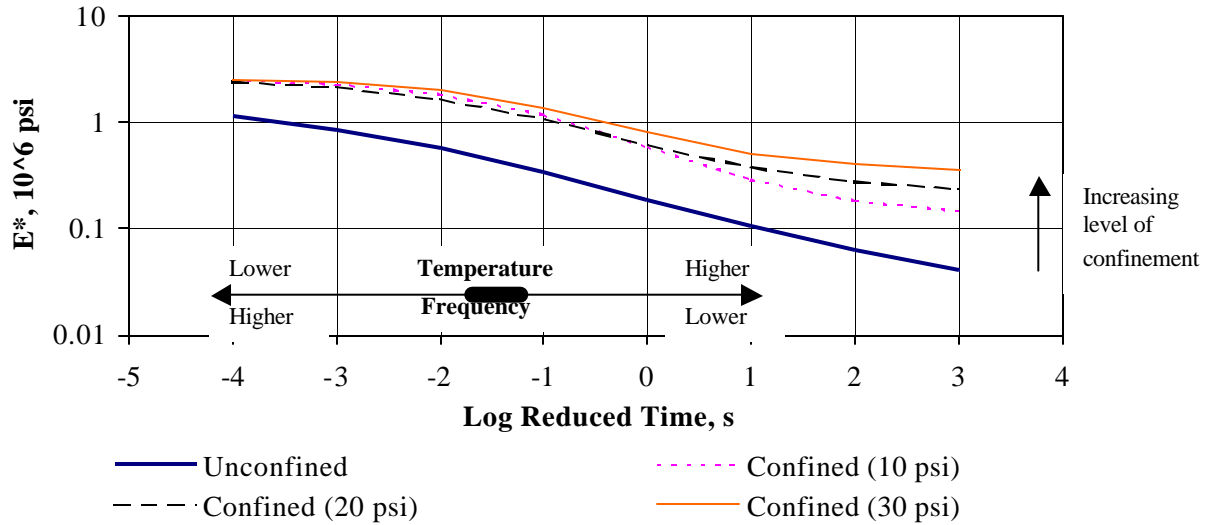


Figure 38. E^* Master Curves for the AR-ACFC Open Graded Mixture

The difference in E^* results between the unconfined and confined tests at higher temperatures, however, stay significant as the confinement level is increased (250% increment from unconfined conditions to a 10-psi confinement, 61% from 10 to 20-psi confinement, and 62% increment from 20 to 30-psi confinement). In addition, this difference between the different levels of confinements is negligible at lower (cold) temperatures. However, the difference between the unconfined and confined tests is still significant at the lower temperatures.

6.3.3. Crumb Rubber Specimen

Because of the similarity in some of the test results obtained at 100 and 130°F, that is, the insignificant change in E^* values at the higher temperatures, it was decided to conduct E^* tests on a crumb rubber specimen (80% crumb rubber and 20% urethane) and observe its behavior. Figure 39 shows the result of E^* at 70, 100, 130°F.

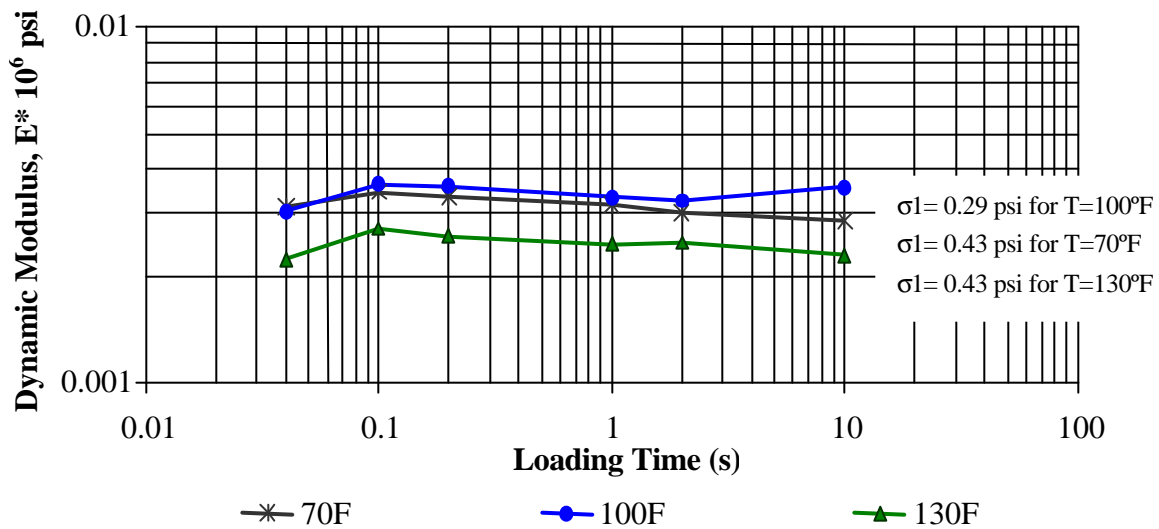


Figure 39. Crumb Rubber Sample: Effect of Loading Time and Temperature on the Measured Dynamic Modulus (Unconfined Test)

It is observed that the E^* values remain almost the same throughout the test at the different frequencies (loading time) and the three test temperatures. Note that the vertical scale of the plot highlights some differences, but in reality those differences are minimal. It can be concluded from this plot that there are no significant changes in E^* values measured for the crumb rubber specimen due to temperature or time of loading changes. These results may explain some of the behavior of the asphalt rubber mixture specimens when tested at high temperatures. One possibility for the insignificant changes in the E^* values measured for the AR mixture is that the effect of the asphalt cement on the mix is reduced at the high temperatures, and the crumb rubber start dominating the behavior of the mix at these higher temperatures.

6.4. Comparison of Asphalt Rubber and Conventional Mixtures

A conventional ADOT mixture utilizing PG 76-16 binder was used as a comparison to the AR open and gap graded mixtures. Figure 40 shows the average E^* master curves for the two AR mixtures, using unconfined tests, compared with the conventional PG 76-16 mixture master curve. As it is shown, the PG 76-16 mixture shows a higher modulus values at every temperature and frequency condition.

Figure 41 shows a similar comparison for selected values of test temperatures and loading frequencies. However, it should be also noticed that the difference in air void content between the PG 76-16 mixtures and the AR mixes had an impact on the results. Higher air voids in the mix generally result in lower modulus values. Further comparison of these mixes at similar air voids contents (specifically for the gap graded mix) is needed.

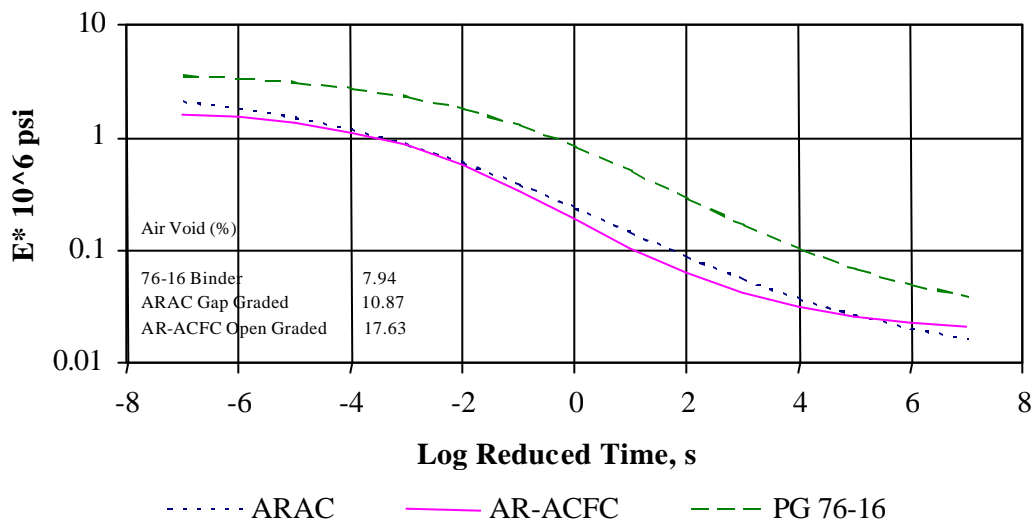


Figure 40. Unconfined Dynamic Modulus Master Curves for ARAC, AR-ACFC and Conventional PG 76-16 ADOT Mixture

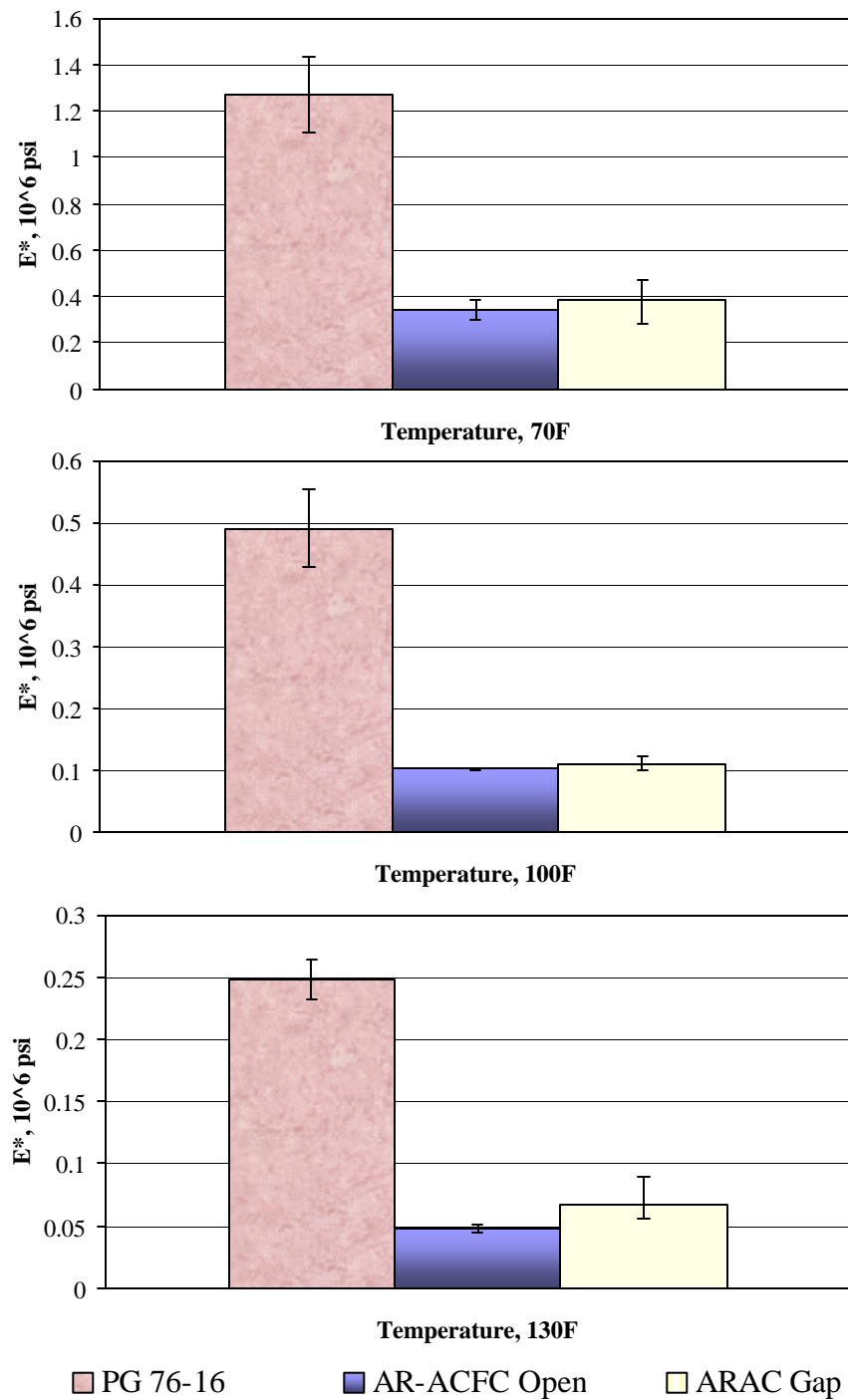


Figure 41. Comparison of Measured Dynamic Modulus E^* values at 10 Hz for the Asphalt Rubber and the PG 76-16 Mixtures at Selected Temperatures

In addition, another comparison was made using another conventional ADOT mixture. This time, the conventional mix utilized was a PG 64-22 binder with similar aggregate source and air voids content (10.53% in average). The data was available from a previous study developed at Arizona State University (38). Figure 42 shows the master curves for the three mixtures. It is observed that the modulus values are more comparable, leading to the observation that the addition of rubber indeed enhances the properties of a PG 58-22 conventional mixture. In fact, at high temperatures and lower frequencies, the AR mixture had a higher modulus than the PG 64-22 conventional mixture; at low temperatures the AR mixtures had lower modulus, both supporting the field observed performance of better resistance to deformation at high temperatures, and to cracking at low temperatures.

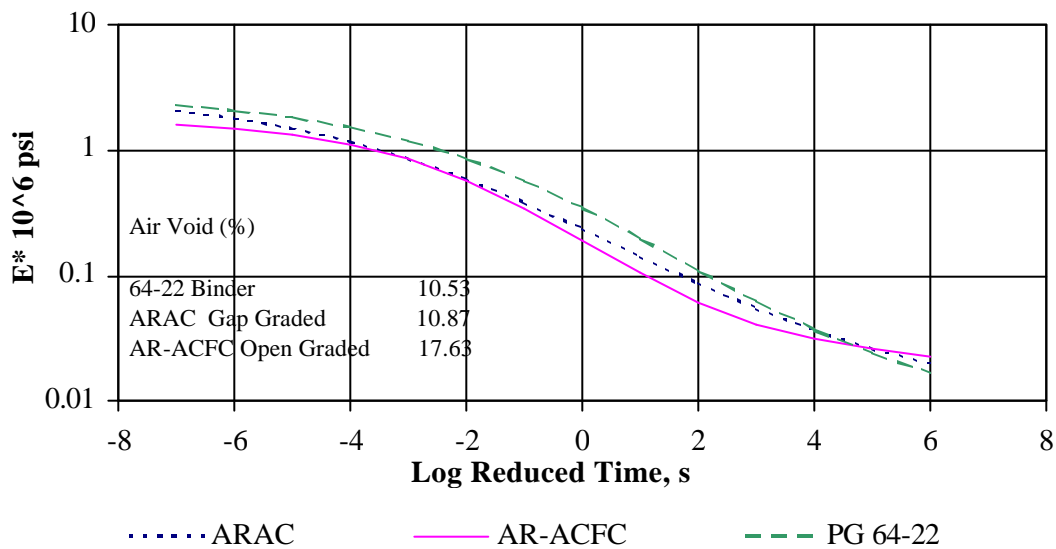


Figure 42. Unconfined Dynamic Modulus Master Curves for ARAC, AR-ACFC and Conventional PG 64-22 ADOT Mixture

6.5. Modular Ratio (R)

Using the Dynamic Complex Modulus (E^*) test results at 14°F and 100°F, both at 10 Hz, for the AR mixes and results available at ASU from previous studies (13, 10, 38), the ratio of the dynamic modulus between the different mixes and that of a reference selected mix can be calculated. A comparison table and ranking can be established for the different mixes. The ratio was calculated using the following equation:

$$R = \frac{E^*_{\text{mix}}}{E^*_{\text{Reference}}} \quad (6.6)$$

Where

R = Modular Ratio

E^*_{mix} = Dynamic Complex Modulus value for a given mixture

$E^*_{\text{Reference}}$ = Dynamic Complex Modulus value for the reference mixture

At cold temperatures, cracking is the most important consideration for an AC mixture. If the mix is too stiff, it will crack easily. Thus, to achieve the desired behavior of less or no cracking of an AC layer at a cold temperature, a lower stiffness is advisable. Therefore, in the ranking shown in Table 11 (E^* at 14°F), the best performance will be that for the mix with the lowest E^* value. Conversely, at high temperatures, rutting or permanent deformation is the most important distress that the AC mixture is affected by. Thus, the desired behavior of an AC mixture at high temperatures is to have as stiff a layer as possible. Therefore, the ranking shown in Table 12 shows that the best mix is the one that has the highest E^* at 100°F.

Table 11. Tabular Summary of the Modular Ratio at 14°F and 10 Hz

Mix ID	Binder Type	AC (%)	Va (%)	Nominal Aggregate	E* (ksi)	R	Rank
AR-ACFC	58-22 (R)	8.8	17.6	9.0-mm OG	1237	0.59	1
ARAC	58-22 (R)	6.8	10.9	19.0-mm GG	1525	0.73	2
WesTrack Section C2	64-22	4.8	9.3	12.5-mm FDGM	1642	0.80	3
ALF Lane 8	Novophalt	4.7	11.9	19.0-mm DGM	1926	0.93	4
ADOT Conventional	64-22	4.1	10.5	19.0-mm DGM	2065	1.00	5
ADOT Conventional	58-28	6.1	6.4	19.0-mm DGM	2245	1.09	6
MnRoad Cell 20	PEN 120/150	6.1	6.3	12.5-mm DGM	2715	1.32	7
ALF Lane 4	AC 20	4.9	9.7	19.0-mm DGM	2727	1.32	8
WesTrack Section C24	64-22	5.8	7.5	12.5-mm CDGM	2833	1.37	9
ADOT Conventional	76-16	4.9	7.9	19.0-mm DGM	3044	1.47	10
ALF Lane 3	AC-5	4.8	7.7	19.0-mm DGM	4101	1.986	11

where: DGM = Dense Graded Mixture

CGDM = Coarse Dense Graded Mixture

FDGM = Fine Dense Graded Mixture

GG = Gap Graded Mixture

OG = Open Graded Mixture

Table 12. Tabular Summary of the Modular Ratio at 100°F and 10 Hz

Mix ID	Binder Type	AC (%)	Va (%)	Nominal Aggregate	E* (ksi)	R	Rank
ADOT Conventional	76-16	4.9	7.9	19.0-mm DGM	490	4.01	1
WesTrack Section R4	64-22	5.2	6.6	12.5-mm FDGM	409	3.35	2
WesTrack Section R23	64-22	5.8	4.9	12.5-mm CDGM	327	2.68	3
ALF Lane 8	Novophalt	4.7	11.9	19.0-mm DGM	267	2.19	4
ALF Lane 12	AC-20	4.1	7.4	37.5-mm DGM	215	1.76	5
ADOT Conventional	58-28	6.1	6.4	19.0-mm DGM	196	1.61	6
ADOT Conventional	64-22	4.1	10.5	19.0-mm DGM	122	1.00	7
MnRoad Cell 20	PEN 120/150	6.1	6.3	12.5-mm DGM	115	0.94	8
ARAC	58-22 (R)	6.8	10.9	19.0-mm GG	107	0.88	9
AR-ACFC	58-22 (R)	8.8	17.6	9.0-mm OG	101	0.83	10

where: DGM = Dense Graded Mixture

CGDM = Coarse Dense Graded Mixture

FDGM = Fine Dense Graded Mixture

GG = Gap Graded Mixture

OG = Open Graded Mixture

For this analysis, the PG 64-22 conventional ADOT mixture, mentioned in the previous section, was used as the reference mixture. At the selected temperature of 14 °F, Table 11 shows that the AR mixes have the lowest E^* values (lowest modular ratio). The lower the modulus at low temperatures, the better the mix resistance to cracking. Table 12 shows the modular ratio at 100°F. The AR mixes are ranked at the bottom of the table. This was attributed to lower stiffness values (from the unconfined tests) observed for these mixtures at high temperatures, and also because these mixes had much higher air void content. However, the field experience with these mixes observed from several projects show that the AR mixtures have excellent performance (great resistance to permanent deformation) at high temperatures. Since the field mixtures are subjected to different levels of confinement, it was decided to further compare the E^* test results at confined testing conditions. Test results using 20-psi level of confinement were available for conventional and AR mixtures (10). For this comparison the ARAC mixture was chosen as the reference mixture. Table 13 and 14 show the modular ratio (10 Hz) at 14°F and 100°F, respectively. It is observed that the AR mixes ranked at the top of Table 13, showing the best performance (lowest dynamic modulus) similar to the unconfined test results. However, Table 14 shows that the ranking is opposite to what was observed in the unconfined tests. The ranking of the AR mixture was increased higher than those of the conventional mixtures. The AR-ACFC Open Graded mixture had the highest stiffness followed by the ARAC Gap Graded mixture. Since this is what is being observed in the field, it is concluded that the confined E^* tests better describe the performance of the AR mixture than the unconfined E^* tests.

Table 13. Tabular Summary of the Modular Ratio at 14°F and 10 Hz for 20-psi Confined Test Results

Mix ID	Binder Type	AC (%)	Va (%)	Nominal Aggregate	E* (ksi)	R	Rank
ARAC	58-22 (R)	6.8	10.9	19.0-mm Gap Graded	1498	1.00	1
AR-ACFC	58-22 (R)	8.8	17.6	9.0-mm Open Graded	1615	1.08	2
ALF Lane 3	AC-5	4.8	7.7	19.0-mm DGM	1947	1.30	3
ALF Lane 8	Novophalt	4.7	11.9	19.0-mm DGM	2351	1.57	4
WesTrack Section C2	64-22	4.8	9.3	12.5-mm FDGM	4233	2.83	5
WesTrack Section C24	64-22	5.8	7.5	12.5-mm CDGM	4601	3.07	6
ALF Lane 4	AC-20	4.9	9.7	19.0-mm DGM	6137	4.10	7

where:

- DGM = Dense Graded Mixture
- CGDM = Coarse Dense Graded Mixture
- FDGM = Fine Dense Graded Mixture
- GG = Gap Graded Mixture
- OG = Open Graded Mixture

Table 14. Tabular Summary of the Modular Ratio at 100°F and 10 Hz for 20-psi Confined Test Results

Mix ID	Binder Type	AC (%)	Va (%)	Nominal Aggregate	E* (ksi)	R	Rank
AR-ACFC	58-22 (R)	8.8	17.6	9.0-mm Open Graded	875	1.02	1
ARAC	58-22 (R)	6.8	10.9	19.0-mm Gap Graded	862	1.00	2
WesTrack Section R4	64-22	5.2	6.6	19.0-mm FDGM	812	0.94	3
ALF Lane 12	AC-20	4.1	7.4	37.5-mm DGM	664	0.77	4
WesTrack Section R23	64-22	5.8	4.9	19.0-mm CDGM	518	0.60	5
ALF Lane 8	Novophalt	4.8	7.7	19.0-mm DGM	314	0.37	6

where:

DGM = Dense Graded Mixture

CGDM = Coarse Dense Graded Mixture

FDGM = Fine Dense Graded Mixture

GG = Gap Graded Mixture

OG = Open Graded Mixture

6.6. Witczak E* Predictive Equation Analysis

Currently, in the development of the new AASHTO 2002 Pavement Design Guide, the Dynamic Complex Modulus of HMA pavements (E*) is one of the fundamental engineering properties used for asphalt mixtures characterization. One of the hierarchical levels for inputting E* in the analysis program is to use the Witczak Dynamic Modulus Predictive Equation (10,36). The equation uses properties of the binder, aggregates; and some volumetric properties of the mixture as an input. Over the last 30 years, the Witczak Dynamic Modulus Predictive Equation evolved and became one of the most rational and comprehensive equation (36). The last two updates were in 1996 by Fonseca and Witczak (37), the equation included a database of 1430 points covering 149 types of conventional asphalt mixes; and in 1999, Andrei and Witczak added 56 additional mixes, 34 of which were modified, and increased the database to 2750 points.

The 1996 Witczak Dynamic Modulus Predictive Equation is shown below:

$$\begin{aligned} \text{Log}E = & -0.261 + 0.008225 \cdot p_{200} - 0.00000101 \cdot (p_{200})^2 + 0.00196 \cdot p_4 - 0.03157 \cdot V_a - \\ & - 0.415 \cdot \frac{V_{b_{eff}}}{(V_{b_{eff}} + V_a)} + \frac{1.87 + 0.002808 \cdot p_4 + 0.0000404 \cdot p_{38} - 0.0001786 \cdot (p_{38})^2 + 0.0164 \cdot p_{34}}{1 + e^{(-0.716 \cdot \log(f) - 0.7425 \cdot \log(\eta))}} \end{aligned} \quad (6.7)$$

The 1999 current version is

$$\begin{aligned} \text{Log}E = & -1.249937 + 0.029232 \cdot p_{200} - 0.001767 \cdot (p_{200})^2 - 0.002841 \cdot p_4 - 0.058097 \cdot V_a - \\ & - 0.802 \cdot \frac{V_{b_{eff}}}{(V_{b_{eff}} + V_a)} + \frac{3.87 - 0.0021 \cdot p_4 + 0.003958 \cdot p_{38} - 0.000017 \cdot (p_{38})^2 + 0.005470 \cdot p_{34}}{1 + e^{(-0.603313 - 0.31335 \cdot \log(f) - 0.393532 \cdot \log(\eta))}} \end{aligned} \quad (6.8)$$

where:

- E Asphalt Mix Dynamic Modulus, in 10^5 psi
- η Bitumen viscosity in 10^6 poise (at any temperature, degree of aging)
- f Load frequency in Hz
- V_a % air voids in the mix, by volume
- V_{b_{eff}} % effective bitumen content, by volume
- p₃₄ % retained on the 3/4 inch sieve, by total aggregate weight (cumulative)
- p₃₈ % retained on the 3/8-inch sieve, by total aggregate weight (cumulative)
- p₄ % retained on the No. 4 sieve, by total aggregate weight (cumulative)
- p₂₀₀ % passing the No. 200 sieve, by total aggregate weight

It is important to notice that both versions not only differ in the value of the coefficients, but also in the number of coefficients: 13 parameters were used for the 1996 version, whereas 14 parameters were used for the current version. This had an impact on the analysis in this report, which will be explained in later sections.

The purpose of this part of the analysis was to evaluate the applicability of the Predictive Equation to the asphalt rubber (AR) mixtures. Primarily because the predictive equation was calibrated with data that did not include data representing AR mixtures, nor included mixtures with high air void content. The actual laboratory measurements of the E^* values presented in the previous sections (6.3.1 and 6.3.2), which were obtained at different temperatures, frequencies, and levels of confinement, were compared with predicted

values computed using the Witczak Predictive Equation. The results are discussed in the next section.

6.6.1. Assessing the applicability of the current version of the Predictive Equation on the Asphalt Rubber mixtures

The predicted E^* values for the AR mixtures were obtained using the volumetric properties of the AR mixtures (VA%, aggregate gradation, $V_{beff}\%$). The input for the predictive equation also required for the AR binder. These were established from the conventional binder tests outlined in Chapter 2. Table 15 contains a summary of the parameters used in the Witczak Dynamic Modulus Predictive Equation.

6.6.1.1. Unconfined Test Results

Figure 43 and 44 show the plots of predicted versus measured E^* obtained for the unconfined tests in both arithmetic and logarithmic spaces. It is quite clear that the AR-ACFC mixture was not well predicted by the equation, while the ARAC mixture was well predicted and represented with an $R^2 = 0.95$. However, in the log-space plot, there is a tendency for the equation to over predict the E^* values at medium-to-high temperature range, and medium-to-low frequencies for both mixtures. Using the 1999 version of the Predictive Equation, the ARAC Gap Graded had an adjusted $R^2 = 0.95$ and a Se/Sy ratio of 0.25; while the statistics were $R^2 = 0.19$ and a Se/Sy ratio of 0.98 for the AR-ACFC Open Graded mixture. For both mixtures combined, the statistics were an $R^2 = 0.56$ and a Se/Sy ratio of 0.69 was obtained.

Table 15. Input Parameters of ARAC and ACFC Mixtures for the Witczak Dynamic Modulus Predictive Equation

Characteristic Material Property		ARAC Gap Graded	AR-ACFC Open Graded
Viscosity	A	-2.4795	-2.4795
	VTs	7.6903	7.6903
Gradation (% Passing)	$\frac{3}{4}$	100	100
	$\frac{3}{8}$	67	100
	#4	39	38
	#200	2.8	2.4
VA (%)		10.87	17.63
Asphalt Binder Percentage (%)		6.8	8.8

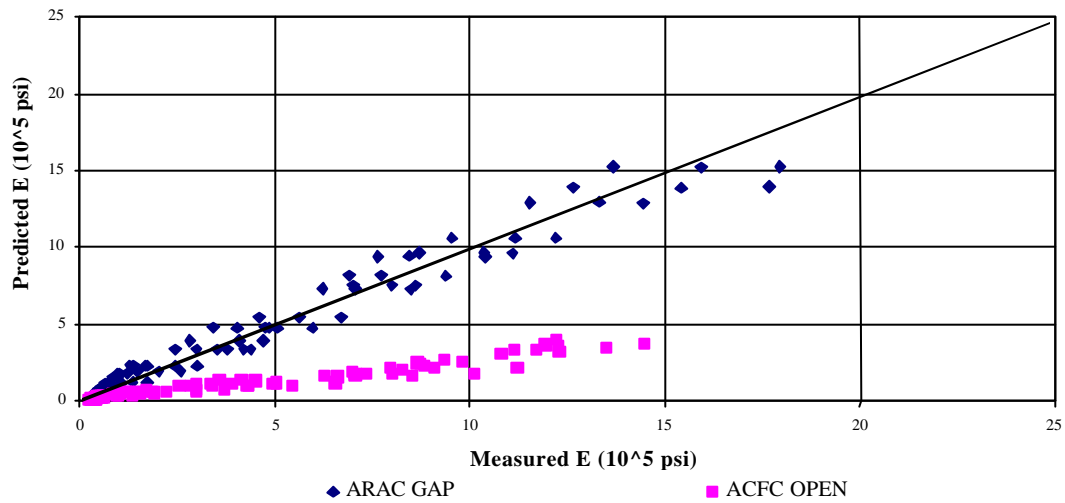


Figure 43. Comparison of Predicted and Measured Dynamic Modulus Values for the Asphalt Rubber Mixtures Using Current Version (1999) of the Witczak Predictive Equation – Arithmetic Space

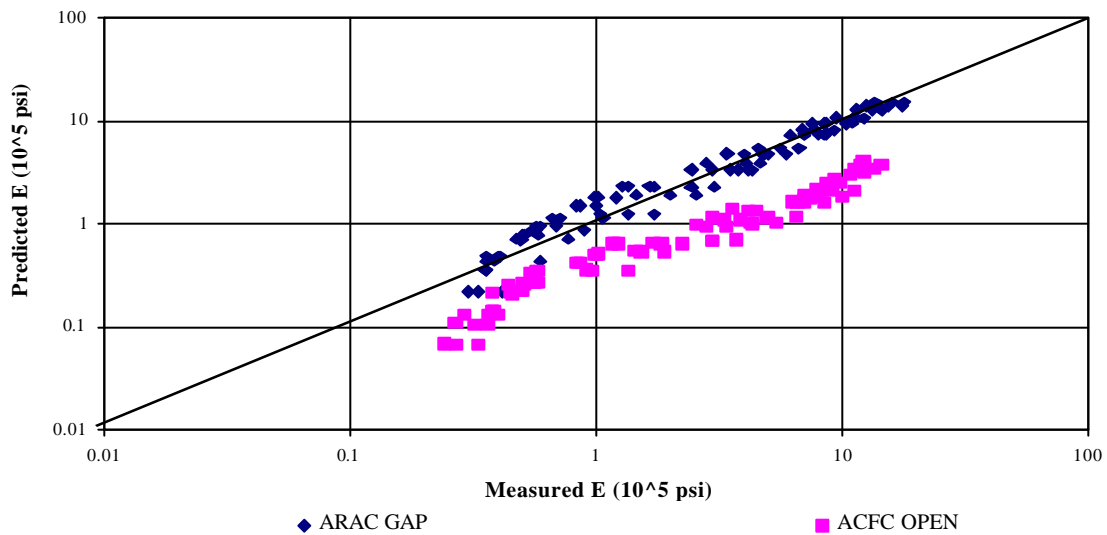


Figure 44. Comparison of Predicted and Measured Dynamic Modulus Values for the Asphalt Rubber Mixture Using Current Version (199) of the Witczak Predictive Equation – Logarithmic Space

The plots clearly show the differences between the results of ARAC and AR-ACFC mixtures. It is also important to realize that both mixtures had the same binder (58-22 with crumb rubber), but had different aggregate gradation and air voids content. In 1999, Andrei and Witczak found that several mixtures with the same type of binder but with different aggregate gradations had quite different results (36). In addition, further evaluation of the aggregate gradation of the AR mixtures and the mixtures in the Predictive Equation database showed that the AR-ACFC mixture was not represented in the database, thus forcing extrapolation and reducing the accuracy in prediction.

In the same way, the air voids (V_a) content played a key role in these differences. The range of different air void contents for the mixes in the database by Andrei and Witczak typically ranged between 5% to 10%. Thus, considering only the air void range, the model will have a good E^* prediction for mixtures with V_a lower than 8% and a fair prediction for mixtures up to $V_a = 12\%$. The ARAC mixture ($V_a = 10.87\%$) was represented in the calibration model, and thus the model provided a good prediction. On the other hand, the AR-ACFC mixture ($V_a = 17.63\%$) had no representation in the model and the E^* prediction did not have good prediction.

6.6.1.2. Confined Test Results

The results from the confined laboratory tests showed that the measured E^* values were higher than those predicted by the equation. Since the difference of predicted/measured E^* values for these levels of confinement was so significant, and the fact that the Witczak

Equation was calibrated with data obtained from unconfined tests, no further analysis was performed with the confined test results.

6.6.2. Witczak et al. Dynamic Modulus Predictive Equation only for AR Mixtures

Because the current version of the predictive equation did not predict with sufficient accuracy the AR-ACFC mixture, and there was a bias in the prediction for both mixtures at the lower frequencies and higher temperatures; an additional effort to revise the coefficient of the equation for AR mixtures was conducted even though the ARAC mixture was well predicted ($R^2 = 0.95$). Nonlinear optimization of the regression coefficients in the logarithmic space was made, using the same format of the equation (number of coefficients) as calibrated by Andrei and Witczak (36). Equation 6.9 shows the new coefficients developed for the AR mixtures alone, and Figure 45 and 46 show the predicted/measured plot for the AR mixtures using this equation.

Proposed Witczak Dynamic Modulus Predictive Equation for Asphalt Rubber mixtures

$$\begin{aligned} \text{Log}E = & -1.047299 - 1.393676 \cdot p_{200} - 12.930698 \cdot (p_{200})^2 + 0.388983 \cdot p_4 - 0.435006 \cdot V_a + \\ & - 0.1956 \cdot \frac{V_{b_{eff}}}{(V_{b_{eff}} + V_a)} + \frac{4.11 - 2.329 \cdot p_4 + 3.4602 \cdot p_{38} - 0.048965 \cdot (p_{38})^2 + 0.005470 \cdot p_{34}}{1 + e^{(-0.003991 - 0.006156 \cdot \log(f) - 0.316338 \cdot \log(\eta))}} \end{aligned} \quad (6.9)$$

As it can be seen from the plot, this new equation with modified coefficients provides good prediction for both the ARAC and AR-ACFC mixtures. The ARAC mixture had an $R^2 = 0.95$ and a Se/Sy ratio of 0.24 while the AR-ACFC mixture statistics were: $R^2 = 0.96$ and a Se/Sy ratio of 0.22, all in the logarithmic space. Finally, both mixes together had an

$R^2 = 0.81$ and a Se/Sy ratio of 0.45 in the arithmetic space and an $R^2 = 0.96$ and a Se/Sy ratio of 0.22 in the logarithmic space.

6.7. Summary of the Dynamic Modulus Tests

Several tests were performed to obtain the Dynamic (Complex) Modulus properties of two Asphalt Rubber (AR) mixtures studied: ARAC Gap Graded and AR-ACFC Open Graded mixtures. Both mixtures utilized a base binder grade of PG 58-22. Additionally, a crumb rubber specimen consisting of 80% crumb rubber and 20% urethane was tested to verify the behavior of AR mixtures at high temperatures. There were cases where the dynamic modulus values at 100 or 130°F were equivalent. It has been surmised that this is due in large measure to the decreased role of the asphalt cement in relationship to the increased role of the rubber particles at higher temperatures.

In addition, unconfined dynamic modulus test results for the two AR mixtures were compared with available test results for conventional mixtures. The two conventional ADOT dense graded mixes include a mix with a PG 76-16 binder, and another one with a PG 64-22 binder. The AR mixtures had generally lower modulus values compared to the PG 76-16 mixture; while they had comparable modulus results with the PG 64-22 mixture. A modular ratio was calculated for the two AR mixtures as well as for several other mixtures available at ASU's database. The modular ratio used the modulus values of a conventional PG 64-22 mixture as a reference, and ranking of the several mixtures were done at 14°F and 100°F, using the test frequency results at 10 Hz.

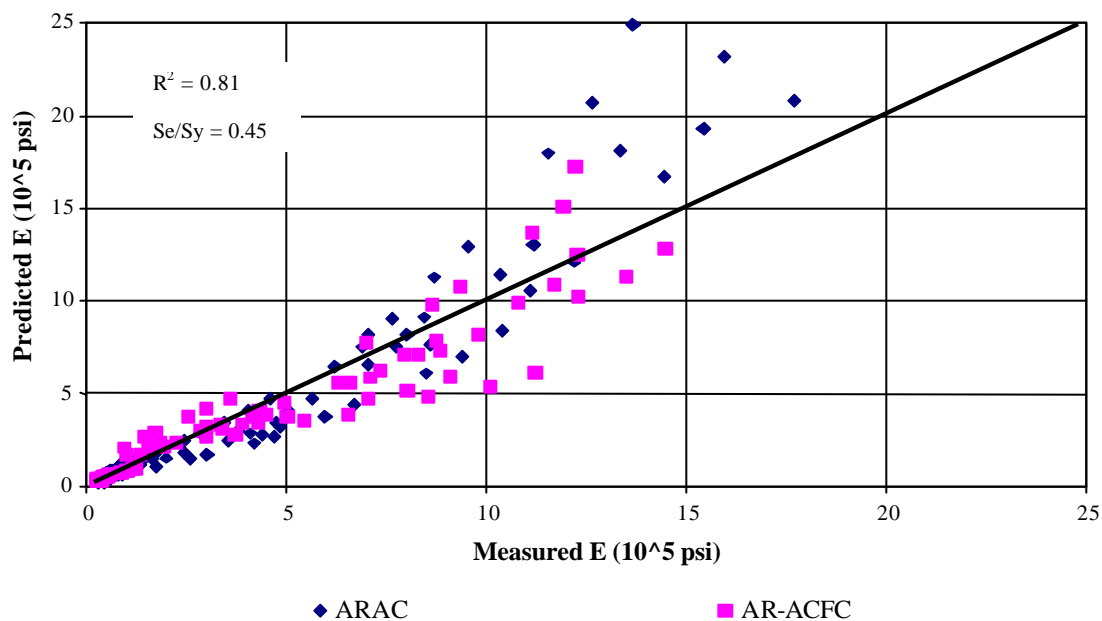


Figure 45. Predicted vs. Measured Dynamic Modulus Values for the AR Mixtures with New Equation Coefficients – Arithmetic Space

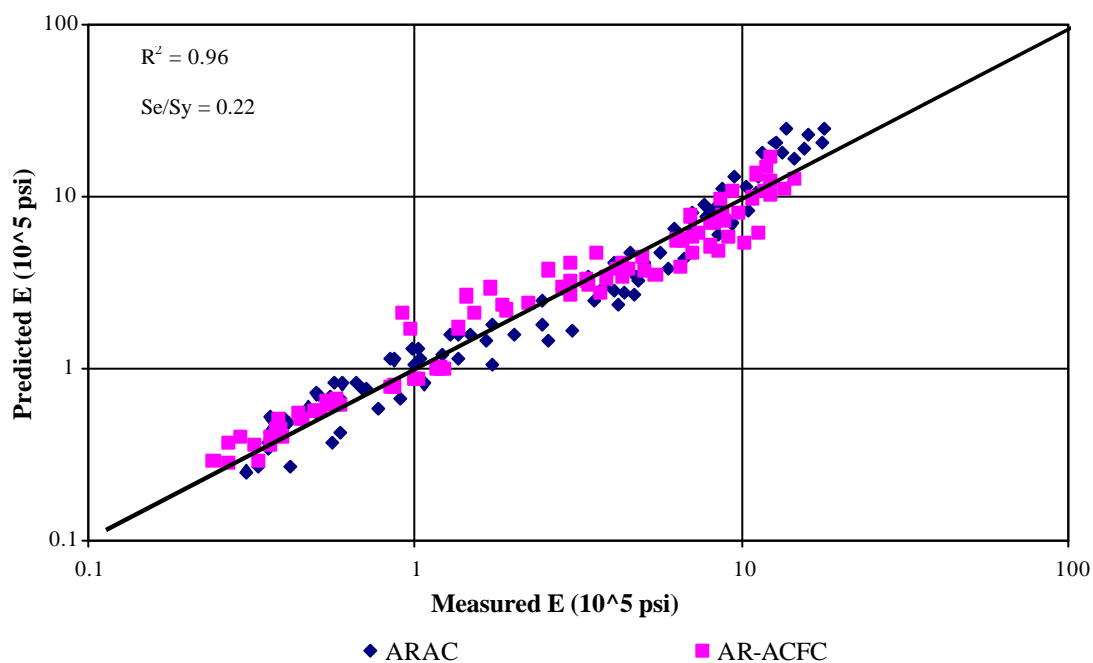


Figure 46. Predicted vs. Measured Dynamic Modulus Values for the AR Mixtures with New Equation Coefficients. – Logarithmic Space

At low temperatures, the AR exhibited the lowest modular ratio (lowest stiffness) and therefore the best performance against cracking. At high temperatures, the unconfined test results did not show any disadvantage of using the AR mixtures as the results yielded low stiffness values (lower modular ratio).

However, when a comparison of the stiffness/modular ratio, was made using the confined test results, the AR mixtures showed the highest stiffness (highest modular ratio) and therefore the best expected performance against permanent deformation. This was an important finding, since this type of behavior (ranking order of mixes) is what is being observed in the field.

Finally, the Witczak Dynamic (Complex) Modulus Predictive Equation was used to check if the Asphalt Rubber mixtures response could be predicted accurately by the predictive equation. It was found that the ARAC mixture could be predicted accurately, while the AR-ACFC was under predicted by the equation. It was supposed that these results were because mixtures that form the Predictive Equation database represented the volumetric characteristics of the ARAC mixture, but did not represent the volumetrics and gradation of the AR-ACFC mixture. An attempt was made to come up with tentative revised coefficients, which would be valid for Asphalt Rubber mixtures. Only the unconfined test results were used in this effort, since the equation was calibrated only with unconfined E^* test results. Despite the limited number of tests used for this new calibration, the revised coefficient and prediction were satisfactory.

Based on the laboratory test results and observations made in this research study, the following conclusions can be made:

- The dynamic modulus tests results obtained in this study showed that the use of crumb rubber modified binders enhances the properties of the asphalt mixture, both at low and high temperatures.
- When conducting dynamic modulus tests on asphalt rubber mixtures using different levels of confinement, a significant increase in the modulus values is observed at high temperatures and low-test frequencies. The increment was not as significant when the test was performed at low temperatures for the AR-ACFC open graded mix.
- When comparing the E^* results at different levels of confinement at high temperatures and low frequencies, it was found that for the ARAC mixture an increment as high as 400% is obtained when changing from the unconfined test to the 10-psi confined test. This increment is drastically reduced as the confinement is increased (25% and 12% when changing from 10 psi to 20 psi and 20 psi to 30 psi, respectively). For the AR-ACFC mixture, these changes are 250%, 61% and 62%, respectively showing that the level of confinement is still considerable for this mixture.
- For some test specimens, it seemed that they were not affected by an increase in temperature from 70 to 130°F or loading frequency. Thus, a crumb rubber specimen (80% crumb rubber and 20% urethane) was tested to verify the behavior of the crumb rubber component under changing conditions of temperature and loading

frequency. It was found that the crumb rubber specimen was unaffected by either of these factors, supporting the research team suspicion that the crumb rubber may have dominated the specimens performance at higher temperatures at the same time when the binder contribution becomes less.

- The Witczak Dynamic (Complex) Modulus Predictive Equation was valid for the ARAC mixture. This was attributed to the fact that the database used for the Predictive Equation had mixtures with similar characteristics (volumetrics) to those for the ARAC mixture. On the other hand, the Predictive Equation was not valid for the AR-ACFC mixture. This was essentially due to its aggregate gradation and the air void content, as both were not represented in the database used for developing the equation.

7. CRACKING TESTS

7.1. FATIGUE CRACKING TESTING

7.1.1. Background for the Flexural Beam Fatigue Test

One objective of this study was to start developing a database of typical ADOT AR mixture fatigue properties and parameters for use with the implementation of the 2002 AASHTO Design Guide. Load associated fatigue cracking is one of the major distress types occurring in flexible pavement systems. The action of repeated loading caused by traffic induced tensile and shear stresses in the bound layers, which will eventually lead to a loss in the structural integrity of a stabilized layer material. Fatigue initiated cracks at points where critical tensile strains and stresses occur. Additionally, the critical strain is also a function of the stiffness of the mix. Since the stiffness of an asphalt mix in a pavement layered system varies with depth; these changes will eventually effect the location of the critical strain that varies with depth; these changes will eventually effect the location of the critical strain that causes fatigue damage. Once the damage initiates at the critical location, the action of traffic eventually causes these cracks to propagate through the entire bound layer.

Over the last 3 to 4 decades of pavement technology, it has been common to assume that fatigue cracking normally initiates at the bottom of the asphalt layer and propagates to the surface (bottom-up cracking). This is due to the bending action of the pavement layer that results in flexural stresses to develop at the bottom of the bound layer. However, numerous recent worldwide studies have also clearly demonstrated that fatigue cracking

may also be initiated from the top and propagates down (top-down cracking). This type of fatigue is not as well defined from a mechanistic viewpoint as the more classical “bottom-up” fatigue. In general, it is hypothesized that critical tensile and/or shear stresses develop at the surface and cause extremely large contact pressures at the tire edges-pavement interface this, coupled with highly aged (stiff) thin surface layer that have become oxidized is felt to be responsible for the surface cracking that develops. In order to characterize fatigue in asphalt layers, numerous model forms can be found in the existing literature. The most common model form used to predict the number of load repetitions to fatigue cracking is a function of the tensile strain and mix stiffness (modulus). The basic structure for almost every fatigue model developed and presented in the literature for fatigue characterization is of the following form (23):

$$N_f = K_1 \left(\frac{1}{\epsilon_t} \right)^{k_2} \left(\frac{1}{E} \right)^{k_3} = K_1 (\epsilon_t)^{-k_2} (E)^{-k_3}$$

where:

N_f = number of repetitions to fatigue cracking

ϵ_t = tensile strain at the critical location

E = stiffness of the material

K_1, k_2, k_3 = laboratory calibration parameters

In the laboratory, two types of controlled loading are generally applied for fatigue characterization: constant stress and constant strain. In constant stress testing, the applied stress during the fatigue testing remains constant. As the repetitive load causes damage in

the test specimen the strain increases resulting in a lower stiffness with time. In case of constant strain test, the strain remains constant with the number of repetitions. Because of the damage due to repetitive loading, the stress must be reduced resulting in a reduced stiffness as a function of repetitions. The constant stress type of loading is considered applicable to thicker pavement layers usually more than 8 inches. For AC thicknesses between these extremes, fatigue behavior is governed by a mixed mode of loading, mathematically expressed as some model yielding intermediate fatigue prediction to the constant strain and stress conditions. Because of the different stress states and damage mechanism for different thicknesses of the asphalt or bound layers, the fatigue model that will be employed in the 2002 Design Guide is the constant strain and constant stress models developed by Shell Oil. These models will be nationally calibrated (field adjusted) in the 2002 Design Guide study. For the ASU / ADOT study; these models will again be calibrated to specifically predict the most accurate comparison to performance of actual ADOT AC conventional and AR mixtures.

7.1.2. Testing Equipment

Flexural fatigue tests are performed according to the AASHTO TP8 (13), and SHRP M-009 (24). The flexural fatigue test has been used by various researchers to evaluate the fatigue performance of pavements (26,27,28,29,30). Figure 47 shows the flexural fatigue apparatus. The device is typically placed inside an environmental chamber to control the temperature during the test.

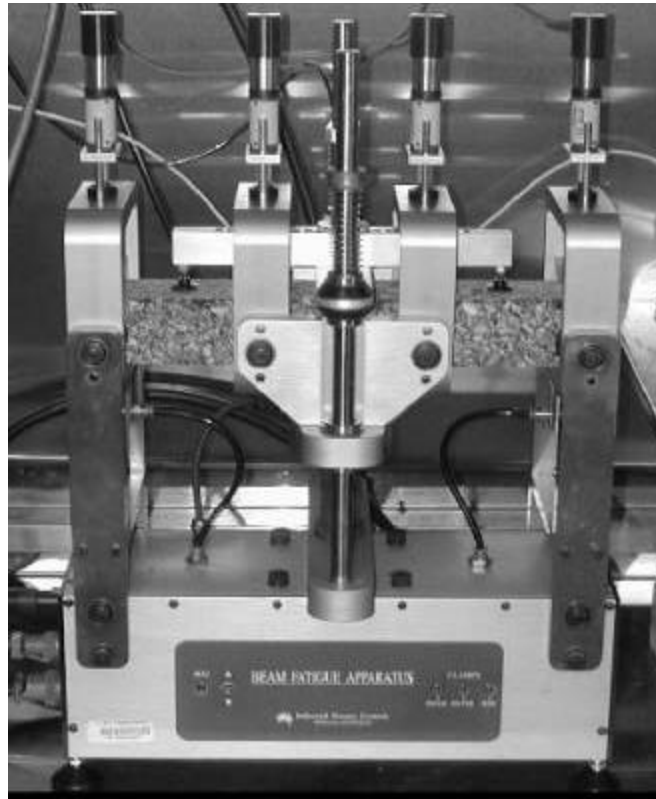


Figure 47. Flexural Fatigue Apparatus

The cradle mechanism allows for free translation and rotation of the clamps and provides loading at the third points as shown in Figure 48. Pneumatic actuators at the ends of the beam center it laterally and clamp it. Servomotor driven clamps secure the beam at four points with a pre-determined clamping force. Haversine or sinusoidal loading may be applied to the beam via the built-in digital servo-controlled pneumatic actuator. The innovative “floating” on-specimen transducer measures and controls the true beam deflection irrespective of loading frame compliance. The test is run under either a controlled strain or a controlled stress loading.

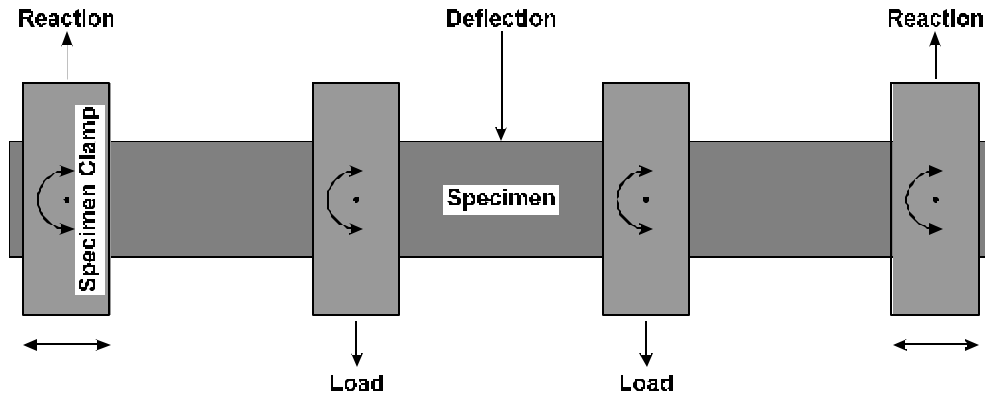


Figure 48. Loading Characteristics of the Flexural Fatigue Apparatus

In the constant stress mode, the stress remains constant but the strain increases with the number of load repetitions. In the constant strain test, the strain is kept constant and the stress decreases with the number of load repetitions. In either case, the initial deflection level is adjusted so that the specimen will undergo a minimum of 10,000 load cycles before its stiffness is reduced to 50 percent or less of the initial stiffness. In this study, all tests were conducted in the control strain type of loading.

7.1.3. Test Procedure and Calculations

The test utilized in this study applied repeated third-point loading cycles as was shown in Figure 48. The sinusoidal load was applied at a frequency of 10 Hz. The maximum tensile stress and maximum tensile strain were calculated as:

$$\sigma_t = 0.357 P / b h^2 \quad (7.1)$$

$$\epsilon_t = 12 \delta h / (3 L^2 - 4 a^2) \quad (7.2)$$

where,

σ_t = Maximum tensile stress, Pa

ϵ_t = Maximum tensile strain, m/m

P = Applied load, N

b = Average specimen width, m

h = Average specimen height, m

δ = Maximum deflection at the center of the beam, m

a = Space between inside clamps, 0.357/3 m (0.119 m)

L = Length of beam between outside clamps, 0.357 m

The flexural stiffness was calculated as follow.

$$E = \sigma_t / \epsilon_t \quad (7.3)$$

where,

E = Flexural stiffness, Pa

The phase angle (ϕ) in degrees was determined as follow.

$$\phi = 360 f s \quad (7.4)$$

where,

f = Load frequency, Hz

s = Time lag between P_{\max} and δ_{\max} , seconds

The dissipated energy per cycle and the cumulative dissipated energy were computed using Equations 7.5 and 7.6, respectively.

$$w = \pi \sigma_t \varepsilon_t \sin \phi \quad (7.5)$$

$$\text{Cumulative Dissipated Energy} = \sum_{i=1}^{i=N} w_i \quad (7.6)$$

where,

w = Dissipated energy per cycle, J/m³

w_i = w for the i^{th} load cycle

During the test the flexural stiffness of the beam specimen was reduced after each load cycle. The stiffness of the beam was plotted against the load cycles, the data was best fitted to an exponential function as follow.

$$E = E_i e^{bN} \quad (7.7)$$

where,

E = Flexural stiffness after n load cycles, Pa

E_i = Initial flexural stiffness, Pa

e = Natural logarithm to the base e

b = Constant

N = Number of load cycles

Once Equation 7.7 was formulated, the initial stiffness S_i can be obtained. Failure was defined as the point at which the specimen stiffness is reduced to 50 percent of the initial stiffness. The number of load cycles at which failure occurred was computed by solving Equation 7.7 for N , or simply:

$$N_{f,50} = [\ln (E_{f,50} / E_i)] / b \quad (7.8)$$

where,

$N_{f,50}$ = Number of load cycles to failure

$E_{f,50}$ = Stiffness at failure, Pa

7.1.4. Material And Specimen Preparation

7.1.4.1. Materials

All beam specimens were prepared using the hot mix asphalt rubber mixes that were obtained during construction.

7.1.4.2. Mold Assembly

The AASHTO TP8-94 (13), and SHRP M-009 (24), flexural fatigue testing protocol, require preparation of oversize beams that later have to be sawed to the required dimensions. The final required dimensions are $15 \pm 1/4$ in. (380 ± 6 mm) in length, $2 \pm 1/4$ in. (50 ± 6 mm) in height, and $2.5 \pm 1/4$ in. (63 ± 6 mm) in width. The procedure does not specify a specific method for preparation. Several methods have been used to prepare beam molds in the laboratory including full scale rolling wheel compaction, miniature rolling wheel compaction, and vibratory loading.

In this study beams were prepared using vibratory loading applied by a servo-hydraulic loading machine. A beam mold was manufactured with structural steel that is not hardened. The mold consists of a cradle and two side plates as shown in Figure 49. The inside dimensions of the mold are $1/2$ inch (12 mm) larger than the required dimensions of

the beam after sawing in each direction to allow for a 1/4 inch (6 mm) sawing from each face. A top loading platen was originally connected to the loading shaft assembly in the middle as shown in Figure 50. Note that the top platen is made of a series of steel plates welded at the two ends to distribute the load more evenly during compaction. The loading shaft was connected to the upper steel plate rather than extending it to the bottom plate so that an arch effect is introduced that would assist in distributing the load more uniformly. In addition, it was found that if the bottom surface of the bottom plate is machined to be slightly concave upward, it would counter balance any bending that might occur during compaction and produce more uniform air void distribution.



Figure 49. Manufactured Mold for Beam Compaction

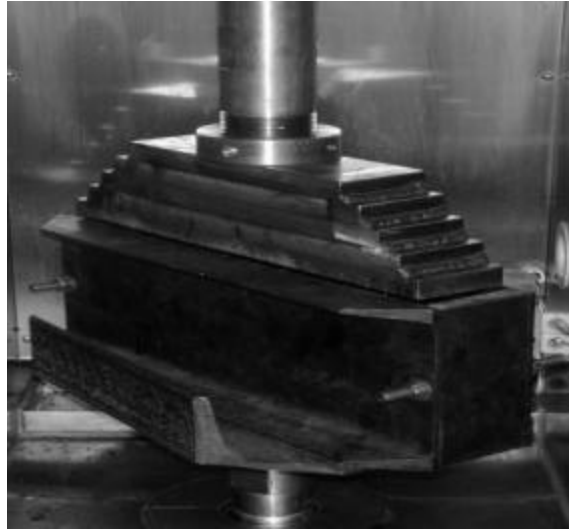


Figure 50. Top Loading Platen

7.1.4.3. Specimen Preparation

The asphalt rubber concrete mixture was heated for two hours at 329°F (165°C). The mold was heated separately for one hour at 329°F (165°C). The mixture was placed in the mold in one load. The mold was then placed on the bottom plate of the loading machine and the top platen was lowered to contact the mixture.

A small load of 0.2 psi (1.4 kPa) was then applied to seat the specimen. A stress-controlled sinusoidal load was then applied with a frequency of 2 Hz and a peak-to-peak stress of 400 psi (2.8 MPa) for the compaction process. Since the height of the specimen after compaction was fixed, the weight of the mixture required to reach a specified air void value was pre-calculated. Knowing the maximum theoretical specific gravity and the target air voids, the weight of the mixture was determined. During compaction the

loading machine was programmed to stop when the required specimen height was reached. Immediately after compaction, the temperatures of some beams were measured using an infrared thermometer and were about 248°F (120°C).

After compaction, specimens were left to cool to ambient temperature. The specimens were brought to the required dimensions for fatigue testing by sawing 1/4 inch (6 mm) from each side (Figure 51). The specimens were cut by using water cooled saw machine to the standard dimension of 2.5 in. (63.5 mm) wide, 2.0 in. (50.8 mm) high, and 15 in. (381 mm) long. Finally, the air void content was measured by using the saturated surface-dry procedure (AASHTO T166, Method A) for the Gap Graded mixture. The air voids of the Open Graded mixture were measured using the CoreLok device.



Figure 51. Specimen sawing

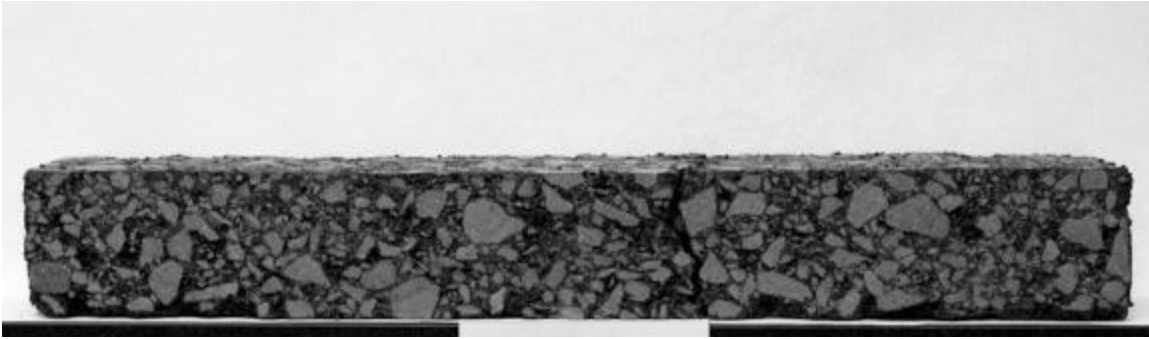


Figure 52. Asphalt rubber GAP graded mix specimen

7.1.5. Testing Factorial

A full testing factorial was used for each mix. Three temperature levels (40, 70, 100 °F) were used for the gap graded mixture; whereas two temperature levels (40, 70 °F) were used for the open graded mixture. One load mode (control strain) using six levels of strain, at one replicate, each was used for each test temperature.

7.1.6. Test Conditions

In summary the following conditions were used:

- Air voids: 11% for gap graded specimens and 18% for open graded specimens.
- Load condition: Constant strain level, 6 levels of the range (300-1750 μ strain)
- Load frequency: 10 Hz
- Test temperature: 100, 70, and 40 °F (37.8, 21.1, and 4.4 °C) for gap graded specimens and 70 and 40 °F (21.1, and 4.4 °C) for open graded specimens.

Specimens that fell outside of the desired air void content within $\pm 1.0\%$ had to be

discarded. The tests were performed according to the AASHTO TP8, and SHRP M-009 procedures. Initial flexural stiffness was measured at the 50th load cycle. Fatigue life or failure under control strain was defined as the number of cycles corresponding to a 50% reduction in the initial stiffness. The loading on most specimens was extended to reach a final stiffness of 30% of the initial stiffness instead of the 50% required by AASHTO TP8 and SHRP M-009. The control and acquisition software load and deformation data were reported at predefined cycles spaced at logarithmic intervals.

7.1.7. Test Results and Analysis for the Flexural Beam Fatigue Test

Tabular summaries of the fatigue test results are presented in Appendix F. Fatigue relationships (flexural strain versus the number of loading cycles) for each test temperature are shown in Figure 54 and 55.

Figure 53 shows the fatigue curves for the ARAC mixture. These plots were obtained from controlled strain tests conducted at 40, 70, 100 °F. The regression equations for each temperature ($N_f = k_1 \epsilon^{k_2}$) are also shown on the plot along with the coefficient of determination (R^2) for each relationship. A summary of the regression equations is shown in Table 16. The high R^2 values are indication of excellent models' accuracy. The relationships obtained are rational in that lower fatigue life (number of repetitions) is obtained as the temperature decreases.

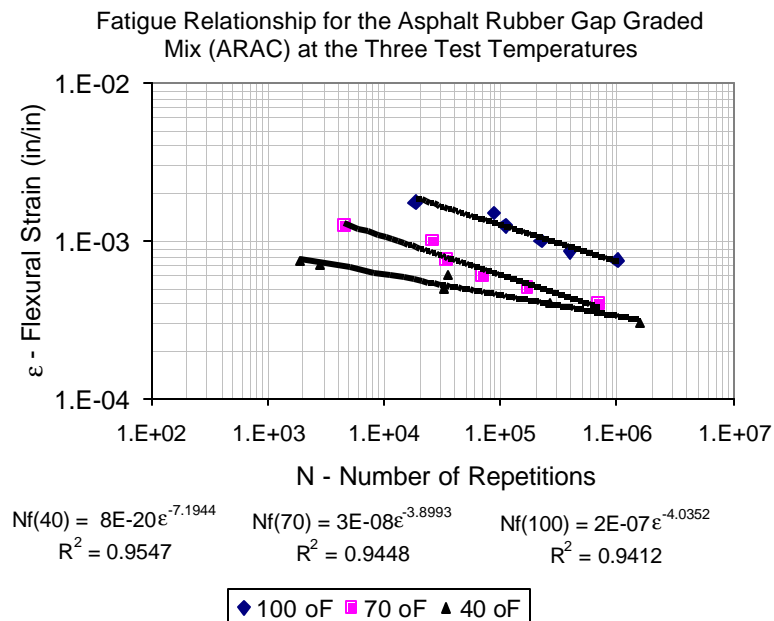


Figure 53. Controlled Strain Fatigue Relationships for the ARAC Mixture

Table 16. Summary of Regression Coefficients for the Fatigue Relationships

MIX TYPE	Test Temperature °F								
	100			70			40		
	K1	K2	R ²	K1	K2	R ²	K1	K2	R ²
ADOT PG 76-16	1.00E-10	4.607	0.99	1.00E-11	4.724	0.97	2.00E-10	4.171	0.74
ARAC	2.00E-07	4.035	0.94	3.00E-08	3.899	0.94	8.00E-20	7.194	0.96
AR-ACFC				2.00E-07	3.850	0.98	1.00E-13	5.521	0.97

* $N_f = K1 * (1/e_t)^{K2}$

* At 50% of Initial Stiffness

Figure 54 shows similar relationships for the AR-ACFC mixture. Initially, no fatigue tests were scheduled for this mixture. However, limited testing was conducted at the end of the testing program for comparative purposes. Therefore, only two test temperatures are shown in this plot. The regression equations for each temperature are shown on the plot with their respective R^2 values. Both R^2 values are indicative of excellent models' accuracy. The relationships are also rational in that lower fatigue life is obtained for the the lower test temperature.

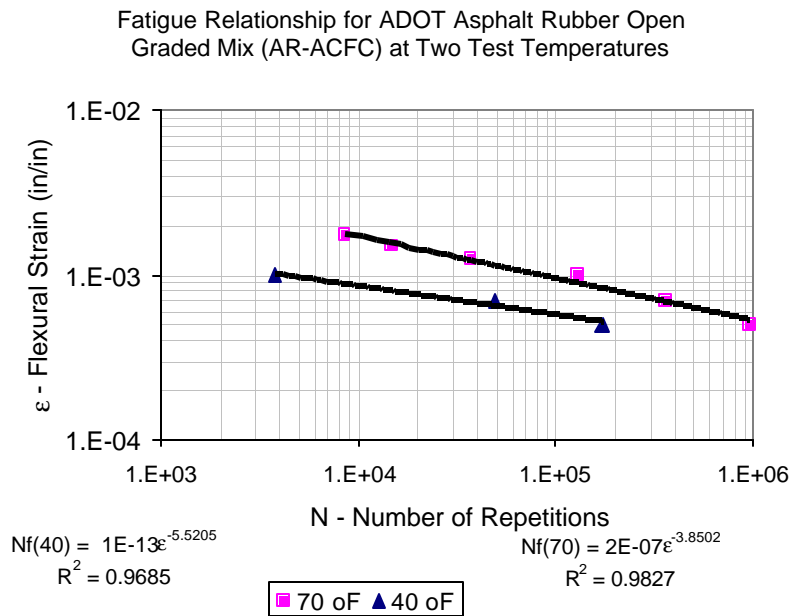


Figure 54. Controlled Strain Fatigue Relationships for the AR-ACFC Mixture

Figure 55 shows a comparison of the two AR mixtures along with ADOT conventional PG 76-16 mix. the comparison is made at the test temperature of 70°F and at 50% reduction of initial stiffness for each mix. Note that the air voids for the PG 76-16 mix is 7% whereas the air voids for the ARAC and AR-ACFC mixtures are 11% and 18%, respectively. In addition, it is worth mentioning that the binder content for the PG 76-16 is 4.20% compared to 6.8% for the ARAC and 8.8% for the AR-ACFC mix.

The relationship observed in Figure 55 has excellent measures of models accuracy. The relationships are also rational in that higher binder content mixtures yielded higher fatigue life despite the air void content variations between the mixtures. It is also clearly noted that both of AR mixtures would result in higher fatigue life than the conventional Chevron PG 76-16 mix. The ARAC mix result is approximately 3 times longer in fatigue life, whereas, the AR-ACFC mix results in 15 to 16 times longer fatigue life than the PG 76-16 mixture.

Table 17 summarizes the K1-K3 Coefficients of the generalized fatigue model for the three mixtures. Two sets of coefficients are included: one for the analysis done at 50% reduction of initial stiffness; the other for the analysis conducted at 30% reduction of initial stiffness. Both type of analysis yielded good to excellent measures of model accuracy. It is also noted that the models developed for the AR-ACFC mixture used only tests conducted at two temperatures (40 and 70 °F) compared to the other two mixes where data were available for three test temperatures (40, 70, 100 °F).

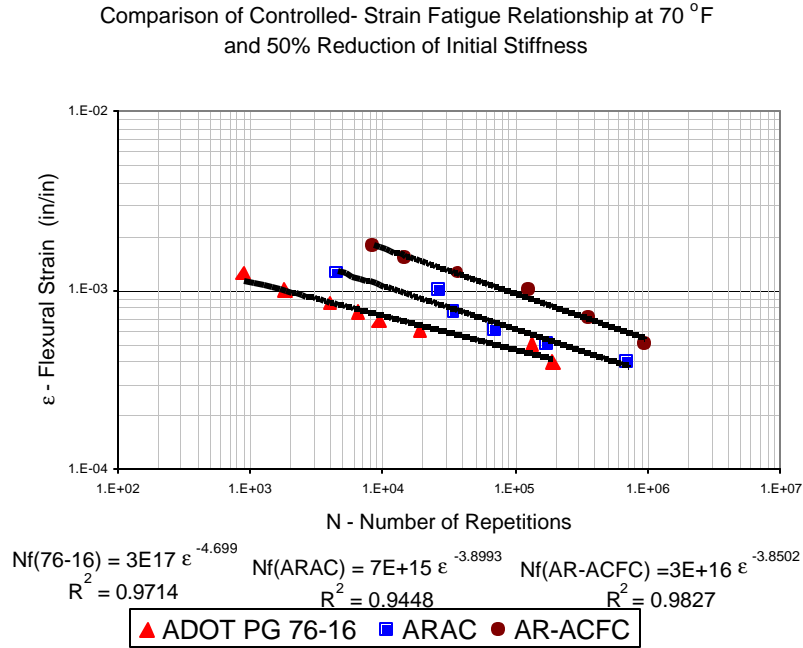


Figure 55. Controlled Strain Fatigue Relationships for SRB, ARAC, and AR-ACFC mixes

Table 17 Summary of the Regression Coefficients for Generalized fatigue Equation

MIX TYPE	50% OF INITIAL STIFFNESS, S_o @ N=50 Cycles				30% OF INITIAL STIFFNESS, S_o @ N=50 Cycles			
	K1	K2	K3	R^2	K1	K2	K3	R^2
ADOT PG 76-16	1.32E-03	4.954	1.531	0.97	9.99E-01	3.616	1.163	0.82
ARAC	2.50E-02	4.231	1.267	0.75	3.52E-05	3.921	0.520	0.95
AR-ACFC	7.81E+03	2.997	1.530	0.99	2.12E+08	1.998	1.705	0.97

* $N_f = K1 * (1/\epsilon_f)^{K2} * (1/E_o)^{K3}$

* Note that only Temperatures were conducted for the AR-ACFC mix.

7.1.8. Summary for the Flexural Beam Fatigue Test

Constant strain Flexural tests were performed according to the AASHTO TP8 and SHRP M-009 procedures to evaluate the fatigue performance of the two asphalt rubber mixtures.

- The fatigue models developed for the AR mixtures in this study had excellent measures of accuracy and were rational in that lower fatigue life was obtained as the test temperature decreased. Furthermore, a comparison was made of the fatigue life obtained for the AR mixes with an ADOT PG 76-16 conventional dense graded mix.
- The fatigue life was found to be higher for asphalt rubber mixes compared to the conventional PG 76-16. The comparison was done at 70 °F and at 50% reduction of initial stiffness for all mixtures. The ARAC mix resulted in approximately a 3 times greater fatigue life than the conventional mix. On the other hand, the AR-ACFC mix resulted in 15 times greater fatigue life than the conventional mix. These order of magnitudes of fatigue life for the three mixtures were rational considering that the PG 76-16 mix had 4.20% binder content whereas the ARAC and AR-ACFC mixtures had 6.8% and 8.8%, respectively.

7.2. THERMAL CRACKING

7.2.1. Indirect Tensile Tests

The indirect tensile test has been used extensively in structural design research for flexible pavements since the 1960's and to a lesser extent in HMA mixture design research. It is the test recommended for mixture characterization in the Long Term Pavement Performance (LTPP) program and to support structural designs in the 1986 and 1993 AASHTO Design Guide.(31,32). In fact, the indirect tensile test is one of the most popular tests used for HMA mixture characterization in evaluating pavement structures. The primary reason for its popularity is that cores from thin lifts can be tested directly in the laboratory (13).

The indirect tensile test is the test specified in AASHTO T-283 for evaluating an HMA mixture's susceptibility to moisture damage. Properties that have been used for evaluating moisture damage and fracture-related distresses are the resilient modulus (repeated loadings) and the indirect tensile strength and failure strain (constant rate of loading) (33). Although the reliability of the indirect tensile test to detect and predict moisture damage is questionable, no other test has been found to provide consistent results at a higher reliability. In addition, SHRP recommended that the indirect tensile creep test method be used for characterizing HMA mixtures for thermal cracking predictions (13).

The indirect tensile method is used to develop tensile stresses along the diametral axis of the test specimen. The test is conducted by applying a compressive load to a cylindrical

specimen through two-diametrically opposite arc-shaped rigid platens, as shown in Figure 56. The test specimen is placed with its axis horizontal between the platens of the testing machine.

Based upon the theory of elasticity, the strain can be expressed in three dimensions. Ideally, the three-dimensional analysis can be reduced to a two-dimensional analysis for special element size and loading conditions. For the case of a circular disk, the two dimensional analysis can be categorized as plane stress (13).

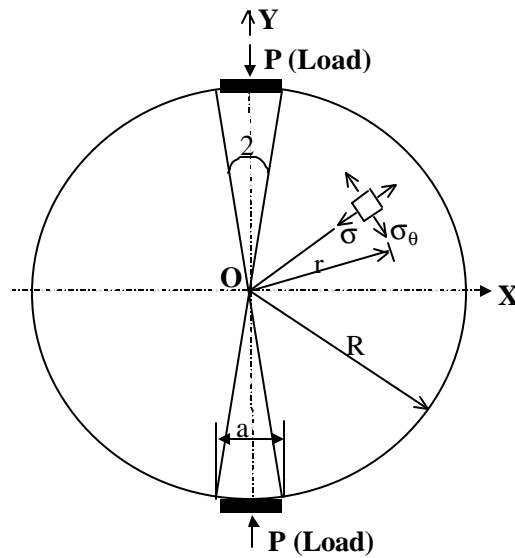


Figure 56. Schematic Diagram of the Indirect Tensile Test

7.2.2. Background for the Indirect Tensile Strength Test

The indirect tensile strength is measured by applying load at a constant rate of deformation of 12.5 mm/min (0.5 in/min). The strength test was stopped when the applied load went to zero (i.e., total failure of the specimen occurred). The horizontal tensile stress at the center of the test specimen is calculated using equation 7.9, while the tensile strain is calculated using equation 7.10 (13).

$$\text{Horizontal Tensile Stress} = \sigma_{xy} = \frac{2P}{\pi t d} \quad (7.9)$$

where:

- d = the diameter of the specimen.
- P = the applied load.
- t = the thickness of the test specimen or core.

$$\text{Horizontal Tensile Strain} = \epsilon_{xx} = \delta_{xx} \left(\frac{2(1 + 3\mu)}{d(a + b\mu)\pi} \right) \quad (7.10)$$

where:

- δ_{xx} = Horizontal deformation across the test specimen.
- μ = Poisson's ratio.
- a, b, d = Integration constants that are specimen geometry dependent.

The only unknowns in the equation are Poisson's ratio and the integration constants. The integration constants are dependent on the geometry of the test specimen. The determination of Poisson's ratio requires both horizontal and vertical deformation measurements made on the specimen or it can be calculated from a regression equation

developed by Mirza and Witczak, as shown below (34).

$$\mu = 0.15 + \frac{0.35}{1 + \exp(3.1849 - 0.04233 \times \text{Temp})} \quad (7.11)$$

Temperature in the above equation is expressed in degree Fahrenheit.

Parameters from the indirect tensile strength test that can be considered for mixture cracking performance include: Indirect Tensile Strength (S_t), Horizontal Strain at Failure (ϵ_{ff}), Total Fracture Energy (Γ_{fr}), Fracture Energy to Failure (Γ_{fa}). These indirect tensile strength parameters are defined below (13):

- The maximum horizontal tensile stress at the center of the specimen and the horizontal tensile strain were calculated according to the chart shown in Figure 57.
- The indirect tensile strength is the maximum stress developed at the center of the specimen in the radial direction during the loading operation for a fixed geometry.
- The fracture energy is calculated as the area under the load-vertical deformation curve as shown in Figure 58.
- The energy until failure is calculated from the results of this test as shown in Figure 59.

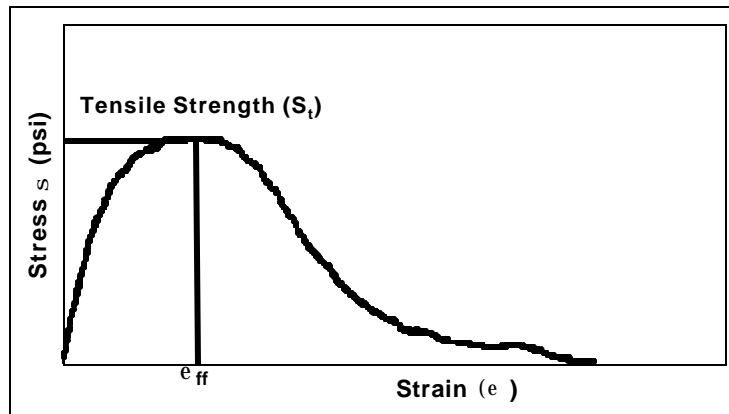


Figure 57. Illustration Showing the Determination of the Indirect Tensile Strength

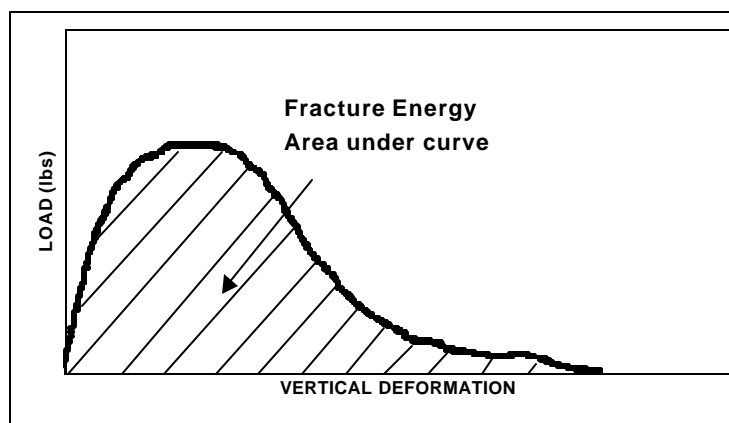


Figure 58. Determination of Total Fracture Energy

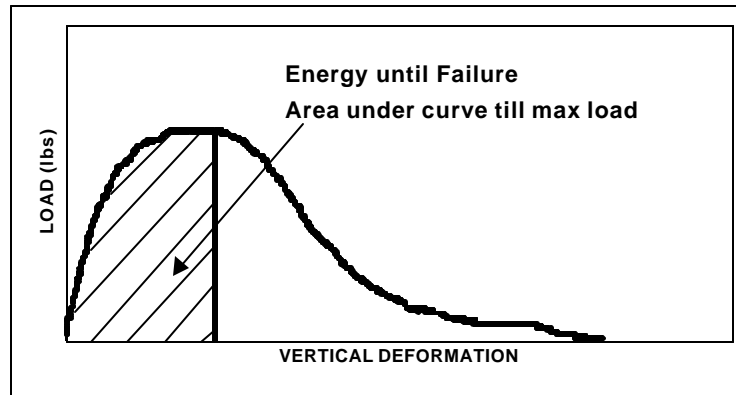


Figure 59. Determination of Energy to Peak Load

7.2.3. Background for the Indirect Tensile Creep Tests

The static creep test in the indirect tensile mode uses a singular load-unload cycle. A constant static load is applied to the specimen for a time of 1,000 seconds and horizontal deformations are recorded during the loading time. The applied load is a percentage of the horizontal tensile strength of the material (equation 7.9).

The horizontal deformations are recorded for another 1,000 seconds after the load is removed to measure the recovery of the specimen. The stresses and strains are calculated using equations 7.9 and 7.10.

Both horizontal and vertical LVDT's are used during the test to measure the deformations under the static load to calculate Poisson's ratio. Poisson's ratio also can be calculated using equation 7.11, when only horizontal deformations are measured.

7.2.3.1. Strain-Time Response Curve

The phenomenon of the static creep test is shown in Figure 60, which illustrates the typical strain-time response of an HMA mixture. Figure 60 shows the salient components of the load/unload cycle. The total strain (ϵ_T) can be divided into recoverable and nonrecoverable components or time-dependent and time-independent components, just as they are for the triaxial compressive creep test. Equation 7.12 describes the four components composing the total strain (13).

$$\epsilon_T = \epsilon_e + \epsilon_p + \epsilon_{ve} + \epsilon_{vp} \quad (7.12)$$

where:

ϵ_T = the total strain.

ϵ_e = the elastic strain, recoverable and time-independent.

ϵ_p = the plastic strain, irrecoverable and time-independent.

ϵ_{ve} = the visco-elastic strain, recoverable and time-dependent.

ϵ_{vp} = the visco-plastic strain, irrecoverable and time-dependent.

The elastic and visco-elastic strain components exist during both loading and unloading conditions, while the plastic and visco-plastic components exist during the loading portion.

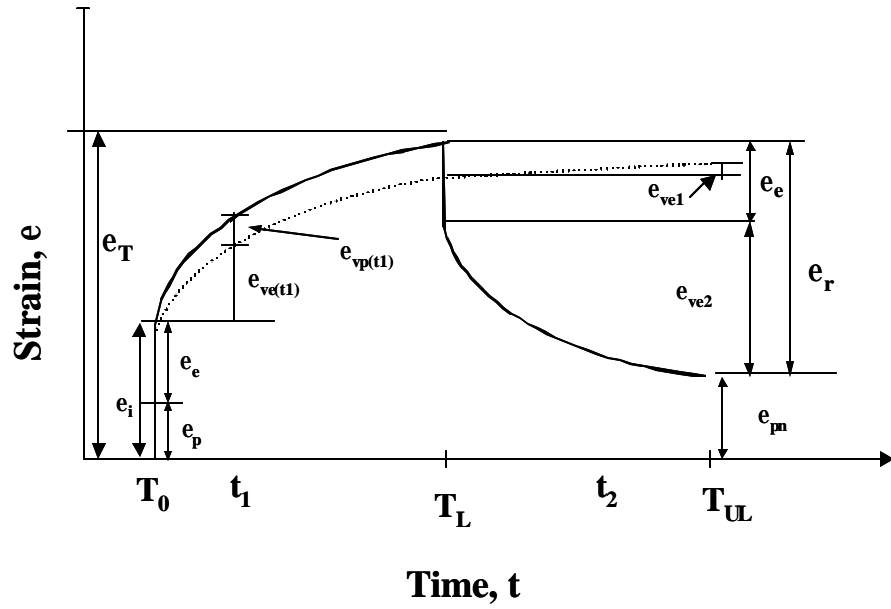


Figure 60. Typical Strain-Time Response for HMA Mixtures for a Static Creep Test

7.2.3.2. Modulus/Compliance Components

The modulus from the creep test is calculated using equation 7.9, so the compliance is defined as:

$$D(t)_h = E(t)^{-1} = \frac{\delta_{xx} * t}{p(a + b\mu)} \quad (7.13)$$

The mathematical form to represent the compliance from the indirect tensile test is similar to the compliance determined from the triaxial compressive creep test and is given by equation 7.14.

$$D(t) = D_1 t^{m1} \quad (7.14)$$

where:

$D(t)$ = total compliance at any time.

t = loading time.

D_1, m_1 = material regression coefficients.

The regression coefficients " D_1 " and " m_1 " are generally referred to as the compliance parameters as shown in Figure 61. These parameters are the general indicators of the creep behavior of the materials, similar to those determined from the triaxial compressive creep test. The Paris law's fracture parameters can be also calculated in accordance with the procedure recommended by Roque, et al. (35)

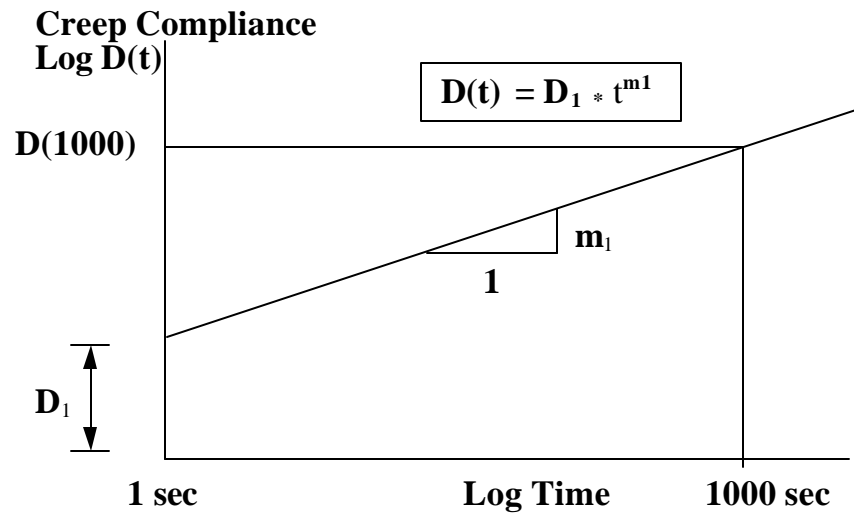


Figure 61. Illustration of Creep Compliance versus Time from a Static Creep Test

7.2.4. Test Conditions for the Indirect Tensile Strength and Creep Tests

Both indirect tensile cracking tests were carried out according to the procedure described in the draft indirect tensile tests protocol for the AASHTO 2002 Design Guide level 1 and level 2 (13). All test specimens were sawed from gyratory fabricated specimens. The test specimen was approximately 38 mm (1.5 in) in thickness and 150mm (6 in) in diameter. At least two replicates were tested for each AR mix and at each test condition. Vertical or horizontal LVDT's were used on the specimen for measuring the horizontal and vertical deformation using a gage length of 76.2 mm (3 in) for both. The tests were carried out at three temperatures: 0°C (32°F), -10°C (14°F) and -15°C (5°F). A typical test setup is shown in Figure 62.



Figure 62. Indirect Tensile Tests Set-Up.

7.2.5. Tests Results and Analysis

7.2.5.1. Indirect Tensile Strength Test

Results for the indirect tensile strength tests for both the AR mixes and an ADOT SRB PG64-22 conventional mixture are summarized and reported in Appendix G. A master summary table for all mixtures at three test temperatures reported in Appendix G is shown in Table 18. The table includes results of tensile strength, strain at failure, fracture energy, and energy until failure. Figure 63 through 67 are summary plots of the test results of all of the above properties.

Table 18. Master Summary of the Indirect Tensile Strength Tests.

Mix	Temp (°F)	Target Air Voids (%)	Max Load (lbs)	Tensile Strength (psi)	Strain @ Failure	Fracture Energy (lbs x inch)	Energy Until Failure (lbs x inch)
AR-ACFC	32	18.0	1237	83	3.47E-03	256	129
ARAC	32	11.0	1766	105	2.47E-03	295	133
SRB PG64-22	32	7.0	3943	277	1.43E-03	330	231
AR-ACFC	14	18.0	1932	137	1.47E-03	300	143
ARAC	14	11.0	2401	144	1.10E-03	282	133
SRB PG64-22	14	7.0	5753	437	9.85E-04	232	142
AR-ACFC	5	18.0	2249	157	2.15E-03	208	111
ARAC	5	11.0	3292	190	1.30E-03	188	86
SRB PG64-22	5	7.0	6078	446	7.05E-04	121	97

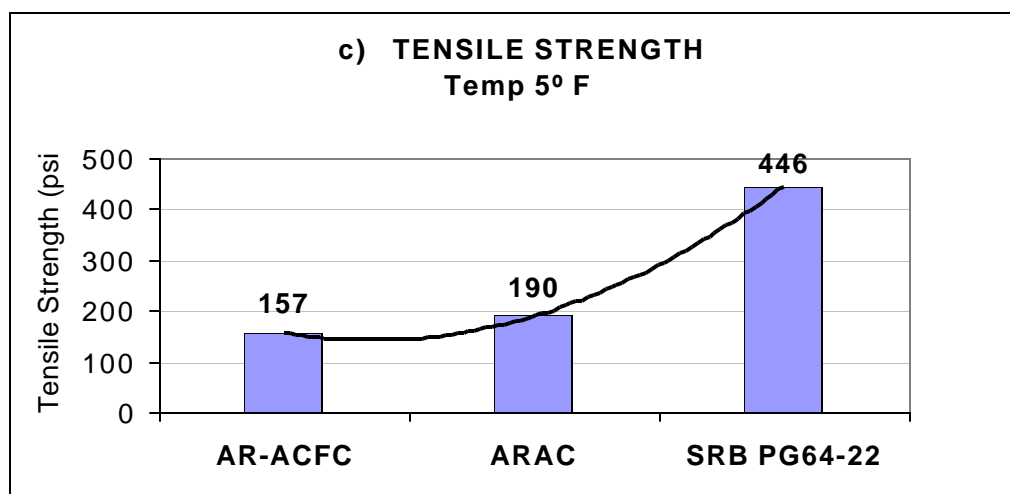
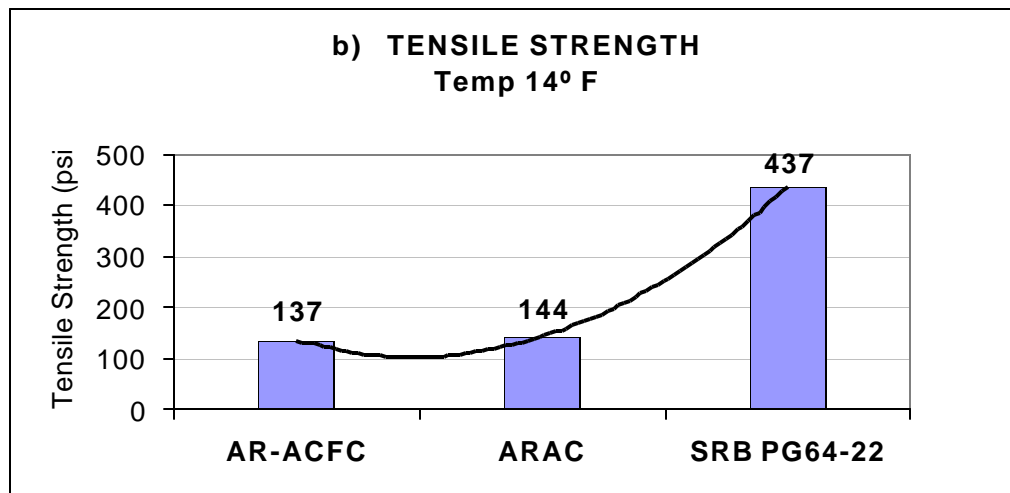
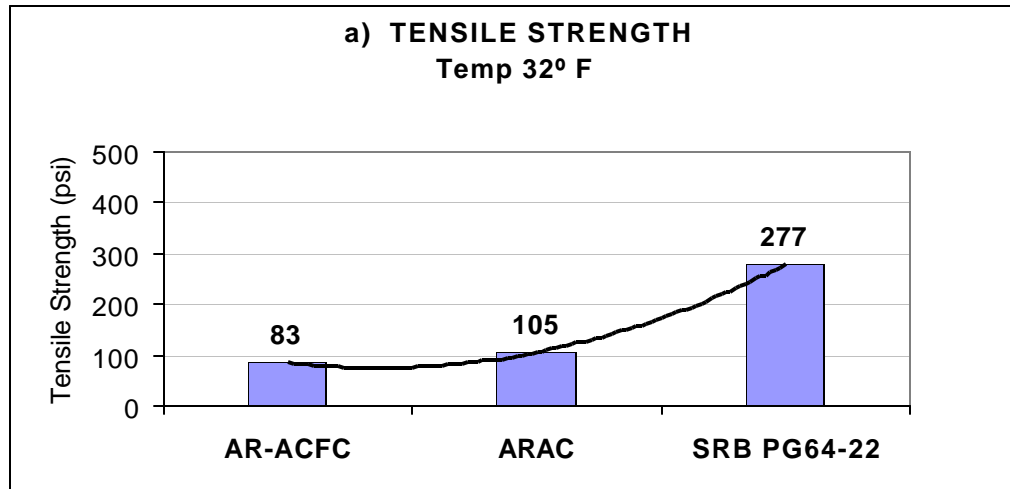


Figure 63. Indirect Tensile Strength Test – Tensile Strength Results

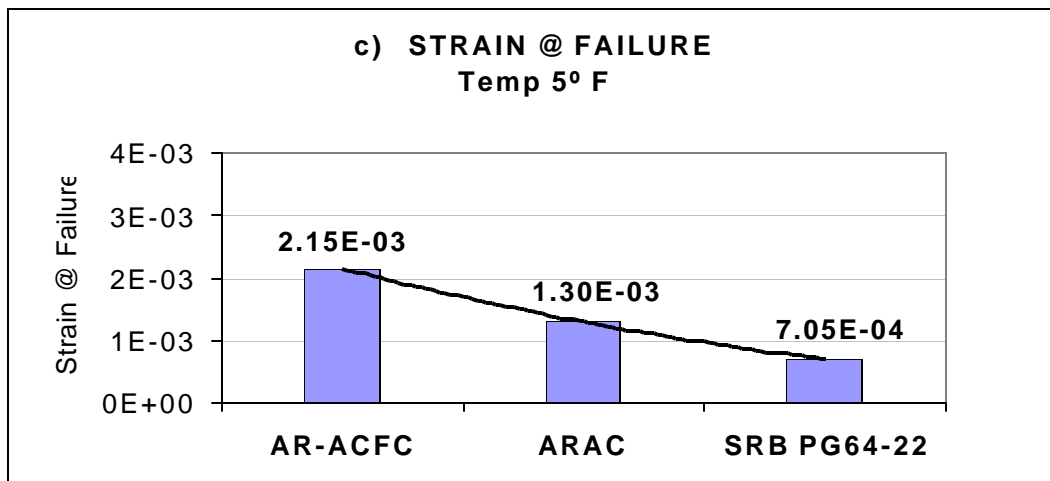
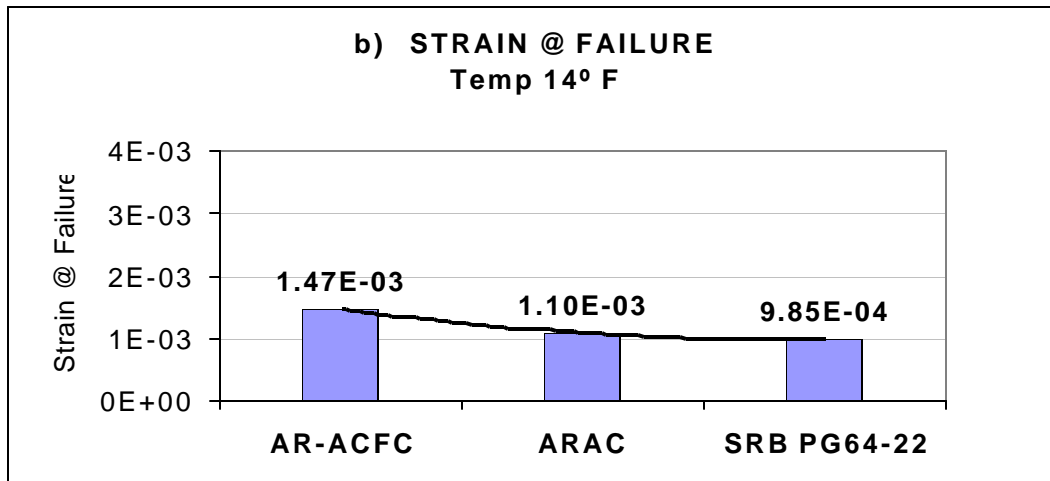
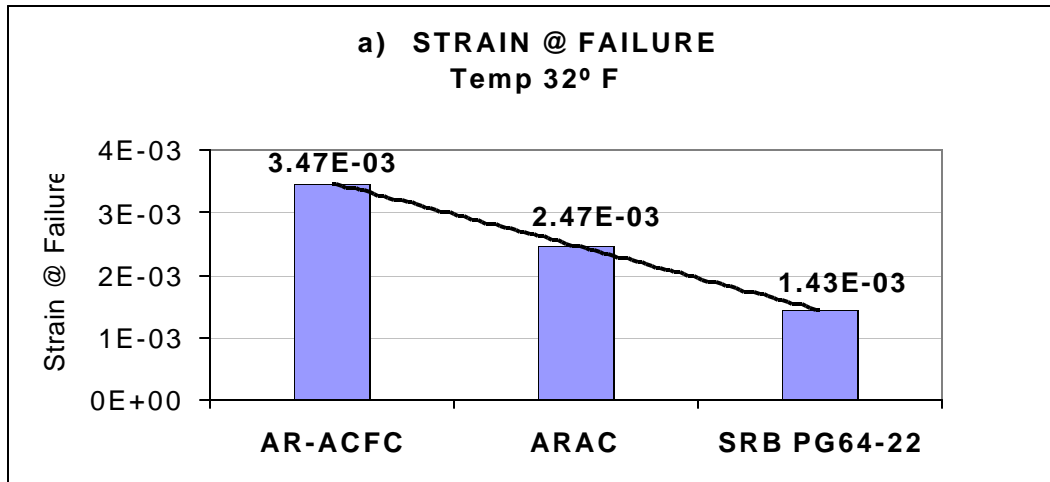


Figure 64. Indirect Tensile Strength Test – Strain at Failure

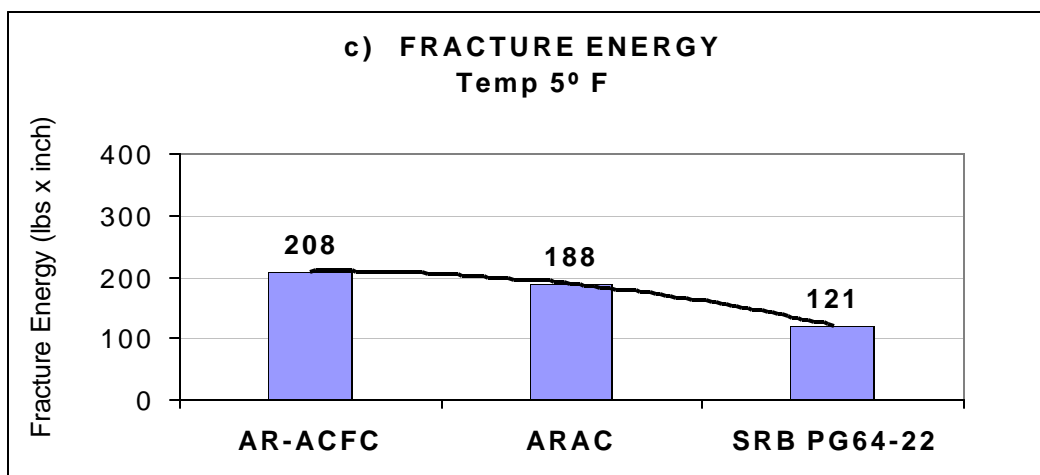
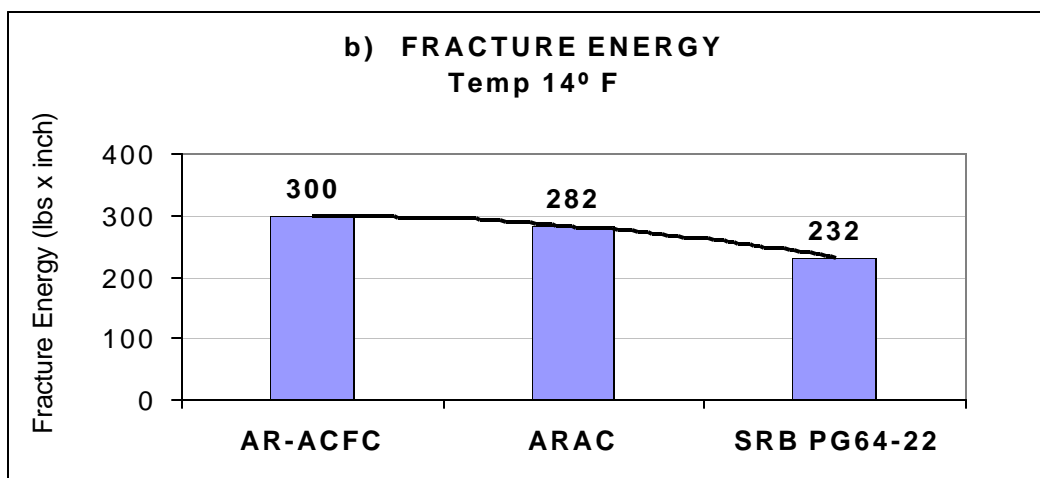
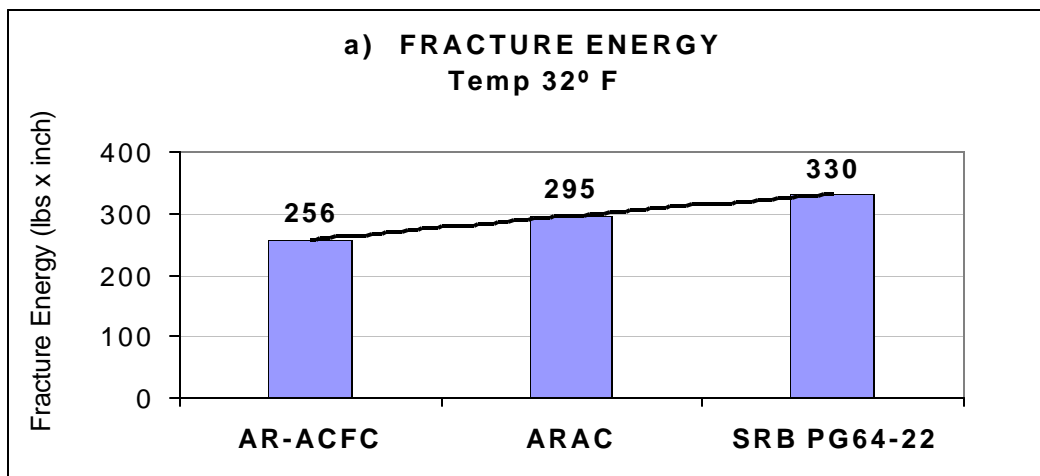


Figure 65. Indirect Tensile Strength Test – Fracture Energy

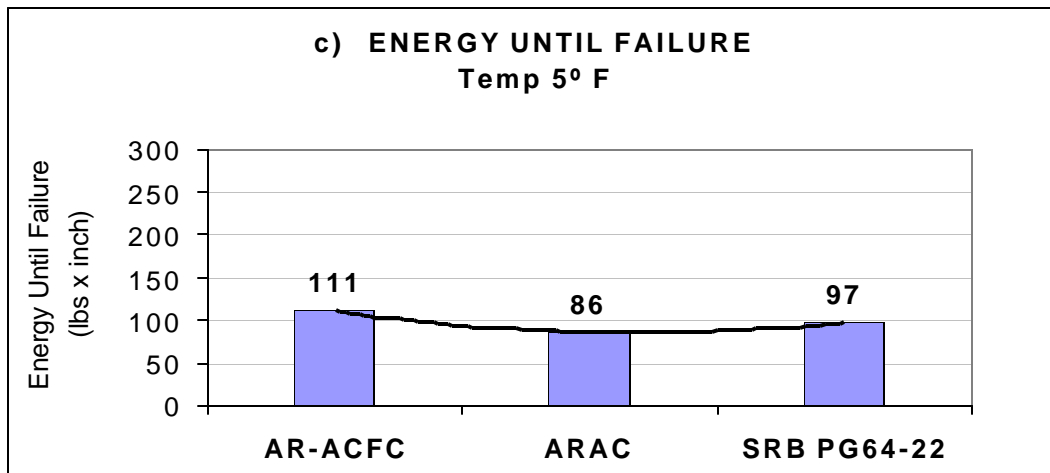
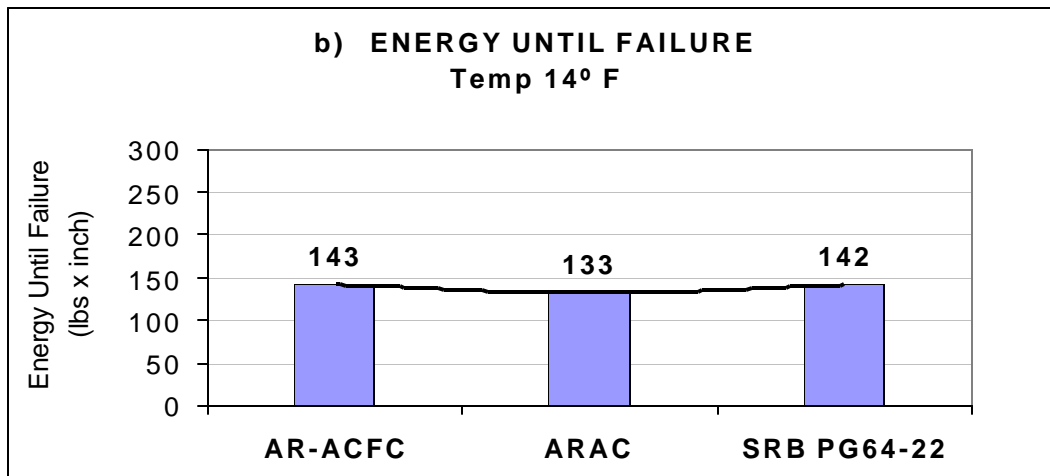
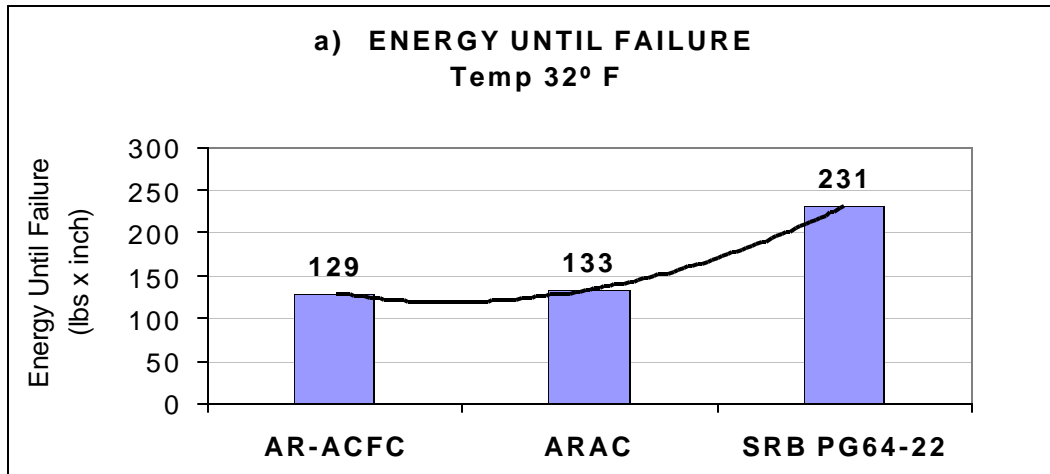


Figure 66. Indirect Tensile Strength Test – Energy Until Failure

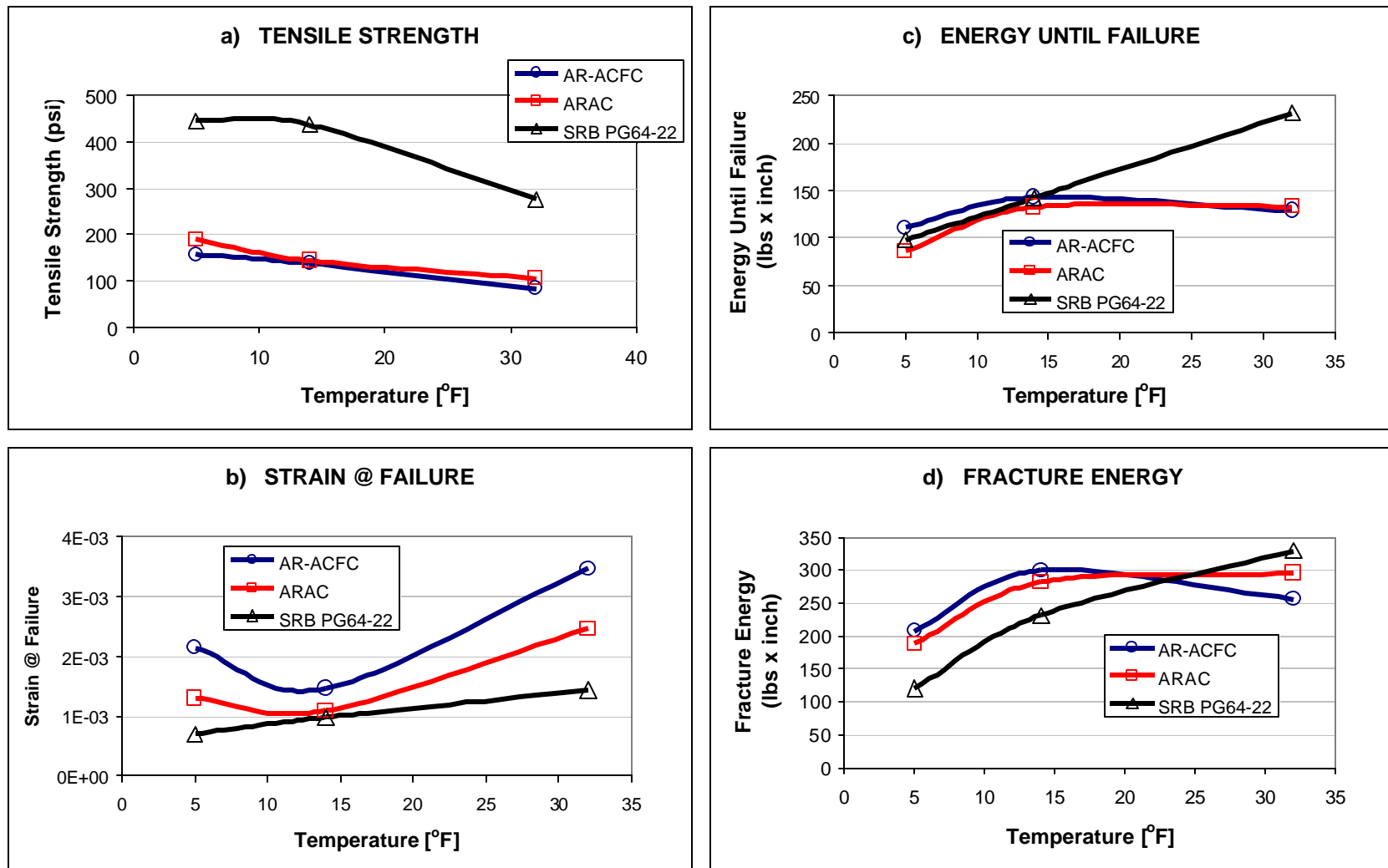


Figure 67. Indirect Tensile Strength Test – Summarized Results

Comparing the results of the tensile strength (Figure 63) for all three mixtures, it can be observed that the difference between the two AR mixtures are relatively small and do not exceed 25%. At the same time the SRB PG64-22 mix has 2.5 to 3 times higher strength than the AR mixtures. The difference between the mixtures strength is increasing as the temperature decreases. Higher thermal cracking would be expected for mixtures with lower tensile strength values.

The strain at failure results are shown in Figure 64. It can be observed that the AR-ACFC mix has 140% larger strain than the SRB PG64-22 mix and 40% larger strain than the ARAC mix. This trend was consistent as the temperature decreased, but the difference between the mixtures also decreased. Generally, the higher the tensile strain at failure, the less susceptible the mix to thermal cracking.

The most interesting result was observed for the fracture energy (Figure 65) and energy until failure (Figure 66). At the higher temperature (32°F), the SRB PG64-22 mix exhibited the highest fracture energy, followed by the ARAC mix and the AR-ACFC mix. The difference between the mixes not exceeds 28%. At the lower temperature of 14°F the order is reversed with similar percentages difference between the mixtures. At 5°F this reversed trend was even larger. Generally, lower thermal cracking should be expected as the energy at failure or fracture energy is increased. Figure 65 and 66 favor this trend at the colder temperature (14 and 5°F).

Another interesting and important observation in Figure 65 is that the fracture energy of the AR-ACFC mix is 82% retained when the temperature drops from 32°F to 5°F. This percentage is about 62% for the ARAC mixture. However, this drop in fracture energy is significant for the conventional SRB PG64-22 mix which retains about 31% of its energy at 5°F.

Figure 67 contains plots which summarizes the previous analyses for the four indirect tensile strength test parameters. In Figure 67 (a), the highest strength is observed for the SRB PG64-22 mix at all three test temperatures; whereas lower strength values and little difference is observed for the AR mixes. These results are not consistent to what is being observed in the field. Figure 67 (b) on the other hand shows that higher tensile strains are obtained for the AR mixtures at the three test temperatures. The difference between the AR mixtures and the SRB PG64-22 mix is lower at 14°F, but it is distinct at the other two temperatures.

The most interesting result was obtained from the fracture energy and energy until failure parameters (Figure 67 (c) and (d)). Higher fracture energy and energy until failure was obtained for the AR mixes at 14°F and 5°F. Higher energy values result in lower thermal cracking, which is consistent with field observations for the AR, mixes.

Another important observation in Figure 67 (c) and (d) is the reduction in the energy levels measured as temperature decreases from 32°F to 5°F. It is observed that the AR

mixes energy loss is in the range of 18 to 38%; whereas as a significant loss for the SRB PG64-22 mix (70%) was obtained.

7.2.5.2. Indirect Tensile Creep Test

The test results for the indirect creep test for the two asphalt rubber mixtures are summarized and reported in Appendix G. Test results from a standard ADOT mixture were not available. A master summary table for all mixtures and test temperatures reported in Appendix G is shown in Table 19. The table contains average values for the strain at time 1000 sec, in addition the creep compliance parameters (intercept, slope, and compliance at time 1000 sec). Figure 68 through 72 present summarized plots of all the properties reported in Table 19.

Table 19. Master Summary of Indirect Tensile Creep Test.

Mix	Temp (°F)	Target Air Voids (%)	P (lbs)	ϵ_{Tx} at t = 1000sec (me)	D(t) t = 1000sec (1/psi)	D1 10^{-6} (1/psi)	m_1
AR-ACFC	32	18.0	40.3	159.5	3.43E-05	0.41	0.75
ARAC	32	11.0	40.2	142.0	4.02E-05	3.23	0.36
AR-ACFC	14	18.0	100.3	51.7	6.08E-06	1.19	0.23
ARAC	14	11.0	100.3	29.0	3.65E-06	0.54	0.28
AR-ACFC	5	18.0	149.9	86.0	6.69E-06	2.17	0.16
ARAC	5	11.0	149.8	62.0	3.57E-06	0.86	0.23

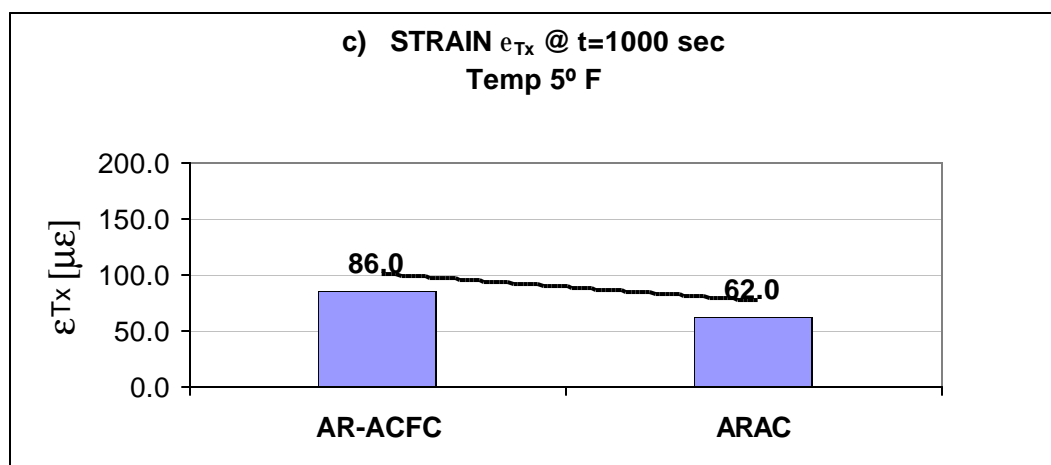
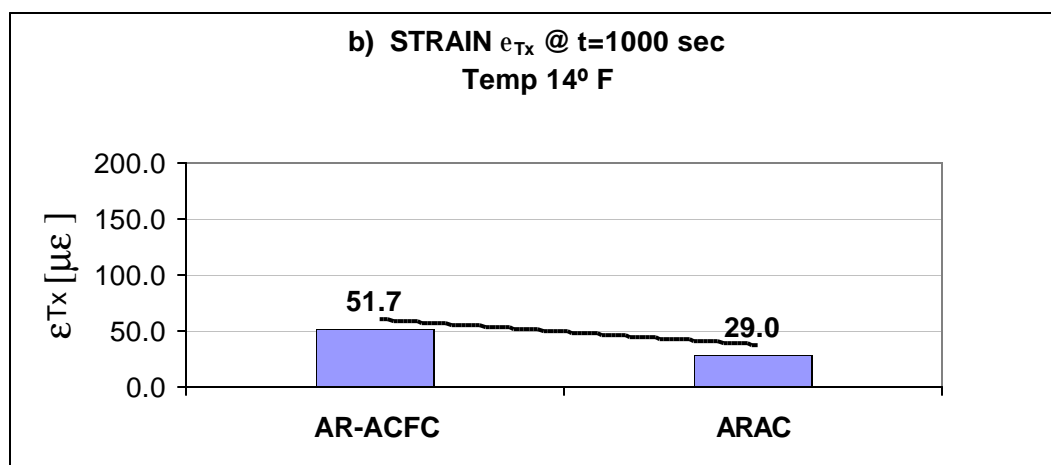
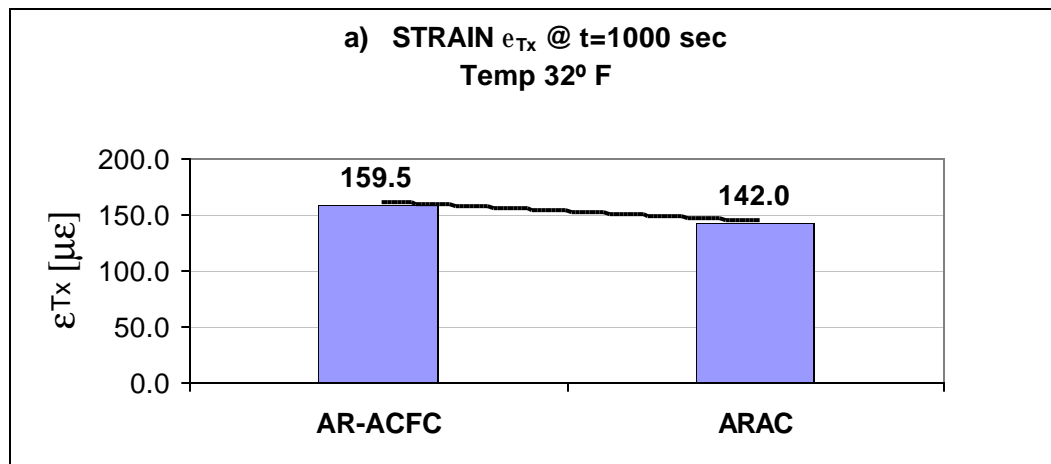


Figure 68. Indirect Tensile Creep Test – Strain at t= 1000s

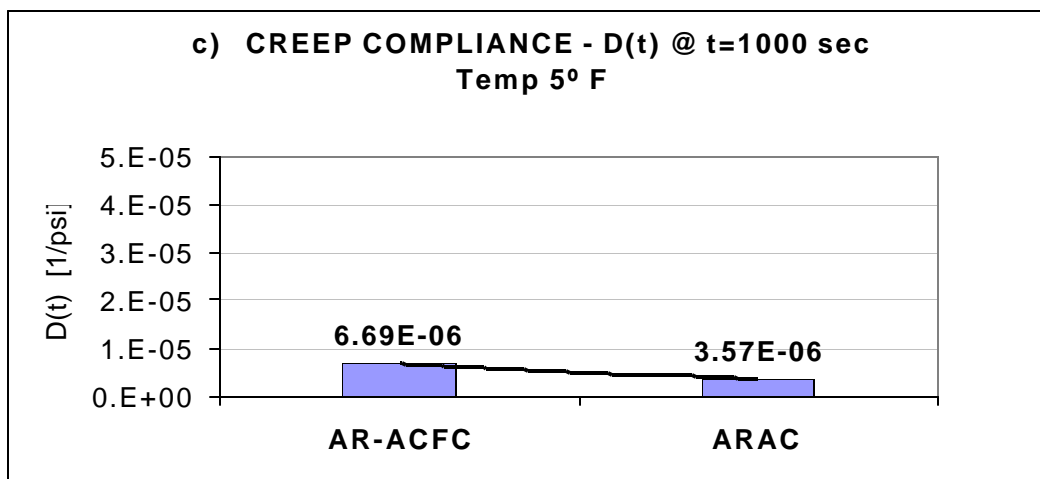
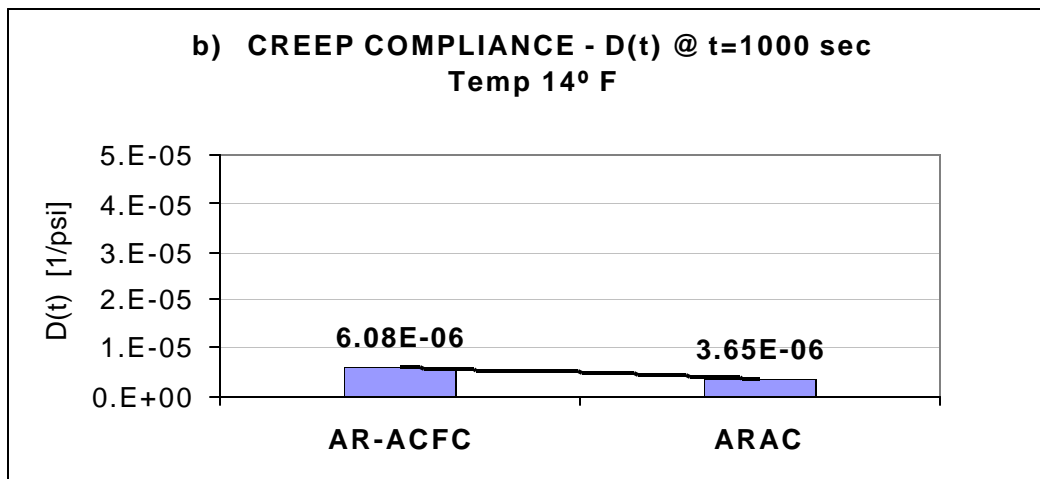
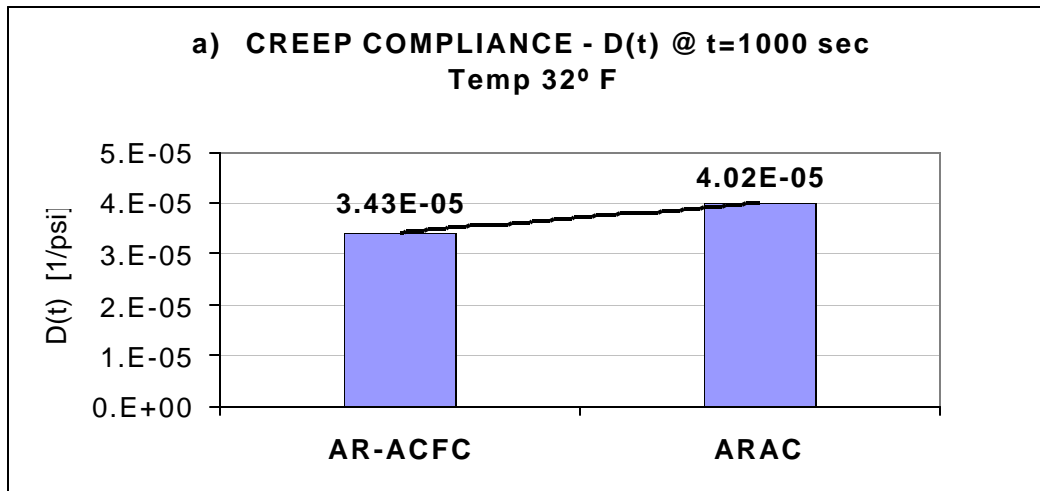


Figure 69. Indirect Tensile Creep Test – Creep Compliance at $t= 1000s$

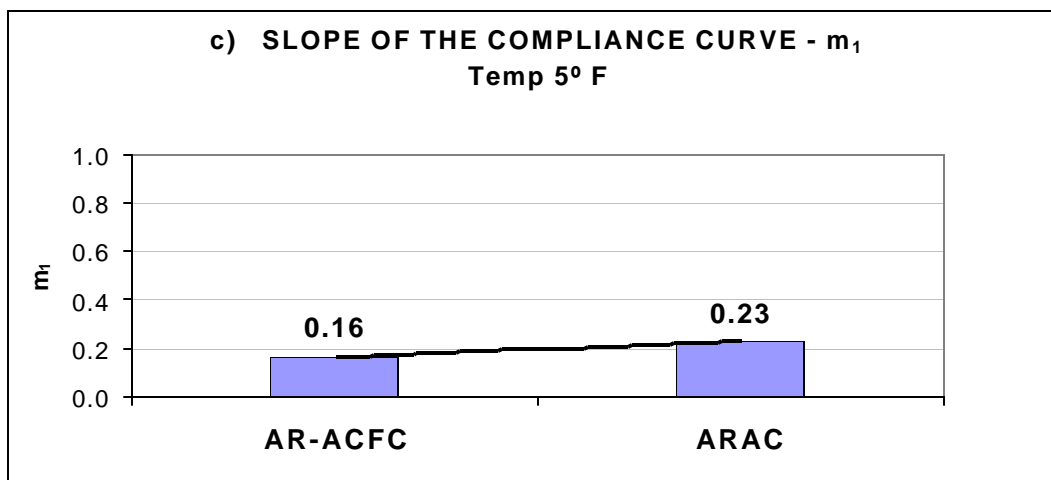
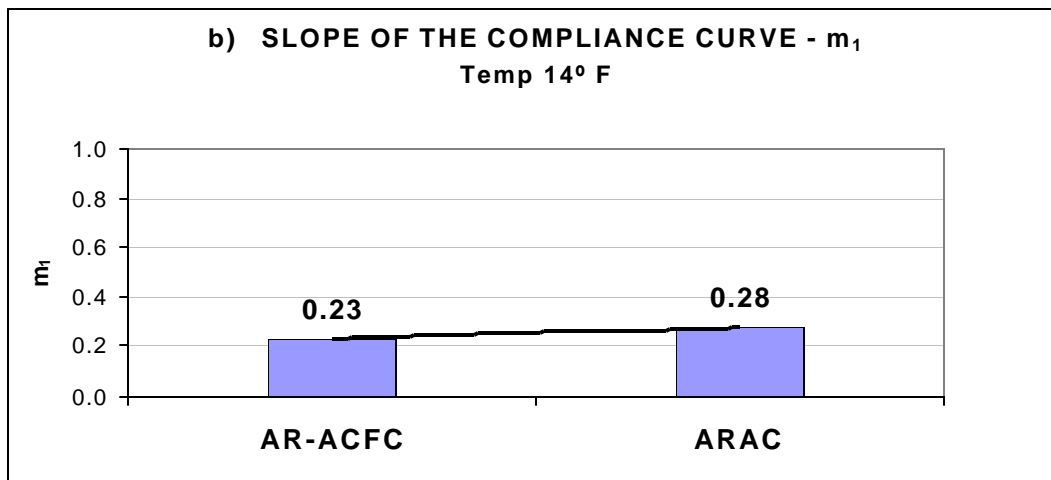
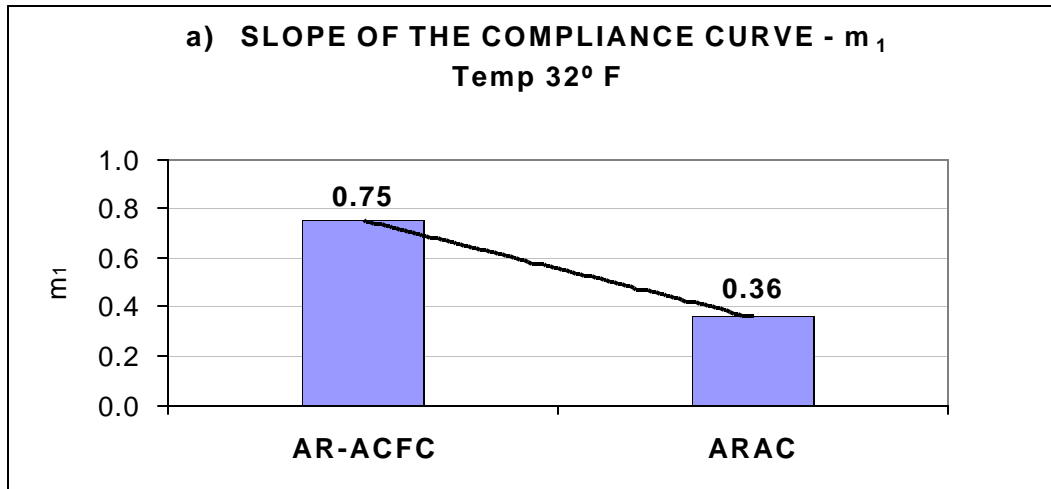


Figure 70. Indirect Tensile Creep Test – Slope of the Compliance Curve

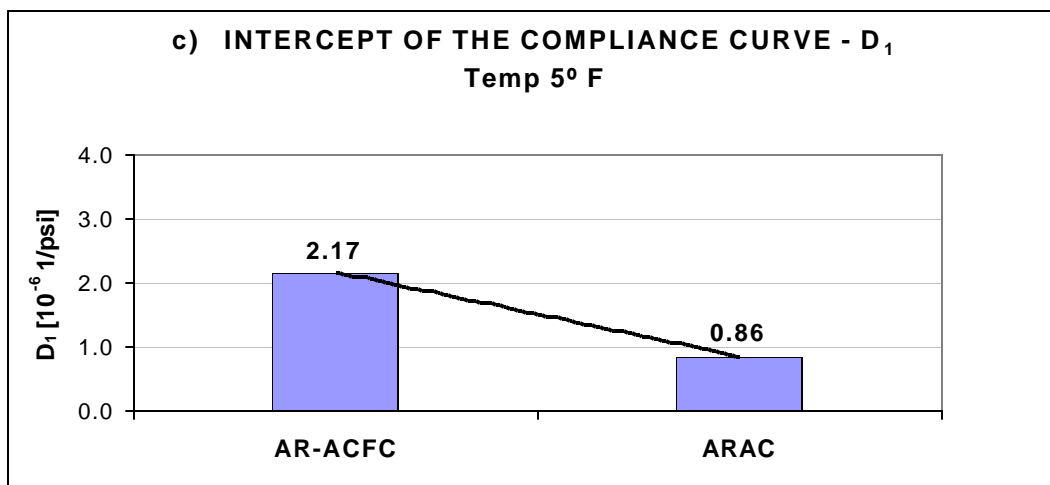
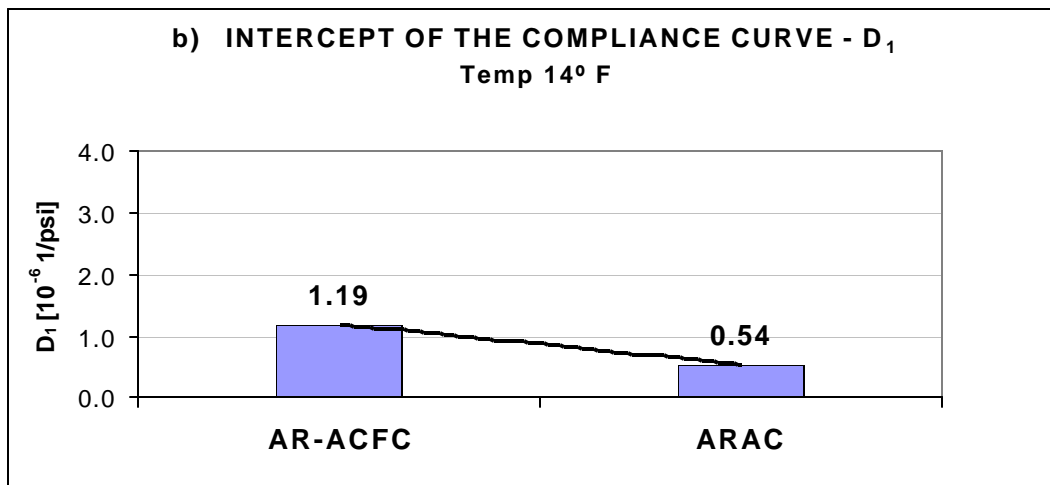
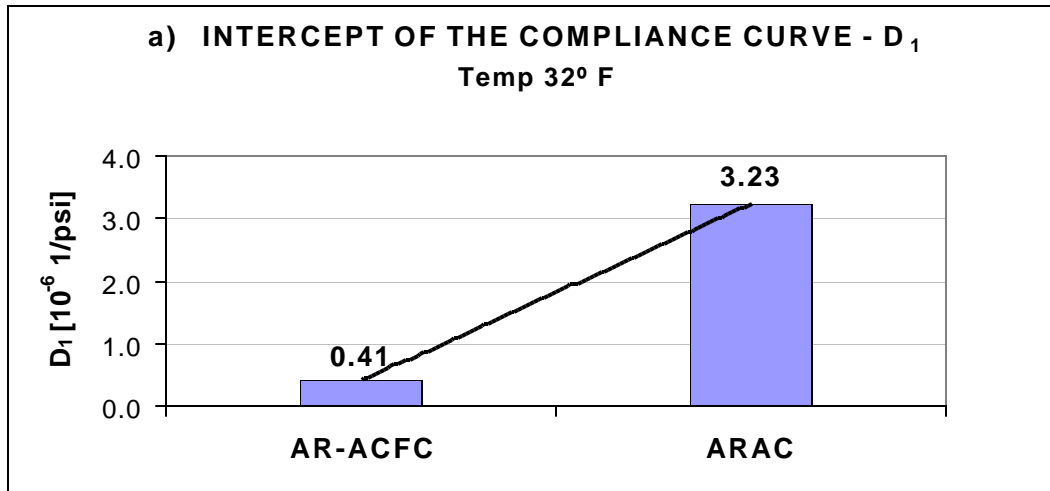


Figure 71. Indirect Tensile Creep Test – Intercept of the Compliance Curve

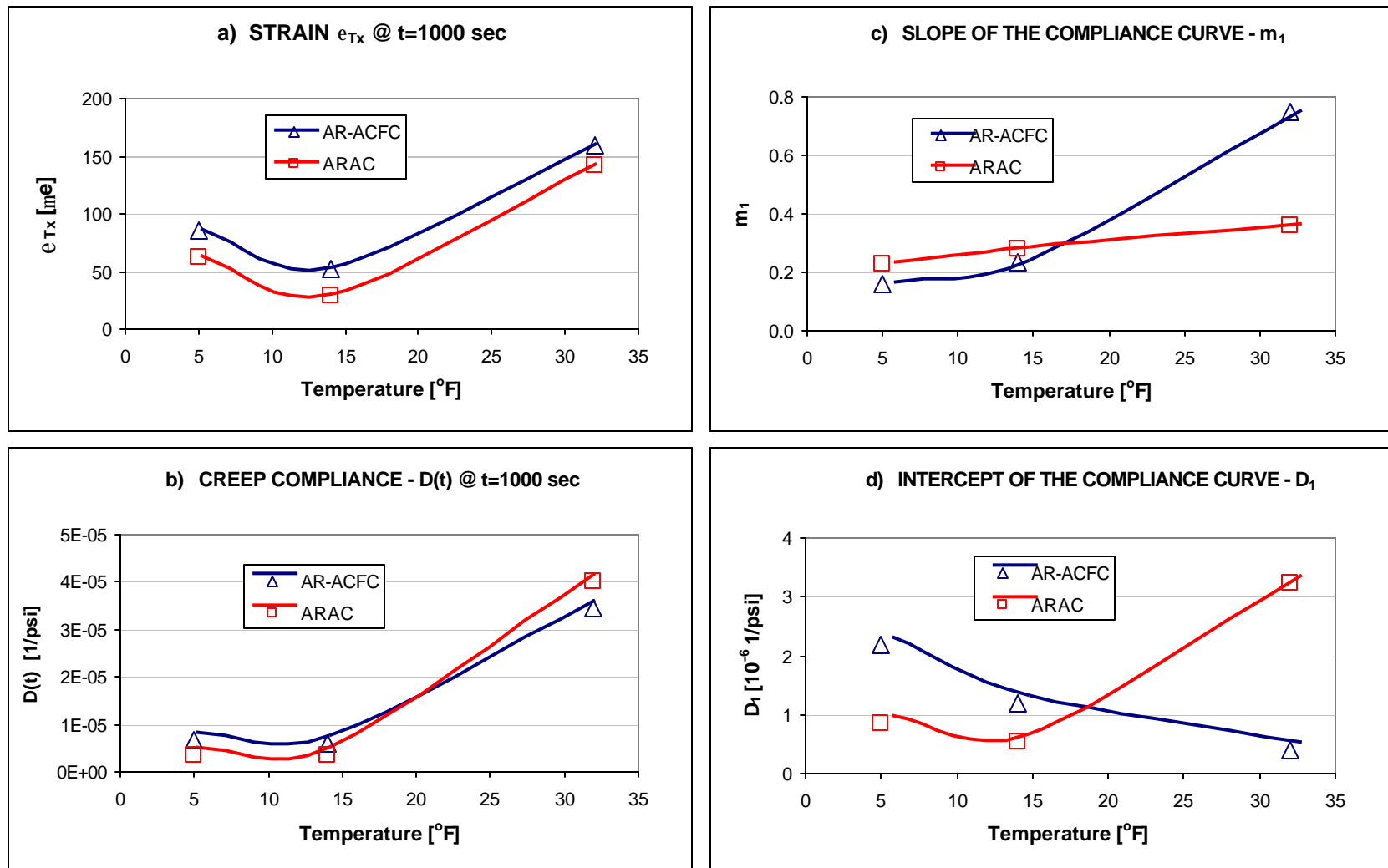


Figure 72. Indirect Tensile Creep Test – Summary of the Results

The results of strain at time 1000sec (Figure 68) show that the AR-ACFC mix has 12% higher strain at temperature 32°F, 78% higher strain at 14°F, and 38% higher strain at 5°F. The lowest strain that both mixture had is at 14°F.

Considering the creep compliance parameters, slope (Figure 70) and intercept (Figure 71) similar trends to the indirect tensile strength test are observed. At higher temperature, the AR-ACFC mix has higher slope and lower intercept than the ARAC mix. The differences are very significant, 2 times larger slope and almost 8 times smaller intercept. At 14°F the order is reversed but with no so significant differences. At 5°F, the difference between the mixtures is increasing.

7.2.6. Summary for the Indirect Tensile Tests

Both indirect tensile cracking tests were carried out according to the procedure described in the draft indirect tensile tests protocol for the AASHTO 2002 Design Guide. The tests were carried out at three temperatures: 32F, 14F and 5F. Based on test results and analysis the following conclusions are made:

- The test results of the Indirect Tensile Strength showed that the SRB PG64-22 mix had about 3 times higher strength compared to AR mixtures. This is not consistent with field observations, where the AR mixes show superior performance compared to standard asphalt concrete mixtures when resistance to thermal cracking is considered. Based on this knowledge, it can be concluded that the tensile strength is not good indicator of performance for AR mixtures.

- The results of strain at failure showed that the AR-ACFC and ARAC mixes had higher values than the SRB PG64-22 mix. Asphalt rubber mixtures with higher strain at failure have higher resistance to thermal cracking.
- The results of energy until failure and fracture energy from the indirect tensile strength test, as well as the results of creep compliance from the indirect tensile creep test indicated that AR mixtures, and especially the AR-ACFC mix, are not sensitive for decrease in temperature compared to the SRB PG64-22 mixture. Higher energy values are indicative of more resistant to thermal cracking. At 32°F, the SRB PG64-22 mix performed better than the AR mixtures, but when the temperature dropped to a level between 32°F and 14°F, the SRB PG64-22 mix very rapidly lost its “good properties (performance)”, while the AR-ACFC and ARAC mixes kept their “good performance” as higher energy is necessary to fracture the specimen. This relative insensitivity for changes in temperature makes the AR mixtures, and especially the AR-ACFC mix better resistance to thermal cracking in the field.
- In summary, while indirect tensile strength test parameter did not provide good explanation to the thermal cracking behavior of the AR mixes, the strain at failure and energy parameter from the same test provided better indication of the field behavior of the mixes.
- Perhaps finding of “the turning point” (temperature at which the trend of mixtures’ properties change) may help determining the temperature below

which the asphalt rubber mixtures could be most efficient in their resistance to thermal cracking.

8. SUMMARY, CONCLUSIONS AND RECOMMENDATIONS

8.1. Summary

In the spring of 2001, ADOT in cooperation with FNF Construction Inc. entered into a research and testing plan with Arizona State University (ASU). The plan involves characterizing AR mixes and binders in order to determine their properties for future use in the AASHTO 2002 Pavement Design Guide. This first project, named Buffalo Range TI-Canyon Diablo is located on Interstate 40 at Mile Posts 224.7 to 229.9, close to Winslow Arizona. The AR overlay project was constructed by FNF Construction Inc. The project consisted of removing by milling off 2.5 inches of the old cracked pavement full width and replacing it with 2 inches of the AR gap graded mix followed by 0.5 inch of AR open graded mix. The construction took place in June of 2000. Materials for the ARAC – Gap Graded mixture and AR-ACFC – Open Graded mixture were collected during construction.

The focus of the laboratory experimental program at ASU was on conducting tests that were recommended by the NCHRP 9-19 Project. These tests dealt with recommending Simple Performance Tests (SPT) for the evaluation of asphalt mixtures. The goal was to also compare the performance of these AR mixtures to other conventional asphalt mixtures that are also being tested at ASU.

Conventional binder consistency tests (penetration, softening point and viscosity) were conducted on the Crumb Rubber Modified (CRM) binder to determine whether there

were any unique characteristics or difficulties in handling the material. Consistency tests across a wide range of temperatures were conducted according to the accepted American Society for Testing and Materials (ASTM) practices.

Triaxial Shear Strength tests were conducted at unconfined and confined conditions at 100°F. These tests provided the standard cohesion and the angle of internal friction parameters of the mixtures. The Mohr-Coulomb failure envelope was developed for each tested mixture. The test results obtained were compared to results available at ASU for conventional ADOT dense graded mixtures.

Repeated Load and Static Creep Permanent Deformation tests were conducted at 100 and 130°F using unconfined and confined SPT protocols. Many test parameters were evaluated including the tertiary flow: flow time and flow number of repetitions. Both parameters / tests were among the selected SPT candidates. The test results obtained were compared to results available at ASU for conventional ADOT dense graded mixtures. In addition, few test specimens for the ARAC gap graded mix were prepared and tested at lower air void content (7%) than that reported in the field (11%) to study the effect of air void variations on the gap graded mixture.

Dynamic Complex Modulus (E^*) tests were conducted at unconfined and confined conditions, and the E^* master curves were developed for each mixture. The E^* test results for the AR mixes were also compared with conventional dense graded mixtures

test results available from previous studies at ASU. A modular (E^*) ratio was calculated and a ranking order was established for a variety of mixtures using a conventional PG 64-22 mixture as a reference.

Constant Strain Fatigue tests were conducted at different test temperatures (40, 70 and 100°F) using the beam fatigue apparatus proposed by the Strategic Highway Research Program (SHRP). Indirect Tensile Cracking tests (Strength and Creep) were carried out according to the procedure described in the draft indirect tensile tests protocol for the AASHTO 2002 Design Guide. The tests were carried out at three temperatures: 32, 14 and 5°F.

8.2. Conclusions and Recommendations

8.2.1. Binder Characterization

- The conventional asphalt cement tests were shown to be adequate in describing the viscosity-temperature susceptibility of crumb rubber modified asphalt cement.
- This favorable viscosity-temperature susceptibility relationship (A and VTS parameters) appeared to relate to the observed field performance behavior. Such behavior is characterized as less low temperature cracking and good resistance to permanent deformation at high temperatures.
- The A and VTS parameters developed for the crumb rubber modified binder provide the very necessary input to predict mixture stiffness (E^*) that is the building block used in the new 2002 Design Guide.

- It is recommended to conduct further testing on additional CRM binders to confirm the unique characteristics found in this study; and to provide further insight and experience in handling this material using conventional binder tests.

8.2.2. Triaxial Shear Strength Test

- The results of the cohesion parameter showed that the asphalt rubber open graded mix (AR-ACFC) had much lower resistance to shearing stresses than the other two mixes. This observation must be supported by information that the AR-ACFC is utilized as a mixture for non-structural layer. For this Buffalo Range project the AR ACFC mix was placed in 0.5 in lift, and for this type of application, the shearing stress is not so critical. At the same time, the AR-ACFC mix had the highest value of angle of internal friction, which indicated that this material has the largest capacity to develop strength from the applied loads, and hence the smallest potential for permanent deformation.
- Comparing the results for the SRB PG64-22 and ARAC mixtures it can be observed that although the ARAC mix had smaller cohesion than the SRB PG64-22, it had also larger angle of internal friction, and smaller potential for permanent deformation.
- Analyzing the failure envelope trend lines it can be noticed that at higher confinements levels, there are smaller difference in shear stress between all three mixtures. Theoretically, a confinement level exists at which for the same normal stress, there is equal shear stress for all three mixtures.

8.2.3. Permanent Deformation Tests

- In both unconfined tests (Static Creep and Repeated Load) conducted at 130°F, the ARAC mixture indicated superior performance, much higher resistance to permanent deformation compared to the standard ADOT SRB PG64-22 mixture.
- The ARAC mixture failure (flow) occurred after reaching 5 to 10 times larger strain than the SRB PG64-22 mix. Larger strain at failure are indicative of good mixture stability to the applied loads
- The trends for the Static Creep and the Repeated Load tests were very similar, and the ARAC mix performed very well in both tests. However, better results were observed in the Static Creep test. Therefore, improved mixture stability under static load may also be expected from the ARAC mixture.
- The AR-ACFC mix generally showed lower resistance to permanent deformation (in both unconfined and confined tests) compared to the other tested mixtures. For the unconfined tests, this was attributed to several factors: much higher air voids, lack of confinement that this material normally experience in the field, and higher binder content. Note that the AR-ACFC mix is a material designed for non-structural layers and its thickness usually does not exceed 1 inch. For the confined tests, the laboratory poor performance was attributed to the lack of adequate confinement level applied, which does not represent the level of confinement that the material experiences in the field. Therefore, the open graded friction course (AR-ACFC mix) should not be

compared in a routine testing mode (that was utilized in this study) to materials like the ARAC – Gap graded asphalt concrete or the Salt River Base dense graded mixtures, when resistance to permanent deformation is considered.

- Experience from the confined tests in this study showed that the selected stress level combinations in the laboratory were not effective and further work on selecting appropriate stress levels for these confined tests should be conducted.
- The air voids sensitivity study showed that the ARAC mix compacted to 7% air voids would have much better performance and less potential for permanent deformation than the same mixture compacted to 11% air voids. This finding is consistent with observations found for dense graded mixes. Therefore, it would be advisable to use a similar type of compaction quality control for the AR gap graded mixtures.
- This study showed promising results of utilizing the flow time / flow number of repetitions parameters to evaluate / verify the field performance of the asphalt rubber mixtures. Further studies including different levels of confined tests are recommended.

8.2.4. Dynamic (Complex) Modulus Test

- The dynamic modulus tests results obtained in this study showed that the use of crumb rubber modified binders enhances the properties of the asphalt mixture, both at low and high temperatures.
- When conducting dynamic modulus tests on asphalt rubber mixtures using

different levels of confinement, a significant increase in the modulus values was observed at high temperatures and low-test frequencies. The increment was not as significant when the test was performed at low temperatures for the AR-ACFC open graded mix.

- When comparing the modulus values of unconfined and confined tests, the results showed that the level of confinement chosen would be considerable and would have an impact on the evaluation of the mixture performance. This was especially true for the asphalt rubber (AR-ACFC) open graded mixture.
- The results of the confined dynamic modulus tests ranked both of the asphalt rubber mixture on top in their resistance to low temperature cracking and high temperature permanent deformation.
- In several cases, equivalent unconfined modulus test results were obtained at test temperatures of 100 and 130°F. This behavior was attributed to the decreased role of the asphalt cement and the increased role of the crumb rubber particles, which seemed to dominate the behavior of the mix as the test temperature increased. This type of behavior confirms the observed good field performance of these mixes against permanent deformation or rutting.
- The Witczak Dynamic (Complex) Modulus Predictive Equation was valid for the ARAC mixture. This was attributed to the fact that the database used for the Predictive Equation had mixtures with similar characteristics (volumetrics) to those for the ARAC mixture. On the other hand, the Predictive Equation was not valid for the AR-ACFC mixture. This was essentially due to its aggregate

gradation and the air void content, as both were not represented in the database used for developing the equation.

- This study showed very promising results of utilizing the dynamic modulus test to evaluate / verify the field performance of the asphalt rubber mixtures. Because of the type of aggregate grading that these mixtures have (gap and open graded), further evaluation using confined testing is recommended to verify conclusions arrived at in this study. In addition, when comparing dense, gap and open graded mixtures, confined dynamic modulus tests are recommended to rank and compare the expected field performance of the different mixtures. It is emphasized that this is not contradictory to findings of NCHRP 9-19 Simple Performance Project, where the unconfined dynamic modulus test was recommended as one of the three candidates for the simple performance test. It is important to recognize that all of the mixtures evaluated under the first phase of NCHRP 9-19 Project were dense graded mixes, and the confinement level was not found to be a discriminating factor.

8.2.5. Fatigue Cracking Testing

- The fatigue models developed for the AR mixtures in this study had excellent measures of accuracy and were rational in that lower fatigue life was obtained as the test temperature decreased.
- The fatigue life was found to be higher for asphalt rubber mixes compared to the conventional PG 76-16. The comparison was done at 70 °F and at 50%

reduction of initial stiffness for all mixtures. The ARAC mix resulted in approximately a 3 times greater fatigue life than the conventional mix. On the other hand, the AR-ACFC mix resulted in 15 times greater fatigue life than the conventional mix. These order of magnitudes of fatigue life for the three mixtures were rational considering that the PG 76-16 mix had 4.20% binder content whereas the ARAC and AR-ACFC mixtures had 6.8% and 8.8%, respectively.

8.2.6. Thermal Cracking Tests

- The test results of the Indirect Tensile Strength showed that the SRB PG64-22 mix had about 3 times higher strength compared to AR mixtures. This is not consistent with field observations, where the AR mixes show superior performance compared to standard asphalt concrete mixtures when resistance to thermal cracking is considered. Based on this knowledge, it can be concluded that the tensile strength may not be a good performance indicator for asphalt rubber mixtures.
- The results of strain at failure showed that the AR-ACFC and ARAC mixes had higher values than the SRB PG64-22 mix. Asphalt rubber mixtures with higher strain at failure have higher resistance to thermal cracking.
- The results of energy until failure and fracture energy from the indirect tensile strength test, as well as the results of creep compliance from the indirect tensile creep test, indicated that AR mixtures, and especially the AR-ACFC mix, are

not sensitive for decrease in temperature compared to the SRB PG64-22 mixture. Higher energy values are indicative of more resistant to thermal cracking. At 32°F, the SRB PG64-22 mix performed better than the AR mixtures, but when the temperature dropped to a level between 32°F and 14°F, the SRB PG64-22 mix very rapidly lost its “good properties (performance)”, while the AR-ACFC and ARAC mixes kept their “good performance” as higher energy was necessary to fracture the specimen. This relative insensitivity for changes in temperature makes the AR mixtures, and especially the AR-ACFC mix better resistance to thermal cracking in the field.

- In summary, while indirect tensile strength test parameter did not provide good explanation to the thermal cracking behavior of the AR mixes, the strain at failure and energy parameter from the same test provided better indication of the field behavior of the mixes.
- It is recommended to conduct future studies to find “the turning point” temperature (temperature at which the trend of mixtures’ properties change). This may help determining the temperature below which the asphalt rubber mixtures could be most efficient in their resistance to thermal cracking.

9. REFERENCES

1. Scofield, L.A., "History, Development, and Performance of Asphalt Rubber at ADOT", Report Number AZ-SP-8902, December 1989.
2. Sousa, J.B., Pais, J.C., Saim, R., Way, G.B., Stubstad, R.N., "Development of a Mechanistic Overlay Design Method Based on Reflective Cracking Concepts", Rubber Pavements Association/ADOT, August, 2001.
3. Way, G.B., "Prevention of Reflection Cracking Minnetonka-East", ADOT, Report Number 1979GWI, August 1979.
4. Zhu, H., Carlson, D.D., "A Spray Based Crumb Rubber Technology In Highway Noise Reduction Application", Rubber Pavement Association, October 1999.
5. Way, G.B., "Flagstaff I-40 Overlay Project", 4R Conference & Road Show, Cincinnati, Ohio, December 1989.
6. Way, G.B., "Flagstaff I-40 Asphalt Rubber Overlay Project Nine Years of Success", Transportation Research Board, 78th Annual Meeting, Washington D.C., January, 2000.
7. Lukanen, E.O., Stubstad, R.N. and Briggs, R.C. "Temperature Predictions and Adjustment Factors for Asphalt Pavement", Federal Highway Administration, Publication No. FHWA-RD-98-085, Washington, DC, June 2000.
8. Radd, L., Saboundjian, S. and Minassian, G. "Field Aging Effects on the Fatigue of Asphalt Concrete and Asphalt-Rubber Concrete", Transportation research Board, Annual meeting CR Rom, Paper No. 01-3097, Washington, DC, January 2001.
9. www.instrotek.com/corelok.htm
10. Witczak, M.W. and Kaloush, K.E., "Performance Evaluation of CitgoFlex Asphalt Modified Mixture using Advanced Material Characterization Tests". Department of Civil Engineering, University of Maryland, College Park, Maryland, 1998.
11. Witczak, M.W. and Mirza, M.W., 1995, "Development of a Global Aging System for Short and Long Term Aging of Asphalt Cements", Journal of the Association of the Asphalt Paving Technologists, Vol. 64, 1995, pp.393-430.
12. American Society for Testing and Materials, "1998 Annual Book of ASTM Standards", Vol. 04.03, 1998.
13. Witczak, M. W., Kaloush, K. E., Pellinen, T., El-Basyouny, M., & Von Quintus, H. (2002) Simple Performance Test for Superpave Mix Design. NCHRP Report 465. Arizona State University, Tempe AZ.
14. Kaloush, K. E. "Simple Performance Test for Permanent Deformation of Asphalt Mixtures", Ph.D. Dissertation, Arizona State University, Tempe AZ, May 2001.

15. Witczak, M. W. and Kaloush, K. E. "Performance Evaluation of Asphalt Modified Mixtures Using Superpave and P-401 Mix Gradings". Technical Report to the Maryland Department of Transportation, Maryland Port Administration, University of Maryland, College Park, Maryland, 1998.
16. Hafez, I. "Development of A Simplified Asphalt Mix Stability Procedure for Use in Superpave Volumetric Mix Design". Ph.D. Dissertation, Civil Engineering Department, University of Maryland, College Park, Maryland, 1997.
17. Mirza, M.W. and Witczak, M. W. "Bituminous Mix Dynamic Material Characterization Data Acquisition and Analysis Programs Using 458.20 MTS Controller". Program Background and Users Guide, University of Maryland, College Park, Maryland, May 1994.
18. Monismith, C.L., Ogawa, N., and Freeme, C. "Permanent Deformation of Subgrade Soils Due to Repeated Loadings". Transportation Research Record 537, Transportation Research Board, National Research Council, Washington, D.C., 1975.
19. Kaloush, K., Mirza, M.W., Uzan, J. and Witczak, M.W., "Specimen Instrumentation Techniques for Permanent Deformation Testing of Asphalt Mixtures". Journal of Testing and Evaluation, ASTM, West Conshohocken, PA, September 2001.
20. Witczak, M.W., Bonaquist, R., Von Quintus, H., and Kaloush, K., "Specimen Geometry and Aggregate Size Effects in Uniaxial Compression and Constant Height Shear Tests". Journal of the Association of Asphalt Paving Technologists, Volume 69, St. Paul, MN, March 2000.
21. Brown, S.F., Cooper, K.E., "The Mechanical Properties of Bituminous Materials for Road Bases and Base courses." Journal of the Association of Asphalt Paving Technologists, Volume 53, St.Paul, Minnesota, 1984.
22. Kenis, W.J., "Predictive Design Procedures." Proceedings of the Fourth International Conference on the Structural Design of Asphalt Pavements, Volume I, The University of Michigan, Ann Arbor, Michigan, August 1977.
23. AASHTO Designation: TP8-94. "Standard Test Method for Determining the Fatigue Life of Compacted Hot Mix Asphalt (HMA) Subjected to Repeated Flexural Bending".
24. SHRP Designation: M-009 "Standard Method of Test for Determining the Fatigue Life of Compacted Bituminous Mixtures Subjected to Repeated Flexural Bending".
25. Monismith, C. L., J. A. Epps, and F. N. Finn. "Improved Asphalt Design". Proceedings, Journal of the Association of Asphalt Paving Technologists Vol. 54, 1985.

26. SHRP-A-404. "Fatigue Response Of Asphalt-Aggregate Mixes". Asphalt Research Program, Institute Of Transportation Studies, University Of California, Berkeley. Strategic Highway Research Program, National Research Council, Washington, D.C., 1994.
27. Harvey, J., and Monismith, C.L., "Effect of Laboratory Asphalt Concrete specimen Preparation Variables on Fatigue and Permanent Deformation Test Results Using Strategic Highway Research Program A-003A Proposed Testing Equipment," Record 1417, Transportation Research Board, Washington, D.C., 1993.
28. Tayebali, A. A., Deacon, J. A., and Monismith, C. L., "Development and Evaluation of Dynamic Flexural Beam Fatigue Test System". Transportation Research Record No: 1545, Washington, D.C., 1996, pp. 89-97.
29. Tayebali, A. A., Deacon, J. A., and Monismith, C. L., "Development and Evaluation of Surrogate Fatigue Models for SHRP" A-003A Abridged Mix Design Procedure. Journal of the Association of Asphalt Paving Technologists Vol. 64, 1995, pp. 340-366.
30. Witczak, M.W., Mamlouk, M., and Abojaradeh, M.. "Flexural Fatigue Tests". NCHRP 9-19, Subtask F6 Evaluation Tests. Task F Advanced Mixture Characterization. Interim Report, Arizona State University, Tempe, Arizona, July 2001.
31. "Development Of The 2002 Guide For The Design Of New And Rehabilitated Pavement Structures – Stage A Report", NCHRP Project 1-37A Interim Report, ERES Consultants, Inc., Report prepared for the National Cooperative Research Program, Washington, DC, April 1999.
32. "LTPP Data Analysis Technical Assistance", FHWA Contract No. DTFH61-96-C-00003, ERES Consultants, Federal Highway Administration, Washington, D.C.
33. Von Quintus, H. L., J.A. Scherocman, C.S. Hughes, and T.W. Kennedy, "Asphalt-Aggregate Mixture Analysis System – AAMAS", NCHRP Report 338, National Cooperative Highway Research Program, National Research Council, Washington, D.C., March 1991.
34. Witczak, M. W., et al., "Development Of Relationships To Predict Poisson's Ratio For Paving Materials", Inter-Team Technical Report for NCHRP 1-37A, Report prepared for the National Cooperative Research Program, Washington, D.C., 1999.
35. Lytton, R. L., et al., "Development And Validation Of Performance Prediction Models And Specifications For Asphalt Binders And Paving Mixes", Report No. SHRP-A-356, Strategic Highway Research Program, National Research Council, Washington, DC, 1993.
36. Pellinen, T. K. "Investigation of the Use of Dynamic Modulus as an Indicator of Hot-Mix Asphalt Performance". Ph.D. Dissertation. Arizona State University, Tempe, AZ. 2001.

37. Witczak, M.W., Bari, J., & Quayum, M., M. "Superpave Support and Performance Models Management". NCHRP 9-19. Field Validation of the Simple Performance Test. Subtasks C4 through C6. Arizona State University, Tempe, AZ, 2001.
38. Andrei, D., Witczak, M.W., & Mirza, M. W. "Development of a Revised Predictive Model for the Dynamic (Complex) Modulus of Asphalt Mixtures. Development of the 2002 Guide for the Design of New and Rehabilitation Pavement Structures", NCHRP 1-37A. Interim Team Technical Report. Department of Civil Engineering, University of Maryland, College Park, MD, 1999.
39. Witczak, M.W., & Fonseca, O., A., A "Revised Predictive Model for the Dynamic (Complex) Modulus of Asphalt Mixtures". Department of Civil Engineering, University of Maryland, College Park, MD.